PREPARATION OF CLAY-POLYMER NANOCOMPOSITE FOR THE RETARDATION OF WASTE WATER INFILTRATION IN LANDFILL SITES

MERT BİLDİREN

SEPTEMBER 2007

PREPARATION OF CLAY-POLYMER NANOCOMPOSITE FOR THE RETARDATION OF WASTE WATER INFILTRATION IN LANDFILL SITES

A THESIS SUBMITTED TO
THE GRADUATE SCHOOL OF NATURAL AND APPLIED SCIENCES
OF
MIDDLE EAST TECHNICAL UNIVERSITY

BY

MERT BİLDİREN

IN PARTIAL FULFILLMENT OF THE REQUIREMENTS
FOR
THE DEGREE OF MASTER OF SCIENCE
IN
GEOLOGICAL ENGINEERING

SEPTEMBER 2007

Approval of the thesis:

PREPARATION OF CLAY-POLYMER NANOCOMPOSITE FOR THE RETARDATION OF WASTE WATER INFILTRATION IN LANDFILL SITES

submitted by **MERT BİLDİREN** in partial fulfillment of the requirements for the degree of **Master of Science in Geological Engineering Department, Middle East Technical University** by,

Prof. Dr. Canan Özgen _____
Dean, Graduate School of **Natural and Applied Sciences**

Prof. Dr. Vedat Doyuran _____
Head of Department, **Geological Engineering**

Prof. Dr. Asuman G. Türkmenoğlu _____
Supervisor, **Geological Engineering Dept., METU**

Examining Committee Members:

Prof. Dr. A.M.Cemal Göncüoğlu _____
Geological Engineering Dept., METU

Prof. Dr. Asuman G. Türkmenoğlu _____
Geological Engineering Dept., METU

Prof. Dr. Mehmet Ekmekçi _____
Geological Engineering Dept., Hacettepe University

Prof. Dr. Teoman Tinçer _____
Chemistry Dept., METU

Assist.Prof.Dr. Fatma Toksoy Köksal _____
Geological Engineering Dept., METU

Date: 04.09.2007

I hereby declare that all information in this document has been obtained and presented in accordance with academic rules and ethical conduct. I also declare that, as required by these rules and conduct, I have fully cited and referenced all material and results that are not original to this work.

Name, Last name :

Signature :

ABSTRACT

PREPARATION OF CLAY-POLYMER NANOCOMPOSITE FOR THE RETARDATION OF WASTE WATER INFILTRATION IN LANDFILL SITES

Bildiren, Mert

M.Sc., Department of Geological Engineering

Supervisor : Prof. Dr. Asuman G. Türkmenoğlu

September 2007, 115 pages

In this thesis study, the use of clay-polymer nanocomposites for their applicability in landfill sites as a product of retardation of waste water infiltration was evaluated. For this purpose, organophilic clays from $HDTMA^+$ organic cation and nanocomposites of montmorillonite were prepared. The bentonite samples B1, B2 and B3 dominantly contain 2:1 layer montmorillonite and 1:1 interstratification of illite/smectite mixed layer as clay minerals. B1 is an unmodified yellow bentonite and B2 is a grey bentonite modified from B1, by the addition of Na_2CO_3 (Soda Ash). They were obtained from Hançılı (Kalecik-Ankara) bentonite deposit which belongs to the Hancılı Formation of Early Pliocene age. B3 is a standard Wyoming (SWy-1) white bentonite and belongs to the Newcastle formation of Cretaceous age.

Their cation exchange and swelling capacity values were determined and the values increase from B1, B2 to B3. In order to produce clay-polymer nanocomposites, firstly organoclays were produced in bentonite samples. Clay-polymer nanocomposite production was achieved by in situ intercalative polymerization successfully with intercalation and partly exfoliation of clay minerals with polyacrylamide (PAM). The samples of sand (S1), sand+bentonite

(S2) and sand+nanocomposite (S3) mixtures were prepared and their permeability was determined. As a result of these values, the permeability of samples decrease from S1, S2 to S3.

The results imply that the permeability of sample decreases as the clay-polymer nanocomposite content increases resulting in a retardation of water penetration throughout the sample. The product has a potential to be used as a retardant for waste water infiltration in landfill sites.

Keywords: clay-polymer nanocomposite, organoclay, waste-water infiltration, exfoliation, bentonite

ÖZ

KATI ATIK SAHALARINDA ATIK SU GEÇİRGENLİĞİNİ AZALTMAYA YÖNELİK KİL-POLİMER NANOKOMPOZİTİ ÜRETİMİ

Bildiren, Mert

Yüksek Lisans, Jeoloji Mühendisliği Bölümü

Tez Yöneticisi : Prof. Dr. Asuman G. Türkmenoğlu

Eylül 2007, 115 sayfa

Bu tez çalışmasında, kil-polimer nanokompozitlerinin atık su geçirgenliğini azaltmaya yönelik bir ürün olarak atık sahalarındaki kullanılabilirlikleri incelenmiştir. Bu amaçla, $HDTMA^+$ organik katyonundan üretilen organik killer ve montmorillonit ve poliakrilamit nanokompozitleri hazırlanmıştır. B1, B2 ve B3 kodlu bentonit örnekleri çoğunlukla 2:1 katmanlı montmorillonit ve 1:1 tabakalı illit/smektit kil mineralleri içermektedir. B1 örneği işlenmemiş sarı bentonittir ve B2 örneği de gri olup B1 örneğinin yüzde 3 oranında soda külüyle (Na_2CO_3) zenginleştirilmesinden elde edilmiştir. Bu örnekler Hançılı (Kalecik-Ankara) bentonit sahasından elde edilmiş olup erken pliyosen yaşlı Hançılı formasyonuna aittirler. B3 örneği ise standart Wyoming (SWy-1) beyaz bentoniti olup, Kretase yaşlı Newcastle formasyonuna aittir.

Örneklerin katyon değiştirme ve şişme kapasitesi değerleri belirlenmiştir ve değerler bu değerler B1 den B2 ve B3'e doğru yükselmiştir. Kil-polimer nanokompoziti üretmek için, ilk olarak bentonit örneklerinden organokiller hazırlanmıştır. Kil-polimer nanokompozit üretimi, yerinde interkalatif polimerizasyon reaksiyonu ile gerçekleştirilmiştir. Kum (S1), kum+bentonit karışımı (S2) ve kum+nanokompozit karışımı (S3) hazırlanmış ve sıvı

geçirgenlikleri tesbit edilmiştir. Bu sonuçlara göre, örneklerin geçirgenlik değerleri S1, S2 ve S3 sırasıyla düşüş göstermektedir.

Sonuçlar göstermektedir ki, örneğin içindeki kil-polimer nanokompozit oranı artarsa, örneğin su geçirgenliği değeri düşer. Bunun sonucu olarak, örneğin içinden geçen su miktarı azalmış olur. Elde edilen ürün katı atık sahalarında su geçirgenliğini azaltmaya yönelik malzeme olarak kullanılma potansiyeline sahiptir.

Anahtar Kelimeler: Kil-polimer nanokompoziti, organokil, atık su süzülümü, eksfoliasyon, bentonit

To my family…

ACKNOWLEDGEMENTS

I would like to express my special thanks to Prof.Dr. Asuman G. Türkmenoğlu for her guidance, understanding, encouragement, care, valuable advices and recommendation. Also, thanks for her supervisorship to my thesis and great help during the writing stage of this thesis.

I would also like to thank to Prof. Dr. Hale Göktürk and Deniz İnam for their advices and help during the organoclay production and analysis stage.

I would also like to send my best gratitude to Prof.Dr. Teoman Tinçer and Prof.Dr. Mehmet Ekmekçi for their great help and advices and their contribution to the analysis stage.

Thanks go to Prof. Dr. Hüsnü Özkan and Nadir Ghazanfari for the XRD measurements and analyses.

Grateful thanks go to my dear friends Mehmet Sinan Öztürk for his contributions to every stage of this thesis and to Kaan Sayıt for mineral identifications.

Finally, I would like to thank to my parents for their enormous support for my whole university education.

TABLE OF CONTENTS

LIST OF TABLES

TABLES

LIST OF FIGURES

FIGURES

CHAPTER 1

INTRODUCTION

1.1. Definition of Materials (Clays and Clay Minerals)

The term 'clay' refers to a naturally occurring material composed primarily of fine-grained minerals, which is generally plastic at appropriate water contents and will harden when dried or fired. Although clay usually contains phyllosilicates, it may contain other materials that impart plasticity and harden when dried or fired (Guggenheim, 1995).

Clays and clay minerals are two terms which are easily confused. A natural clay may not consist of a single clay mineral itself. It may consist of some impurities such as calcite, quartz, feldspars, iron oxides, etc. which are not belonging to the family of clay minerals. Clay minerals belong to the group of phyllosilicates and contain continuous two-dimensional tetrahedral sheets of composition T_2O_5 (T=Si, Al, Be, etc.) with tetrahedra linked by sharing three corners of each, and with the fourth corner pointing in any direction. The tetrahedral sheets are linked in the unit structure to octahedral sheets, or to groups of coordinated cations, or individual cations (Brindley and Pedro, 1972).

Because they are “layered silicates” they contain sheets of linked tetrahedrons and octahedrons (Figure 1) bounded together with the help of some chemical bonds and form layers. For example; one octahedral sheet and one tetrahedral sheet stack together and form a 1:1 type layer structure.

Depending on the layer types and different cations present in their octahedral sheets, clay minerals are classified into categories (Table 1). Smectites fall into the category of 2:1 layer (2 tetrahedral and 1 octahedral sheet) and montmorillonites are the smectite group clay minerals having different species. Because they have high swelling and cation exchange capacities, montmorillonites are the most preferred clay minerals for processing.

Clays and clay minerals have been mined since the Stone Age; today they are among the most important minerals used by manufacturing and environmental industries. Clays and clay minerals occur under a fairly limited range of geologic conditions. The environments of formation include soil horizons, continental and marine sediments, geothermal fields, volcanic deposits, and weathering rock formations (Foley, 1999). In nature clay minerals are formed as “residual” which means in-situ alteration of the pre-existing host rock due to change in pressure, temperature and/or pH conditions, or “detrital” which means transportation and sedimentation from a distant source. They are the secondary minerals and they form by the disaggregation and chemical decomposition of pre-existing rocks. Common silicate materials such as quartz, feldspars, and volcanic glasses, as well as carbonates, noncrystalline iron oxides, and primary clay minerals, are transformed during diagenesis into more stable clay minerals mainly by dissolution and recrystallization (Foley, 1999).

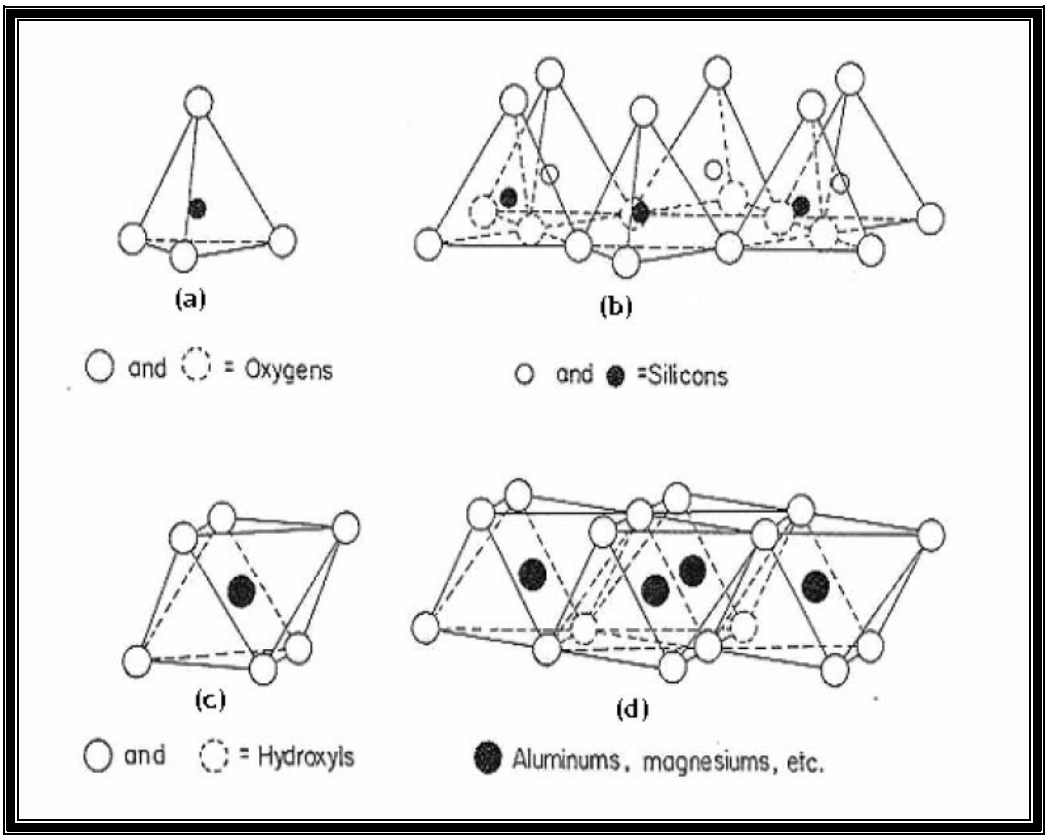

Figure 1. Tetrahedral and octahedral sheet structures in clay minerals (a) single tetrahedral unit, (b) sheet structure of the tetrahedral units, (c) single octahedral unit (d) sheet structure of octahedral units (Grim, 1953)

1.2. Definition of Nanoscience, Nanotechnology, Nanomaterial and Nanocomposite

Before making some definitions about the topic of this study, one has to know that what "nano-" prefix and "nanometer" means. "Nano-" is an ancient Greek word and SI (International System of Units) prefix that denotes a factor of 10^{-9}. Nanometer is a unit of spatial measurement that is 10^{-9} meter or one billionth of a meter and also 10 Ångstroms (Å) equal to 1 nanometer. Figure 2 demonstrates and gives an idea about the smallness of one nanometer when compared to one meter.

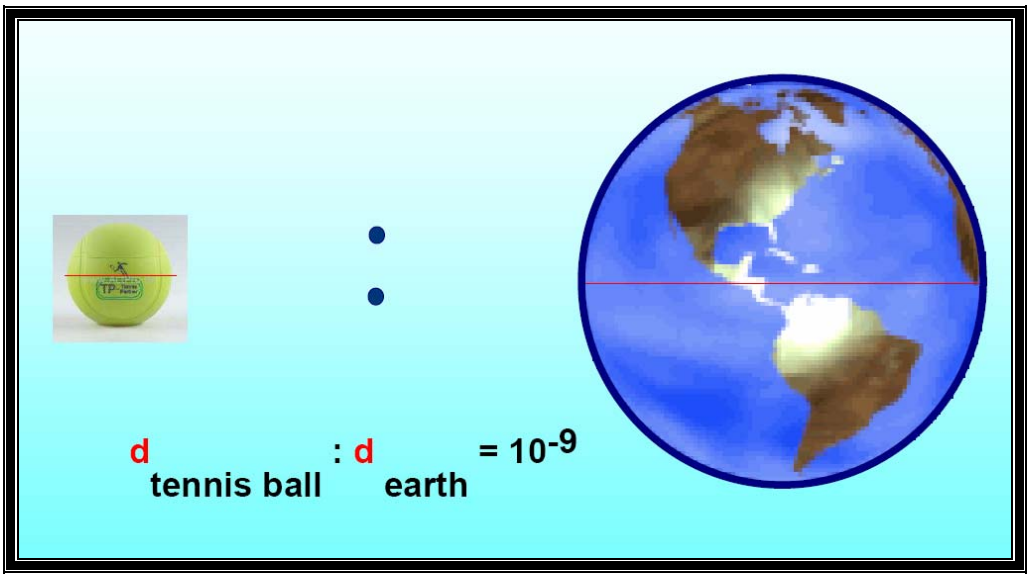

Figure 2. Comparison of tennis ball with earth to illustrate nanometer scale (Süd-Chemie AG, 2005)

Nanoscience is the study of phenomena and manipulation of materials at atomic, molecular and macromolecular scales, where properties differ significantly from those at a larger scale. Nanotechnologies are the design, characterisation, production and application of structures, devices and systems by controlling shape and size at nanometre scale and nanomaterials combine one or more separate components in order to obtain the best properties of each component (composite). In nanocomposite, nanoparticles (clay, metal, carbon nanotubes) act as fillers in a matrix, usually polymer matrix. (Nanocompositech, 2005)

Table 1. Classification of clay minerals ($\underline{x}$ = charge per formula unit) (Bailey, 1980).

Layer Type	Group	Subgroup	Species
1:1	Kaolinite-serpentine	Kaolinite	Kaolinite, dickite, halloysite
	$\underline{x} \sim 0$	Serpentine	Chrysotile, lizardite, amesite
	Pyrophyllite-talc	Pyrophyllite	Pyrophyllite
	$\underline{x} \sim 0$	Talc	Talc
2:1	Smectite	Dioctahedral smectite	Montmorillonite, beidellite
	$\underline{x} \sim 0.2\text{-}0.6$	Trioctahedral smectite	Saponite, hectorite, sauconite
	Vermiculite	Dioctahedral vermiculite	Dioctahedral vermiculite
	$\underline{x} \sim 0.6\text{-}0.9$	Trioctahedral vermiculite	Trioctahedral vermiculite
	Mica	Dioctahedral mica	Muscovite, paragonite
	$\underline{x} \sim 1$	Trioctahedral mica	Phlogopite, biotite, lepidolite
	Brittle mica	Dioctahedral brittle mica	Margarite
	$\underline{x} \sim 2$	Trioctahedral brittle mica	Clintonite, anandite
	Chlorite	Dioctahedral chlorite	Donbassite
	$\underline{x}$ variable	Di,trioctahedral chlorite	Cookeite, sudoite
		Trioctahedral chlorite	Clinochlore, chamosite, nimite

Nanomaterials can be defined as materials which have structured components with at least one dimension less than 100 nm. Materials that have one dimension in the nanoscale are layers, such as a thin films or surface coatings.

Some of the features on computer chips come in this category. Materials that are nanoscale in two dimensions include nanowires and nanotubes. Materials that are nanoscale in three dimensions are particles, for example precipitates, colloids and quantum dots (tiny particles of semiconductor materials).

Clay minerals fall into the nanomaterials category in terms of their dimensions. They have one dimension that is less than 100 nm. Their natural crystal structure consists of generally 1-2 nm basal (001) *d*-spacing and several hundreds of nanometers of other axes (Figure 3). Therefore, clay minerals are the naturally occurring nanomaterials used in nanotechnology. Besides, their abundancy in nature put them into the category of most preferrable materials in nanoscience and nanocomposite production.

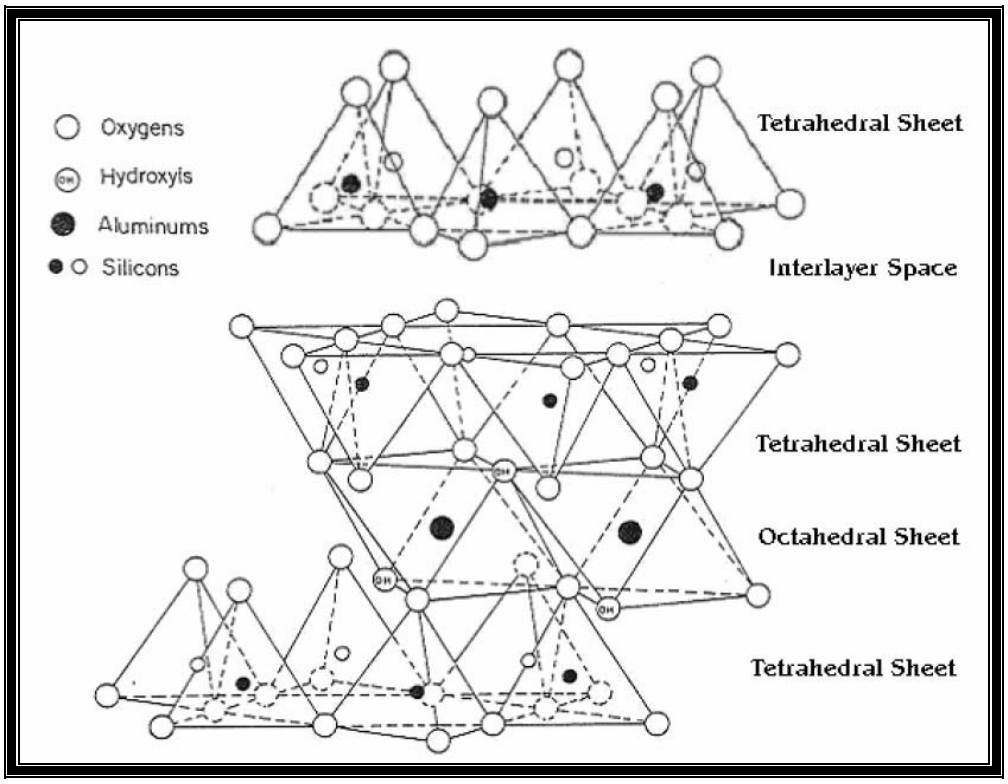

Figure 3. Schematic representation of the crystal structure of a 2:1 type clay mineral showing the relations between tetrahedral and octahedral sheets and interlayer spaces (Clauer and Chaudhuri, 1995).

1.3. Brief History and Application Areas of Nanocomposites

Composites that exhibit a change in composition and structure over a nanometer length scale have been shown over the last 10 years to afford remarkable property enhancements relative to conventionally-scaled composites (Schmidt, 1985; Novak, 1993; Mark, 1996).

The use of polymer nanocomposites in history starts in 1990 when Toyota first used clay/nylon-6 nanocomposites for Toyota car in order to produce timing belt covers. After that other automotive applications started. Mitsubishi covered its GDI (Gasoline Direct Injection) with clay/nylon-6 nanocomposites in their engines and General Motors used clay/polyolefin nanocomposites in their GMC Safari and Chevrolet Astro vans. The potential applications go beyond automotive industry. Up to now, plenty of studies have been and are still being made devoted to several areas.

One of the most promising industries is drink packaging application considering increased barrier properties of polymer clay nanocomposites. For example, gas barriers for fruit juice, dairy products, beer and carbonated drink bottles are the areas that nanocomposites used. The other areas of applications of clay-polymer nanocomposites include, oxygen barriers, reducing agent in solvent transmission in fuel tanks, production of thin films for transparency and haze effects, flammability reduction agent. They are used also as the environmental protection agent for waste water in landfills to diminish the extent to which water would be transmitted through to an underlying substrate (Nanocompositech, 2005). There are some advantages (Table 2) of nanocomposite additives in these products.

Table 2. The major advantages of nanocomposite additives.

- Mechanical properties e.g. strength, modulus and dimensional stability
- Decreased permeability to gases, water and hydrocarbons
- Thermal stability and heat distortion temperature
- Flame retardancy and reduced smoke emissions
- Chemical resistance
- Electrical conductivity
- Optical clarity in comparison to conventionally filled polymers

1.4. Production Techniques of Clay-Polymer Nanocomposites

In order to disperse clay layers into polymer matrix, it is very important considering polymer-clay compatibility. This means it is important to provide organophilic character to the clay by a pretreatment in order to make a successful formation of polymer-clay nanocomposite.

In the case of hydrophilic polymers and silicate layers, pretreatment is not necessary. Most polymers are hydrophobic (lacking affinity for water) and are not compatible with hydrophilic (having affinity for water) clays. Pretreatment involved only clays in order to obtain organic compatibility.

An organophilic clay can be produced from a hydrophilic (having an affinity for water) clay by ion exchange with an organic cation such as an alkylammonium ion (Hexadecyltrimethylammoniumbromide salt). For example, in the case of this study, the sodium and/or calcium ions in montmorillonite (MMT) were exchanged with $HDTMA^+$ (Hexadecyltrimethylammonium) cations by a definite reaction (Equation 1).

$$Na^+\text{-MMT} + HDTMA^+ + Br^- \rightarrow \text{HDTMA-MMT} + NaBr \quad \ldots\ldots\ldots \text{(Eqn.1)}$$

In order to obtain clay-polymer nanocomposite, well established methods are solution induced intercalation, in situ polymerization and melt processing. In solution induced intercalation method, a polymer is solved in an organic solvent, the clay is dispersed in the obtained solution and either the solvent is evaporated or the polymer precipitated. This approach leads to poor clay dispersion, besides other problem like: high costs of solvents required, large amount of solvent needs to be used to achieve appreciable filler dispersion, technical phase separation problem, and health and safety problem (Nanocompositech, 2005).

In situ polymerization consists of dispersing clay mineral layers into matrix by polymerization, mixing the silicate layers with the monomer, and with the help of polymerization initiator and/or the catalyst, nanocomposite is produced.

In the third technique the silicates layers are directly dispersed into the polymers during the melt. In order to use this method, the silicates should need to be previously surface treated through the organo-modification.

1.5. Organically Modified Clays (Organoclays)

Clay minerals have negatively charged surfaces and these surfaces are occupied by exchangeable cations of alkali and alkaline earth metals. The term "organoclay" means a type of clays that are made from the substitution of the cation present in their interlayer with an organic cation (Figure 4) in an aqueous medium. The reaction is given in section 1.4 (see equation 1).

Depending on the charge density of the clay, the onium ions may lie parallel to the clay surface as a monolayer, a lateral bilayer, a pseudo-trimolecular layer, or an inclined paraffin structure as illustrated in Figure 4 (Le Baron et al., 1999).

Organoclays are often prepared using quarternary ammonium cations of the general form $[(CH_3)_3NR]^+$ or $[(CH_3)_2NRR`]^+$ where R and R` are hydrocarbon groups (Inam, 2006). In the studies, $HDTMA^+$ tail group was found to have higher affinity for the exchange sites on clays relative to other surfactants (Haggerty and Bowman, 1994; Li, 1999). Therefore $HDTMA^+$ is the most frequently used surfactant in the research.

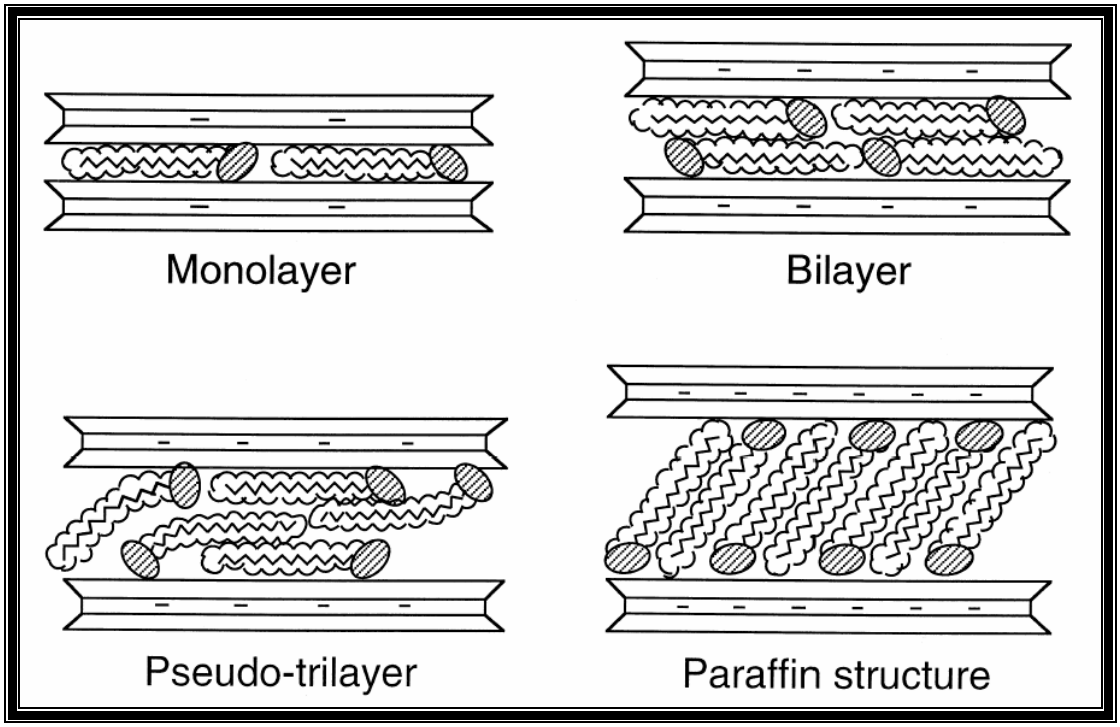

Figure 4. Orientation of alkylammonium ions in the galleries of layered silicates with different layer charge densities (Lagaly, 1986).

Organoclays can be created by exchanging the hydrated exchangeable cations of clay (usually bentonite) with various types of quaternary ammonium cations (Xu et al., 1995). Depending on the property associated with the organic cation (size and/or composition), the surfaces of the clay mineral become less hydrophilic and more hydrophobic, providing improved sorption properties of non-polar organics compared to the original clay (Xu et al., 1997).

Ion exchange with alkylammonium ions is a well-known method to make clay minerals and clays dispersible in organic solvents and to render them compatible with hydrophobic materials in compounding processes (Bergaya and Lagaly, 2001).

1.6. Intercalation and Exfoliation Mechanisms in Clay Minerals

In order to produce a nanocomposite, the clay minerals have to be dispersed homogeneously into the polymer matrix. To do this, first, clay minerals should be made organophilic to provide polymer-clay compatibility, and then intercalated with these polymers and finally exfoliated into the polymer matrix.

In an intercalated nanocomposite (Figure 5), single (and sometimes more than one) extended polymer chain is intercalated between the silicate layers resulting in a well ordered multilayer morphology build up with alternating polymeric and inorganic layers (Alexandre, 2000).

Exfoliated nanocomposites (Figure 5) are defined as having insufficient attractions between each two layer section, which is the reason of why these materials cannot maintain a uniform layer space. However, only a few stacks of clay layers, which are dispersed homogeneously in the polymer matrix, belong to the family of exfoliated nanocomposites. More commonly, the homogeneous dispersion of clay layers and the large interfacial area between polymer and clay make exfoliated clay/polymer nanocomposites desirable for greatly improving properties (Wang et al., 2005). Usually, the clay content of an exfoliated nanocomposite is much lower than that of an intercalated nanocomposite (Okamoto et al., 2003).

Once nanolayer exfoliation is achieved, the improvement in properties can be manifested as an increase in tensile properties, as well as enhanced barrier properties, decreased solvent uptake, increased thermal stability and flame retardance (Okada and Usuki, 1995; Giannelis, 1996).

For true nanocomposites, the clay nanolayers must be uniformly dispersed (exfoliated) in the polymer matrix (Figure 6), as opposed to being aggregated as tactoids or simply intercalated (Le Baron et al., 1999).

The clay interlayer spacing is fixed in an intercalated nanocomposite. On the other hand, in an exfoliated nanocomposite, the average gallery height is determined by clay silicate loading. The difference between ordered and disordered exfoliated nanocomposites is that the former can be detected by X-ray diffraction and the latter is X-ray amorphous (Le Baron et al., 1999).

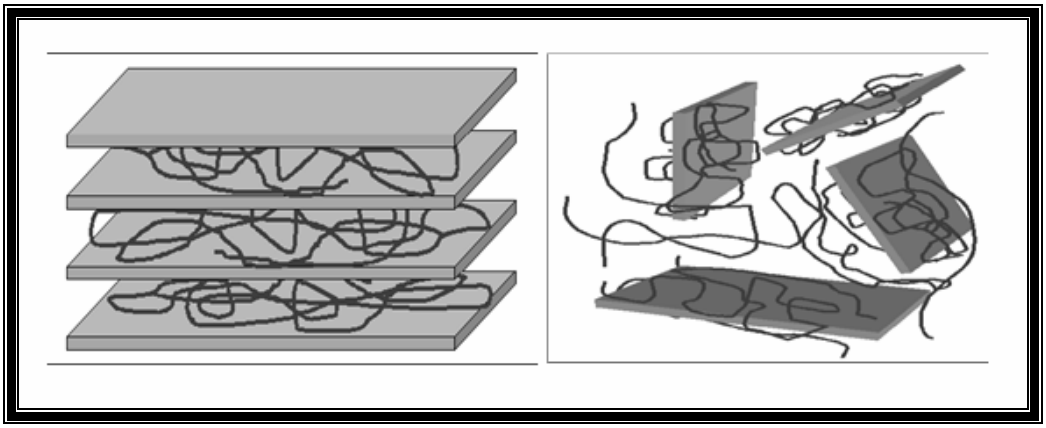

Figure 5. Schematic illustration of two different types of thermodynamically achievable polymer/clay nanocomposites. Left: the intercalated system, where the polymer chains penetrate into and swell the galleries of the silicate layers. Right: the exfoliated or delaminated system, where individual silicate layers are dispersed in the polymer matrix (Dulgerbaki, 2006).

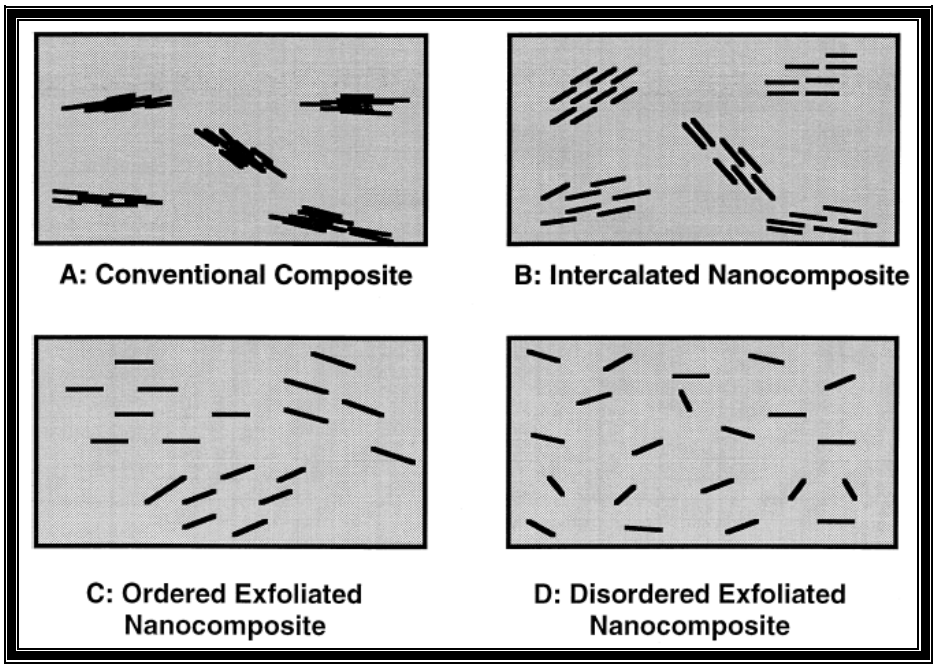

Figure 6. Schematic illustrations of (A) a conventional; (B) an intercalated; (C) an ordered exfoliated; and (D) a disordered exfoliated polymer–clay nanocomposite (Le Baron et al., 1999).

The replacement of inorganic exchange cations by organic onium ions on the gallery surfaces of smectite clays not only serves to match the clay surface polarity with the polarity of the polymer, but it also expands the clay galleries (Figure 7). This fact facilitates the penetration of the gallery space (intercalation) by either the polymer precursors or preformed polymer. Depending on the charge density of clay and the onium ion surfactant, different arrangements of the onium ions are possible (Le Baron et al., 1999).

However, regardless of the initial charge density of the clay and the orientations of the gallery long chain alkylammonium ions, the gallery height is determined by the vertical orientation of the long chain alkylammonium in the solvated intercalates. Cross-hatched ellipses represent the intercalated polymer precursor species (Figure 7) (Le Baron et al., 1999).

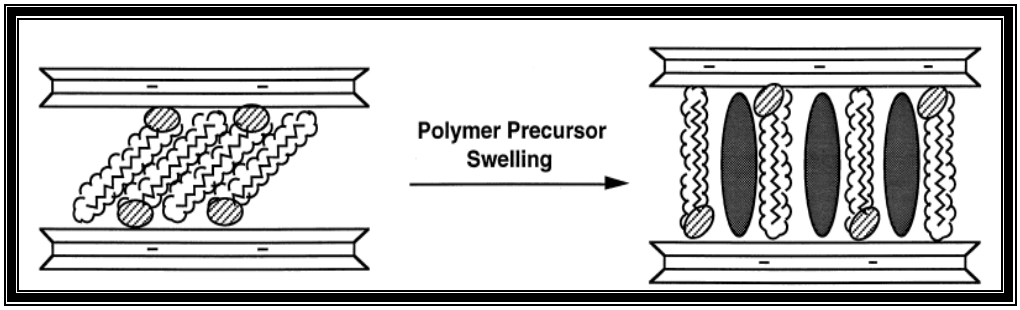

Figure 7. Proposed model for the swelling of alkylammonium exchanged clay with a parafin structure by polymer precursors (Le Baron et al., 1999).

The impermeable clay layers mandate a tortuous pathway for a permeant to transverse the nanocomposite (Figure 8). The enhanced barrier characteristics, chemical resistance, reduced solvent uptake and flame retardance of clay–polymer nanocomposites all benefit from the hindered diffusion pathways through the nanocomposite (Le Baron et al., 1999).

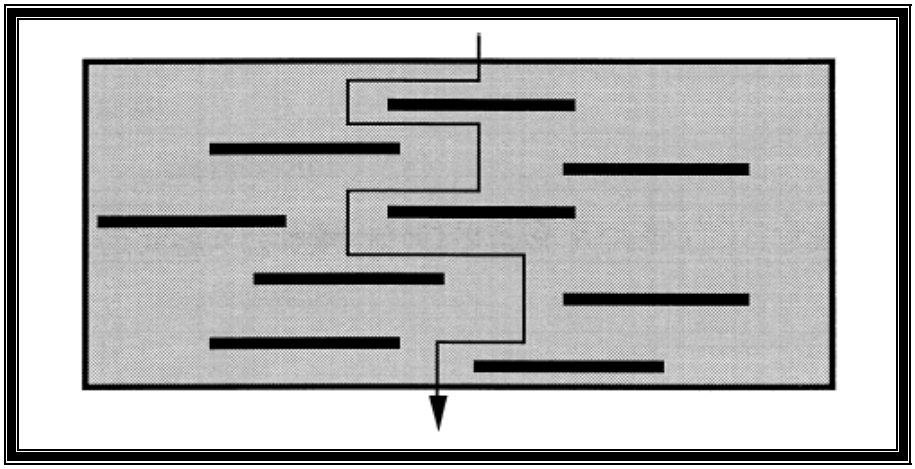

Figure 8. Proposed model for the torturous zigzag diffusion path in an exfoliated polymer–clay nanocomposite when used as a gas barrier (Yano et al., 1993).

1.7. Purpose & Scope

Clay minerals are used in several industries because of their different physical and chemical characteristics. They can be modified with different chemicals by substituting their interlayer cations to produce surface treated hybrid products. They are also abundant in nature. This situation make them very popular in newly developing raw material industries.

The major aims of this study are;

- to substitute the interlayer cation of the clay mineral with an organic cation to produce an organoclay providing the clay-polymer compatibility to trigger the mechanism of intercalation and exfoliation.
- to produce a clay-polymer nanocomposite containing a specific proportions of bentonite (mainly montmorillonite) and polymer (polyacrylamide)
- to investigate and lower the parameters such as permeability and hydraulic conductivity of this nanocomposite in the use of landfill depository sites for the prevention of waste-water leakage.

The study includes several steps. First step is the determination of some physico-chemical characteristics of chosen bentonites. Swelling capacity test, Methylene blue adsorbtion test for cation exchange capacity of samples and some XRD measurements were performed to prove the presence of clay minerals in the samples and to characterize the type of clay minerals.

Second step includes the production of organo-clays with $HDTMA^+$ organic cation and production of clay-polymer nanocomposites with acrylamide monomers through in-situ intercalative polymerization.

Finally, a permeability test was performed to determine the effect of produced nanocomposite which is the result of intercalation and exfoliation of clay minerals into the polymer matrix.

1.8. Previous Works

Clay-polymer nanocomposites and their applications have gained a great importance in recent years. These studies generally focus on the improvement of mechanical, thermal and barrier properties of these products. Followings are the most up-to-date and attributed studies.

Xiong et.al (2007) showed that modified montmorillonites play a great role on the mechanical, thermal and barrier characteristics of the polymer-clay nanocomposites.

Liu (2007) examined the latest studies of surface modification of clay minerals using polymers and established that the polymers improve the physical and chemical characteristics of clay mineral surfaces. The importance of these materials on the application of catalyzer, adsorbent and composite materials were also established.

Sun et al. (2006) stated that clay minerals have high surface/volume ratios and therefore react more than any other inorganic substance, when distributed into the polymer matrix, they show better mechanical and barrier performances.

Inam et al. (2006) prepared organoclays to remove the anionic pollutants in water. They modified the montmorillonite with $HDTMA^+$ organic cation making the clay mineral surface positively charged and showed that organically modified montmorillonites can hold and remove the anionic pollutants in water.

Mandalia and Bergaya (2006) distributed the organoclay minerals into two different polymer matrices and they produced clay polymer nanocomposites. They investigated the characteristics of the organoclays by X-Ray Diffraction, Infrared Spectroscopy, swelling capacity, Thermogravimetric Analysis (TGA) methods, and examined the effect of addition of different amounts of surfactant to the

nanocomposite. They also defined the thermal and mechanical characteristics of nanocomposites.

Bhiwankar and Weiss (2006) investigated the intercalation and exfoliation mechanism of Na-montmorillonite with SPS ionomers. The morphology of nanocomposite was determined by using XRD and Transmission Electron Microscopy (TEM). The thermal, dynamic and mechanical characteristics of produced nanocomposite were assigned.

Önal and Çelik (2006) produced polymethacrylamide/ Na-montmorillonite nanocomposites and characterized them by Fourier-Transform Infrared (FTIR), XRD, Scanning Electron Microscope (SEM) and thermal analysis methods and they investigated the thermal behaviour and water uptake properties of these samples.

Kim et al. (2005) examined the characteristic properties of the organoclays and nanocomposites as moisture barriers and manifested that moisture content and diffusion ratio changes depending on the type of organoclay. Also they determined that the clay content present in the organoclay affect the moisture barrier property of nanocomposites.

Zeng et al. (2005), Ray and Okamoto (2003) and Bergaya and Lagaly (2001) stated the suitability of the production of organoclay from smectite group clays and then they synthesized the clay-polymer nanocomposite with a determined polymer by a suitable method.

Le Baron et al. (1999) checked the structure of organoclay, the interaction between organoclay-polymer and the synthesis of nanocomposite in detail. They also stated that organoclay forms an ideal system for the production of clay-polymer nanocomposite.

Ludulena et al. (2007) produced montmorillonite-polycaprolactone nanocomposites by casting and melt intercalation methods, and compared them in terms of mechanical and thermal properties. They stated that intensive mixing is an

excellent technique to obtain nanocomposites with high mechanical properties in comparison to the neat polymer.

Cho et al. (2005) simulated hybrid barriers of iron filings and organo (hexadecyltrimethylammonium, HDTMA) bentonite in columns to assess the performance of the hybrid barriers. They stated that the incorporation of HDTMA-bentonite into zero valent ion (ZVI) not only can effectively retard the transport of chlorinated organic contaminants from landfill leachate or oil shock in subsurface environment, but also can expedite the reduction rate of trichloroetylene (TCE).

Jo et al. (2007) proposed a constitutive model for tensile behavior of high density polyethylene (HDPE)/clay nanocomposite foams. They suggested that the mechanical properties were improved with nanoclay loading.

Lai et al. (2007) successfully prepared environmentally friendly anticorrosive materials by effectively dispersing nanolayers of Na-montmorillonite (Na-MMT) clay into water-based polyacrylate latex. Materials were subsequently characterized by FTIR spectroscopy, XRD, TEM and Gel Permeation Chromatography (GPC). Effect of material composition on the molecular barrier, optical clarity and thermal stability were also studied by molecular permeability analysis, ultraviolet-visible transmission spectra, differential scanning calorimetry (DSC) and thermogravimetric analysis (TGA), respectively.

Wang et al. (2007) produced chitosan-organic rectorite (OREC) nanocomposite films by a casting/solvent evaporation method. The structures of the films were evaluated by Fourier Transform Infrared – Attenuated Total Reflectance (FTIR-ATR), XRD and SEM. A wide variety of material characteristics for the chitosan/OREC nanocomposite films were investigated, including the water resistance, mechanical property, optical transmittance, anti-ultraviolet capacity and bactericidal activity. Drug-controlled release studies showed a slower and more continuous release for the nanocomposite films in comparison with pure chitosan film, and the drug-delivery cumulative release was proportional to the amount and the interlayer distance of OREC. The chitosan/OREC nanocomposites films provide

promising applications as antimicrobial agents, water-barrier compounds, anti-ultraviolet compounds, and drug-controlled release carriers in antimicrobial food packaging and drug-delivery system.

Yeh et al. (2007) successfully prepared a series of poly(o-methoxyaniline) (PMA)/Na–montmorillonite (MMT) clay nanocomposite (Na–PCN) materials by in situ emulsion polymerization in the presence of inorganic nanolayers of hydrophilic Na–MMT clay with Dodecyl benzenesulfonic acid (DBSA) and Ammonium Persulfate (APS) as surfactant and initiator, respectively. The synthesized Na–PCN materials were characterized by Fourier-transformation infrared (FTIR) spectroscopy, wide-angle powder X-ray diffraction (XRD) and transmission electron microscopy (TEM). Effects of material composition on the optical properties, electrical conductivity, thermal stability and surface morphology of neat PMA and/or a series of Na–PCN materials, in the form of solution, powder-pressed pellet and fine powder, were also studied by ultraviolet–visible spectra, four-point probe technique, thermogravimetric analysis (TGA) and scanning electron microscopy (SEM), respectively.

Barbosa et al. (2007) produced Polyethylene (PE)/Brazilian clay nanocomposites and PE/commercial flame retardant systems via direct melt intercalation. The dispersion analysis and the interlayer distance of the clay particles were investigated by X-ray diffraction (XRD) and transmission electron microscopy (TEM). The flammability behavior of the obtained systems was investigated by horizontal burning tests for HB classification. It was observed that the burning rate of PE/Brazilian clay nanocomposites was significantly reduced in relation to pure PE and PE/flame retardant systems, indicating that the PE/Brazilian clay system was more efficient.

Picard et al. (2007) prepared polyamide 6-montmorilonites and examined them in terms of barrier properties and indicated that the permeation properties have been related to the clay content and dispersion. They suggested that this product can be used for barrier material in desired areas.

Ha et al. (2007) investigated the effect of montmorillonite (MMT) clay modification and concentration on the tensile behavior of MMT/epoxy nanocomposite. They stated that for unmodified MMT/epoxy nanocomposite, as the concentration of clay increased the elastic modulus increased, but the tensile strength was not affected significantly. For surface-modified MMT/epoxy nanocomposite, both the elastic modulus and the tensile strength increased as the concentration of clay increased. Tensile strength and elastic modulus of surface-modified MMT/epoxy nanocomposite were larger than those of unmodified MMT/epoxy nanocomposite, and the modification effect increased with clay concentration. This occurred due to the increased exfoliation of clays along with the improved interfacial strength by the surface modification.

Sarathi et al. (2007) studied the electrical, mechanical and thermal properties of epoxy nanocomposite materials. The thermal behaviour of the epoxy nanocomposites was analyzed by carrying out thermo gravimetric-differential thermal analysis (TG-DTA) studies. The dynamic mechanical analysis (DMA) results indicated that storage modulus of the material increases with small amount of clay in epoxy resin. The exfoliation characteristics in epoxy nanocomposites were analyzed through wide angle X-ray diffraction (WAXD) studies.

Calcagno et al. (2007) prepared PET (polyethylene) nanocomposites using montmorillonite with different organic modifiers (Cloisite 15A, 30B and 10A). TEM, WAXD and DSC were used for the characterization. Nanocomposites of intercalated and exfoliated morphologies were obtained, and an average maximum distance between the platelets was observed in the intercalated morphology. the study allowed the evaluation of the characteristics of the organic modifiers' influence on the intercalation and exfoliation processes in PET. It was observed that PET nanocomposites were intercalated and exfoliated when polar modifiers were present.

Santiago et al. (2007) synthesized a series of composite and nanocomposite hydrogels by copolymerization reaction of partially neutralized acrylic acid (SA) on bentonite micropowder (BT) using N,N-methylenebisacrylamide (MBA) as a

crosslinker and potassium persulfate as an initiator in aqueous solution. These hydrogels were then characterized by X-ray diffraction and scanning electron microscopy. Finally, the thermogravimetric analysis indicated that introduction of clay to the polymer network resulted in an increase in thermal stability.

Osagawara et al. (2006) examined the gas permeability of silicate clay (montmorillonite) particles/epoxy nanocomposites. They stated that the incorporation of increasing amounts of montmorillonite particles reduced the helium gas permeability. Based on Fick's law, gas permeation behavior of the nanocomposite was evaluated. With the increase of montmorillonite loading, gas diffusivity decreased, while gas solubility increased. It has been revealed that dispersion of nanoscale platelets in polymer is effective in improving gas barrier property.

Alexandre et al. (2006) investigated th water transport through nanocomposite-based polyamide 12/montmorillonite by permeation kinetics electron microscopy and X-ray diffraction. Intercalated and semi-exfoliated nanocomposite structures were studied. For low montmorillonite content (≤ 5%) a decrease of water permeability was obtained for both structures and mainly explained by an increase of the tortuosity (decrease of water diffusivity). However, this barrier effect is affected by other phenomena which depend on the structures: the plasticization phenomenon, the water solubility and the role played by the clay/polymer interface.

Peneva et al. (2006) investigated the flammability, microhardness and transparency of nanocomposites based on poly(ethylene-co-acrylic acid) copolymers having different concentration of acrylic acid and different molar mass, their Zn ionomer and ethylene glycidylmethacrylate copolymer as matrixes and on organically modified montmorillonite as a nanofiller. The UV spectra showed that the light transmittance of the materials does not change significantly in the presence of the clay, i.e., the nanocomposite films preserve the polymer transparency. The results have been interpreted by the intercalated structures of the nanocomposites investigated.

Sugama (2006) dispersed the clay minerals MMT into a polyphenylenesulfied (PPS) matrix. When this advanced PPS nanocomposite was used as a corrosion-preventing coating for carbon steel in a simulated geothermal environment at 300°C, a coating of 150μm thickness adequately protected the steel against hot brine-caused corrosion.

Peprnicek et al. (2006) concentrated on poly(vinyl chloride) e PVC e from the point of view of structural characterisation of PVC/clay nanocomposites through X-ray diffraction, thermogravimetric analysis and dynamic rheometric analysis. PVC plasticizer was mixed with clay, natural and organophilic, and the suspension was then compounded with other components. Two factors were followed: effect of shearing alone, and in combination with temperature. They stated that the type of filler and the method of composite preparation affect the mechanical and thermal properties of the composite, through delamination and exfoliation levels. The results showed that the thermal degradation is shifted towards higher temperatures for organophilic clays, compared to chemically untreated natural clay.

Xu et al. (2006) combined unmodified montmorillionite with Poly(ethyl acrylate) (PEA)/poly(methyl methacrylate) (PMMA) emulsion blends. The PEA/PMMA–MMT nanocomposites could be processed at low temperatures. Low temperature processing prevented the commonly observed discoloration associated with many thermoplastic nanocomposites. Differential scaning calorimetry (DSC), Small Angle X-ray Scattering (SAXS), TEM and Atomic Force Microscope (AFM) were used to study the dispersion of MMT and morphology of PEA/PMMA–MMT nanocomposites. Tensile stress, elongation at break and Young's modulus demonstrated a significant reinforcing effect of clay.

Causin et al. (2006) studied the unmodified bentonite and a specifically formulated nanocomposite based on isotactic poly(1-butene) (PB) by wide angle X-ray diffraction (WAXD), small angle X-ray scattering (SAXS), transmission electron microscopy (TEM) and polarized light optical microscopy. They also investigated the polymorphism of the polymer, and examined the interaction between PB and the silicate. Interaction between polymer and clay was studied by

TEM and SAXS also under a quantitative point of view. A significant enhancement of physical mechanical properties was observed, even though exfoliation did not occur, but just a slight intercalation and a reduction in the size of tactoids.

Ahn et al. (2006) examined the rubber toughening of nylon 6 nanocomposites prepared from an organoclay as a means of balancing stiffness/strength versus toughness/ductility. The tensile properties and impact strength of these toughened nanocomposites are discussed in terms of the MMT and rubber contents and morphology. There is a clear trade-off between stiffness/strength versus toughness/ductility.

Zheng et al. (2006) developed the relative permeability theory and the detour theory to study the effects of clay layers in the barrier properties of PCN. The findings provided guidelines for tailoring clay layer length, volume fraction and dispersion for fabricating polymer–clay nanocomposite with the unique barrier properties.

Powell and Beall (2006) reviewed the state of knowledge about polymer/clay nanocomposites and the general trends seen in selected physical properties and the theoretical basis if know for the observed changes. Data indicated that the level of exfoliation in these composites is one of the critical parameters in determining changes in properties. In addition to physical properties such as modulus and impact strength other phenomena such as improved flame retardancy and gas barrier properties are discussed.

Bertini et al. (2006) prepared polypropylene (PP)emontmorillonite nanocomposites using isotactic PP homopolymers with different rheological properties, and a maleic anhydride grafted PP. Morphology and structure of the composites were investigated by using X-ray techniques (WAXD, SAXS) and transmission electron microscopy (TEM). The thermal behaviour and degradation have been studied by means of differential scanning calorimetry (DSC) and thermogravimetric analysis (TGA). The incorporation of the montmorillonite

improves the thermal stability in air atmosphere of all the investigated PPs because of a physical barrier effect of the silicate layers.

Katti et al. (2006) evaluated molecular interactions in organically modified clay and polymer clay nanocomposite using a combination of experimental (photoacoustic FTIR, XRD) and computational (molecular dynamics (MD)) techniques. The FTIR data revealed hydrogen bond and ionic bond interaction between functional end groups of organic modifier and surface oxygen of interlayer clay sheet lying in the organically modified clay; and, the hydrogen bond formation between intercalated polymer and organic modifier and surface oxygen of clay sheet lying in the interlayer clay gallery in the polymer clay nanocomposite. In this work they reported the nature of interactions between clay and polymer, clay and organic modifier in polymer–clay nanocomposites through experiments and molecular dynamics simulations.

Paul et al. (2005) stated the importance of understanding the interlayer swelling and molecular packing in organoclays to the formation and design of polymer nanocomposites. The paper presents recent experimental and molecular simulation studies on a variety of organoclays that show a linear relationship between the increase of *d*-spacing and the mass ratio between organic and clay. A denser molecular packing is observed in organoclays containing surfactants with hydroxyl–ethyl units. Moreover, their simulation results showed that the head (nitrogen) groups are essentially attached to the clay surface while the long hydrocarbon chains tend to adopt a layering structure with disordered conformation which contrasts with the previous assumptions of either the chains lying parallel to the clay surface or being tilted at rather precise angles.

Rehab and Salahuddin (2005) synthesized polyurethane organoclay nano-composites via in situ polymerization method. The organoclay has been prepared by intercalation of diethanolamine or triethanolamine into montmorillonite clay (MMT) through ion exchange process. The nanocomposites with dispersed structure of MMT was obtained as evidence by scanning electron microscope and X-ray diffraction (XRD). The results shows broaden with low intense and shift of the peak

characteristic to *d*-spacing to smaller 2Θ and the MMT is dispersed homogeneously in the polymer matrix. Also, the TGA showed that the nanocomposites have higher decomposition temperature in comparison with the pristine polyurethane.

Jiang et al. (2005) prepared nylon6/clay nanocomposite by mixing organized montmorillonite with nylon6. Solvent permeation resistance of the nano-composite is measured to estimate the resistance to solvent permeation. Their investigation indicated that the crystalline property of nylon6 has a strong impact on the sorption and diffusion of small molecules in the polymer. The improvement in solvent barrier properties of nylon6/clay nanocomposite is attributable to incorporation of an impermeable phase such as the layered silicate, improvement in crystallinity and decrease of crystalline dimension, which are evidenced by XRD, AFM, DSC and polarized optical microscopy (POM) studies.

Kim et al. (2003) prepared water-borne polyurethane-clay nanocomposites The particle size of emulsion was measured and the morphology of these nanocomposites was observed by transmission electron microscope, where the effectively intercalated or exfoliated organoclay was observed. The reinforcing effects of organoclay in mechanical properties of these nanocomposites were examined by dynamic mechanical and tensile tests, and the Shore A hardness was measured. Enhanced thermal and water resistance and marginal reduction in transparency of these nanocomposites were observed compared with pristine polymer.

Delozier et al. (2002) prepared polyimide organoclay hybrids. The resulting nanocomposite films containing %3-8 by weight of organoclay were characterized by differential scaning calorimetry (DSC), dynamic thermogravimetric analysis (TGA), transmission electron microscopy (TEM), X-ray diffraction (XRD) and thin film tensile properties. A significant degree of dispersion was observed in the nanocomposite films of the amide acid and imide. They stated that the polyimide/organoclay hybrid films exhibited higher room temperature tensile moduli and lower strength and elongation to break than the control films.

CHAPTER 2

MATERIALS AND METHODOLOGY

2.1. Raw materials

2.1.1. Bentonites

There are three materials used in this study. The first and second one is Hançılı bentonite (B-1 and B-2), and the third one is a standard Wyoming bentonite SWy-1 (B-3) obtained from the Clay Minerals Society

Bentonite samples (B-1, B-2) were obtained from ÇANBENSAN Trade & Industury Co. Çankırı. The first sample (B-1) is an unmodified yellow bentonite, and it is mainly composed of Ca-montmorillonite (Appendix F). Quartz, plagioclase and gypsum are also present as impurities in the sample.

The second sample (B-2) is the grey bentonite which is modified from B-1. The difference between these two materials is that soda ($NaCO_3$) is added to B-2 about 3% percent by weight for activation to improve the quality of the product. It is mainly composed of dioctahedral Na-montmorillonite (Appendix F). In this sample the impurities are the same as B-1.

The bentonite samples B-1 and B-2 are belong to the bentonite-bearing mudstone in Hançılı formation of Early Pliocene age (Figure 9). Hançılı formation is in the Kalecik-Hasayaz basin. This basin is separated from the rest of the Çankırı basin during Oligocene as a trough for molasic sedimentation. The basin fill consists of the Late Miocene aged, fluvial Aslantaş formation and Lower Pliocene aged, lacustrine Hançılı formation (Türkmenoğlu et al., 1994).

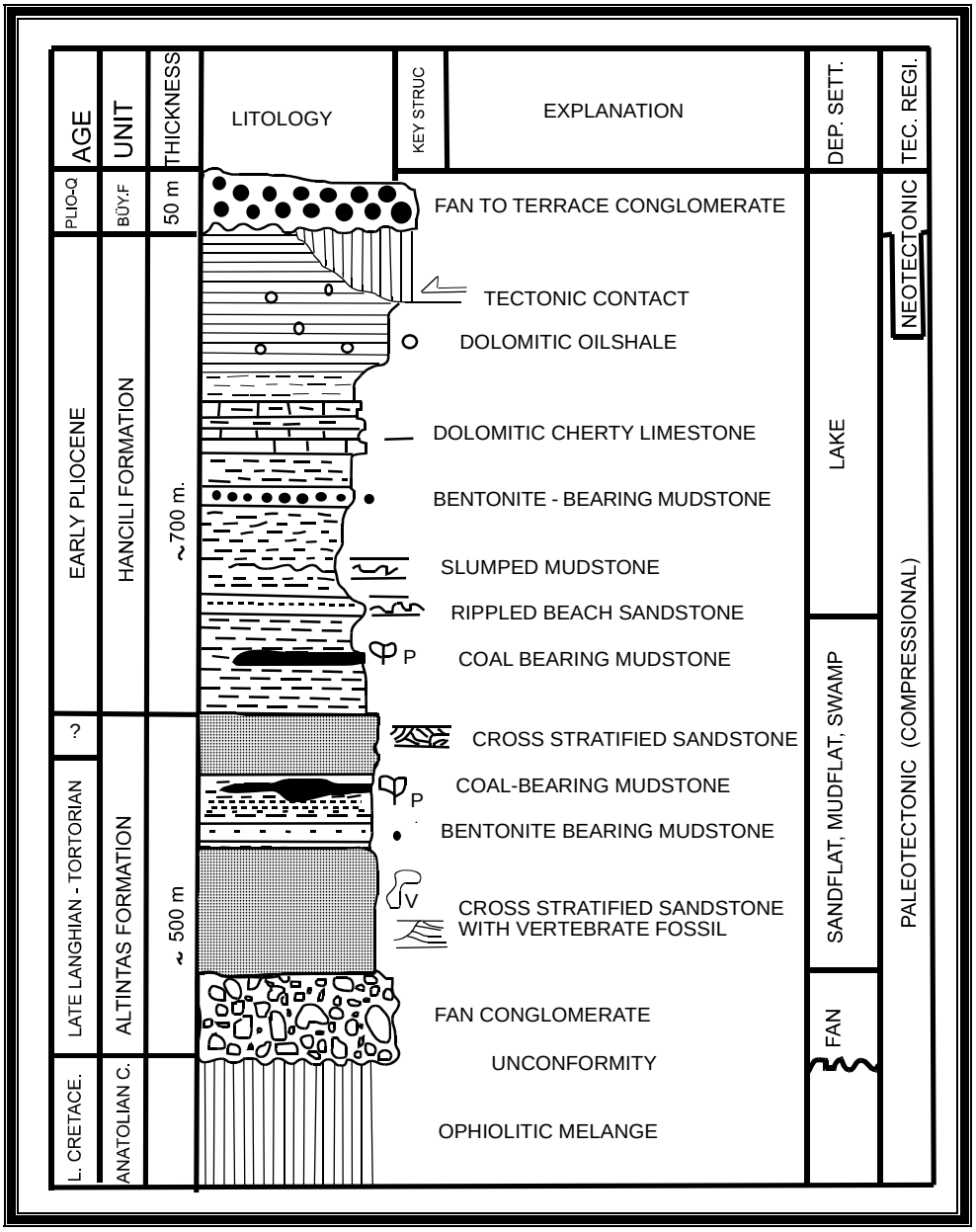

Figure 9. Generalized columnar section of Kalecik-Hasayaz troughs (Koçyiğit et al., 1995)

Türkmenoğlu et al. (1995) stated that this basin is filled with fluvial and lacustrine environment sediments and pyroclastic material originated from the Galatian volcanism. The sedimentary section is generally an alternation of blue-green mudstone and thinly laminated limestone with occasional sandstone lenses. The clay minerals are detritic in origin. Smectite is originated from volcanic (pyroclastic) rocks, while chlorite and illite are derived from ophiolitic and metamorphic sources. The latters also indicate arid-semiarid climate and authigenic

calcite-dolomite-analcime association signifies a saline-alkaline environment (Türkmenoğlu et al., 1995).

The standard bentonite SWy-1 (standard clay sample obtained from Mineral Society, USA) is used to achieve reliability in the experiments which was named as B-3. It is composed of largely sodium montmorillonite and it belongs to Newcastle formation of Cretaceous age. Its location is Crook County in the state of Wyoming, USA (Figure 10).

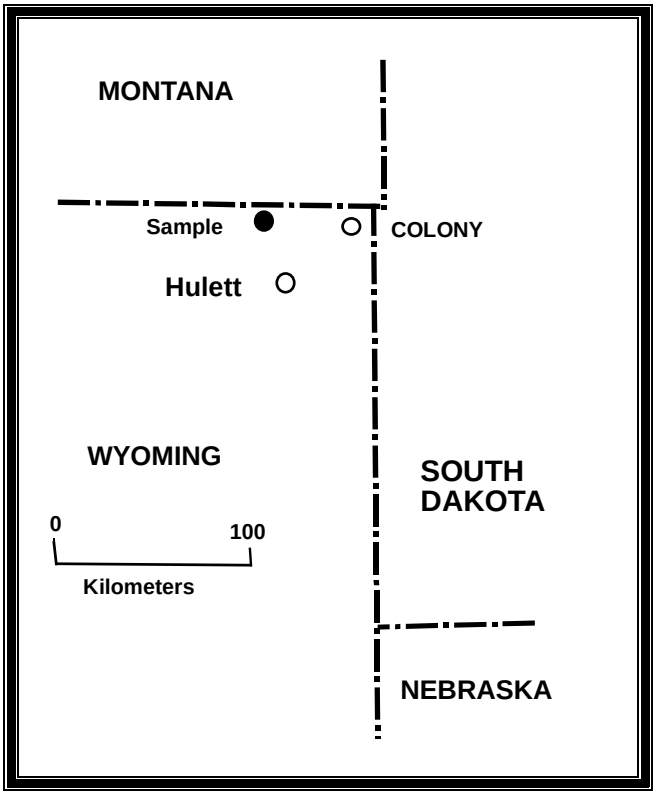

Figure 10. Map of Northeastern Wyoming showing location of Wyoming montmorillonite sample (Van Olphen et. Al., 1979).

Newcastle formation (Figure 11) is composed of sandstone, at places cross-bedded, and interbedded with siltstone, sandy shale, carbonaceous shale, bentonite and impure lignite. Davis (1965), Knetchel (1962), Osterwald (1966) and Slaughter (1965) argue that these bentonites resulted from volcanic ash fall into the sea. The volcanism was thought to be associated with the emplacement of the Idaho batholith. Glass shards attest to the volcanic origin, and sedimentary features in the

Newcastle formation denote the depositional environment. Slaughter and Early (1965) suggest that the marine environment could account for the exchange cation when the replacement series suggest it should have been supplanted by calcium and magnesium. Sodium-rich solutions must have passed through the deposit at some time after alteration. Therefore, it became a sodium smectite rich bentonite.

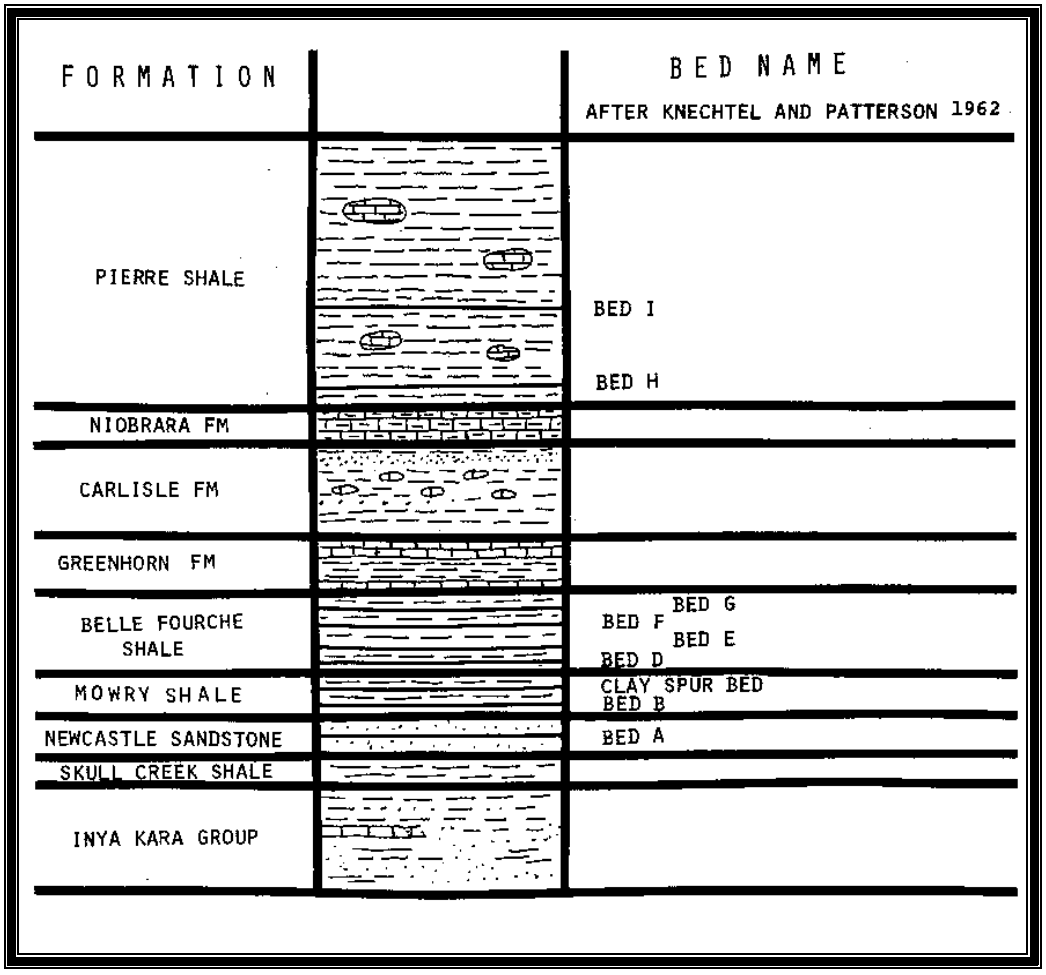

Figure 11. Bentonite beds in the Cretaceous of Wyoming (Van Olphen et. Al., 1979).

2.1.2. Sand

The sand is obtained from the General Directoriate of State Airports Authority, Construction and Real Estate Department, Ankara. It is brought from Murat River, Elazığ. It is the transported alluvions of Murat River (sedimentary origin) and composed of quartz, plagioclase, calcite, clinopyroxene and fossiliferous limestone fragments (Figure 12).

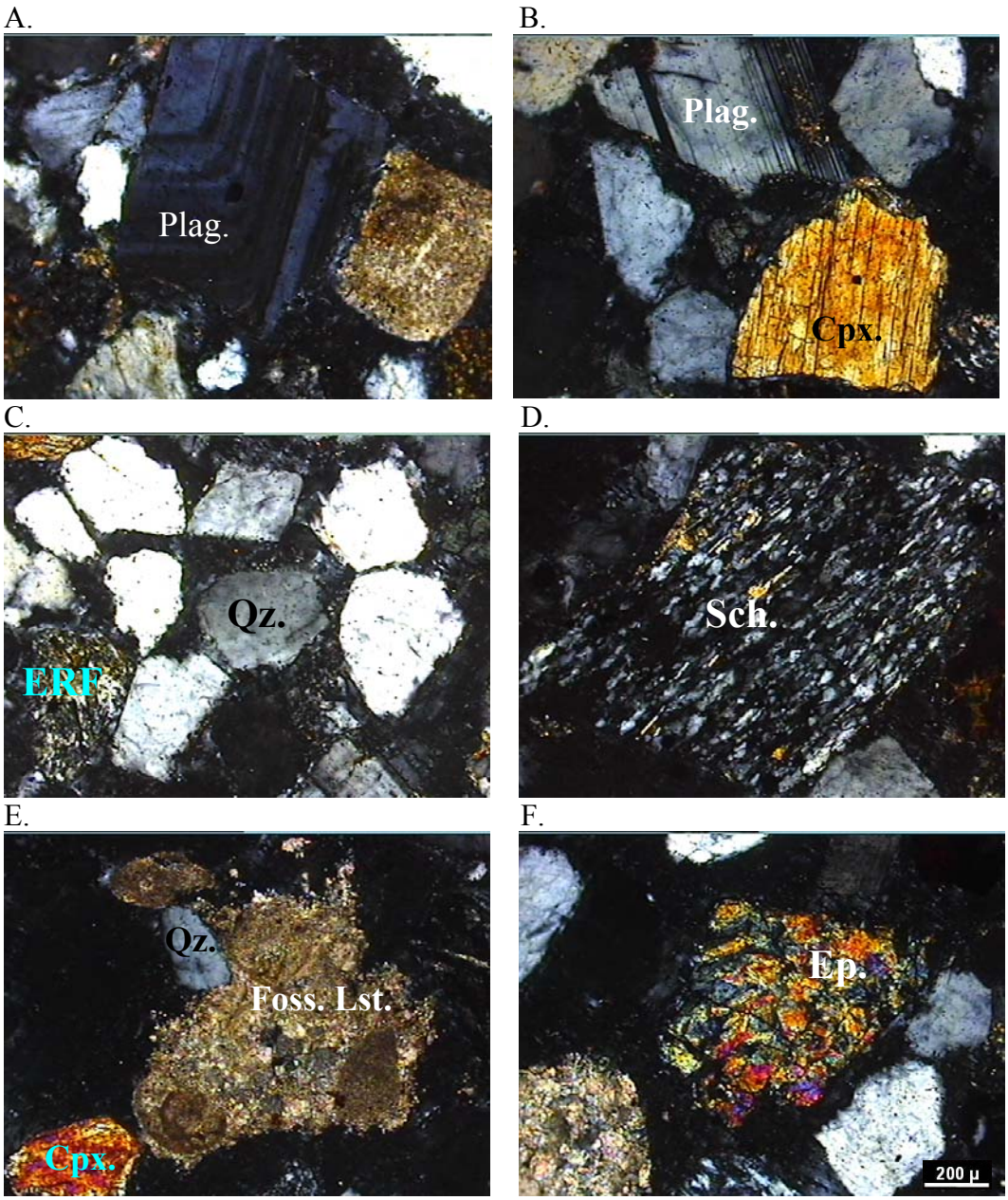

Figure 12. Thin sections (XPL) of sand sample used in permeability test (Plag.: Plagioclase, Cpx: Clinopyroxene, ERF: Extrusive Igneous Rock Fragments, Qz: Quartz, Sch: Schist, Foss. Lst: Fossiliferous Limestone, Ep: Epidote).

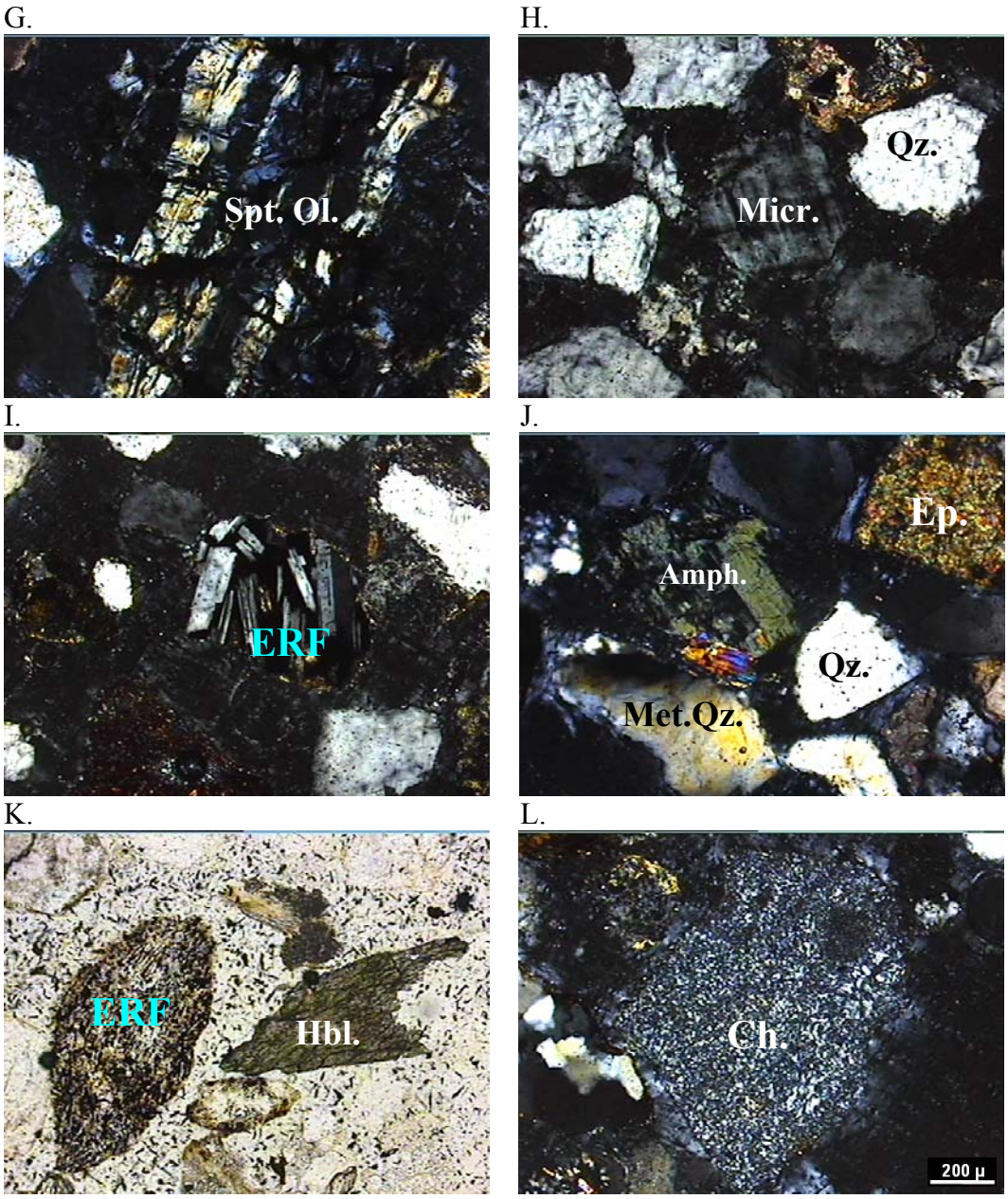

Figure 12 (continued). Thin sections (XPL except for K, which photo was taken using PPL) of sand sample used in permeability test (Spt.Ol: Serpentinized Olivine, Micr: Microcline ERF: Extrusive Igneous Rock Fragments, Qz: Quartz, Ep: Epidote, Met.Qz.: Metamorphic Quartz, Amph.: Amphibole, Ch: Chert, Hbl: Hornblende).

M.

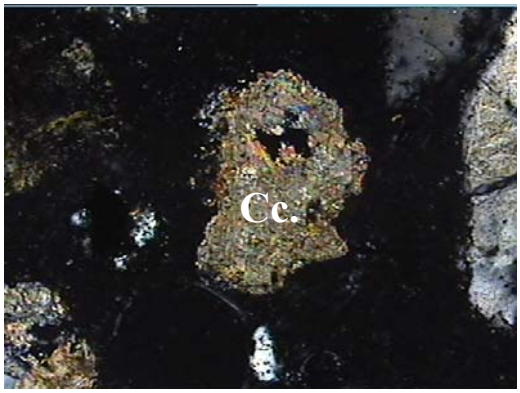

N.

Figure 12 (continued). Thin sections (XPL except for K, which photo was taken using PPL) of sand sample used in permeability test. (Cc: Calcite, Hyp. RF: Hypabyssal Igneous Rock Fragments).

The particle size distribution of sand was determined through sieve analysis in accordance with ASTM D422-63 (2002). The particle size distribution data is given in Table 3 and grain size distribution curve is given in Figure 13. The coefficient of uniformity C_u and coefficient of curvature C_c, defined as $C_u = D_{60}/D_{10}$ and $C_c = (D_{30})^2/D_{10}*D_{60}$, are calculated based on grain size distribution curve.(Ada, 2007)

Table 3. Grain size distribution data for sand material (Ada, 2007).

Sieve No.	Sieve Opening (mm)	Percent Passing (%)
4	4.75	100.00
10	2.00	99.95
20	0.85	75.33
40	0.425	39.62
60	0.25	15.17
140	0.106	3.07
200	0.075	1.64
Pan	-----	-----

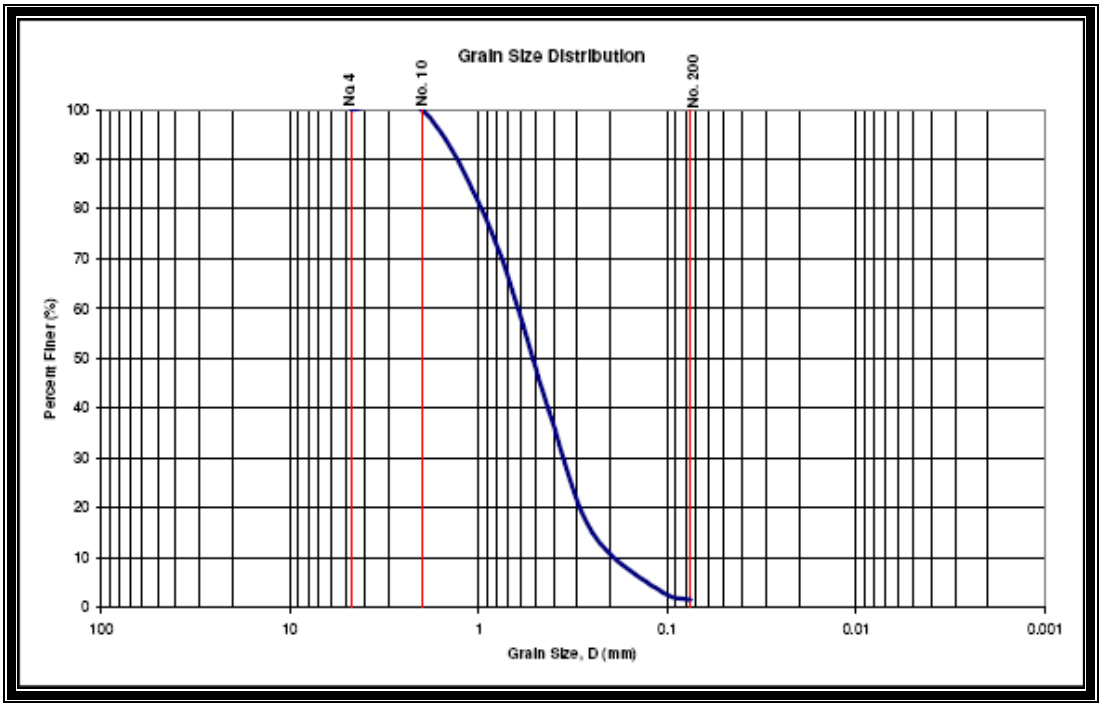

Figure 13. Grain size distribution curve of the sand material (Ada, 2007).

The sand was classified as poorly graded (SP) fine to medium sand (Figure 14) according to Unified Soil Classification System (USCS) in accordance with ASTM D2487-06 (Ada, 2007).

Particle size distribution	Class
ASTMD 422-63	USCS
D_{10} = 0.23 mm D_{30} = 0.38 mm D_{60} = 0.65 mm C_c =0.96 C_u =2.82	SP, fine to medium sand

Figure 14. Classification of sand material according to USCS (Ada, 2007).

Sand is sieved through <2 mm (no:10) sieve to bring the grains to sand particle size. The sieved sand is used for permeability tests.

2.2. Chemicals

2.2.1. Hexadecyltrimethylammonium-bromide Salt

When it is solved in the water, Hexadecyltrimethylammonium-bromide salt is separated into its ions $HDTMA^+$ and Br^-. $HDTMA^+$ is a cationic surfactant (Fig 15). It belongs to the family of quaternary ammonium cations. As mentioned previously, organoclays are often prepared using quarternary ammonium cations of the general form $[(CH_3)_3NR]^+$ or $[(CH_3)_2NRR`]^+$ where R and R` are hydrocarbon groups (Inam, 2006). In the studies, $HDTMA^+$ tail group has been found to have higher affinity for the exchange sites on clays relative to other surfactants (Haggerty and Bowman, 1994; Li 1999).

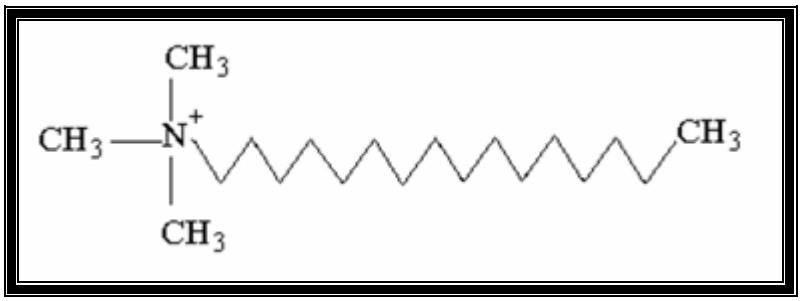

Figure 15. Hexadecyltrimethylammonium ion (R=$C_{16}H_{33}$) (Inam, 2006).

2.2.2. Polyacrylamide

Polyacrylamide is an acrylate polymer (-$CH_2CHCONH_2$-) formed from acrylamide subunits that is readily crosslinked (Figure 16). It is highly water absorbent, hard and brittle. The non-ionic form of polyacrylamide has found an important role in the potable water treatment industry. Trivalent metal salts like ferric chloride and ammonium chloride are bridged by the long polymer chains of polyacrylamide (Inyang and Bae, 2005). The polymer was produced in an aqueous medium with in-situ polymerization by free radical reaction (Figure 17).

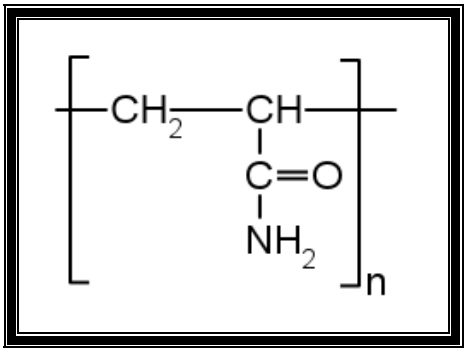

Figure 16. Sketch view of polyacrylamide (Inyang and Bae, 2005).

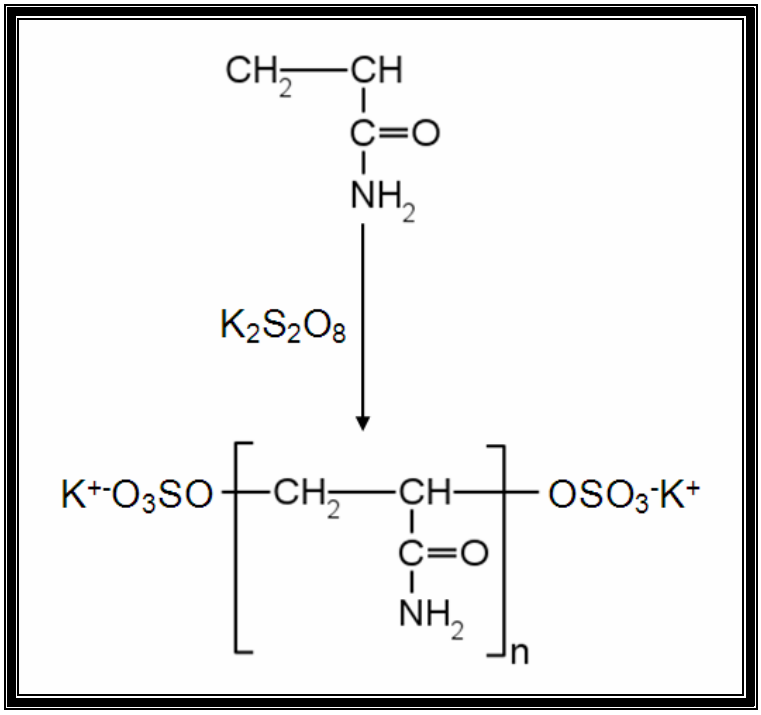

Figure 17. General radical reaction of polyacrylamide with $K_2S_2O_8$

The radical which initiates the polymerization process is potassium persulfate salt ($K_2S_2O_8$). The seperation of persulfate anion to sulfate anions is achieved with trivalent iron cations of ferric chloride $FeCl_3$. Then the polymerization of acrylamide monomers starts (Eqn. 2).

$$S_2O_8^{2-} \rightarrow 2SO_4^- \cdot$$
$$SO_4^- \cdot + Monomer \rightarrow SO_4^- Monomer \cdot \quad \text{.....(Eqn. 2)}$$

Primary radicals generated by the decomposition of initiator were added to monomer to yield primary propogating radicals (Taşkın 2007). Free radical polymerization consists of the elementary reactions of initiation, propagation and termination. Termination refers to the bimolecular reaction of propogating radicals by combination or disproportionation that leads to the deactivation of propagating radical chain ends (Matyjaszewski et al., 2002).

2.3. Methods

2.3.1. Methylene Blue Adsorption (Cation Exchange Capacity) Test

Methylene blue adsorption test is one of the easiest and reliable tests that is used to calculate the cation exchange capacity (CEC) of clay minerals. The spot method employed is a simple titration technique (Appendix A) (Çokça, 1991). If significant amount of methylene blue dye is adsorbed by the soil or ground rock material, this may indicate the presence of swelling clay minerals, although there exists other substances that also adsorbs methylene blue. Low values of adsorption generally indicate low swelling capacity. In other words, low values reveal the presence of either a very low amount of swelling clay or certain amount of swelling clay.

The first experiments were done with 30 gr of clay sample and one experiment took 12 hours to complete and get a correct result. In order to prevent time waste, the second and the third tests of each sample were performed with 7,5 gr of clay sample. The test was performed in METU Geological Engineering Department, Engineering Geology Laboratory.

2.3.2. Swelling Capacity Test

Swelling capacity is simply defined as the volume of soil sample (ml) in 100 ml water for 24 hours. Swelling capacity is used to determine the rate of increase in volume (ml) of a soil sample when hydrated. It is a simple and common test to understand if sample contains swelling clay (Appendix B) The test was performed in METU Geological Engineering Department, Clay Mineralogy Laboratory.

2.3.3. Preparation of Organoclay

The preparation of organoclays is a hard and enduring process. The samples were put into centrifuge tubes as 2 gr samples and shaken laterally for one day with

a laboratory shaker. Approximately 130 gr of B-1 sample corresponding to 65 centrifuge tubes was treated with HDTMA-Br solution and each tube contained 0.88 gr HDTMA-Br salt solved in 15 ml distilled water (See Appendix C). The test was performed in METU Geological Engineering Department, Clay Mineralogy Laboratory.

2.3.4. Preparation of Nanocomposite

The production technique of nanocomposite preparation is in-situ intercalative polymerization by a free radical (Appendix D) Potassium persulfate salt as free radical, initiates the reaction and the monomers are polymerized by the bridging agent named as ferric chloride ($FeCl_3$). 6 samples were produced in the order of 7, 17, 25, 30, 40 and 50% w/w (by mass) polymer content (for example 7 gr of polymer- 93 gr of clay in 7% case). After the observation of intercalation and partly exfoliation of clay particles into polymer matrix from the XRD diffractograms, 25% w/w ratio of polymer-clay was selected for economical reasons. Finally, 130 gr. of clay-polymer nanocomposite was produced. When mixed with water, this product had a plastic property. The test was performed in METU Geological Engineering Department, Clay Mineralogy Laboratory.

2.3.5. XRD Measurements

XRD measurements were done in METU Physics Department, X-ray Laboratory with a Rigaku Miniflex 3500 X-ray instrument. The voltage and current values were 30 kV and 15 mA respectively. The diffractograms were measured between 2 and 40 2theta degrees. Scan speed was 2 deg./min and sampling width was 0.02 deg. The three bentonites (B-1, 2 and 3) and organoclays produced from those bentonites (OB-1, 2 and 3) were powdered and placed randomly into the holder of the instrument. The X-ray diffractograms were named as “random”. They were placed into a glass lamella immediately after the centrifugation and air-dried for about one day and X-ray diffractograms were taken. The X-ray diffractograms of those sample were named as “AD”.

The samples were placed onto glass lamellas and air-dried. Then they were put into a dessicator containing ethylene glycol. The samples were ethylene glycol solvated and kept in the dessicator for a half day at 60 C°. Those samples were named as "EG". Later on, the samples were placed onto glass lamellas and heated up to 300 C° for 1 hr. in an oven and named as "300". Finally, the samples were again placed onto glass lamellas and heated up to 550 C° for 1 hr. and named as "550". Eventually, 5 diffractograms were obtained from each sample named as Random, AD, EG, 300 and 500 (Appendix F and G).

The X-ray diffractograms of produced clay-polymer nanocomposites were taken randomly and named as "CPN". For example, a nanocomposite containing 30% w/w polymer was named as CPN 30. All the XRD samples were prepared in METU, Gelogical Engineering Department, Clay Mineralogy Laboratory (Appendix H).

2.3.6. Thin Section Preparation

Thin section was prepared in METU Geological Engineering Department, Thin Section Preparation Laboratory by technician Orhan Karaman. The photographs of this thin section was taken in Geological Engineering Department, METU with a Nikon polarized microscope under polarized light (xpl) with 10 times magnification.

2.3.7. Preparation of Samples for Permeability Test

There were three samples prepared for permeability tests. First one contains 1200 gr of only sand sieved through <2 mm mesh and named as S-1. Second one contains 130 gr. of B-1 (Unmodified yellow Hançılı bentonite) and 1070 gr. of sand (sieved through <2 mm mesh) and named as S-2. The sample was mixed mechanically with a laboratory mixer at 100 rpm for 5 minutes. Finally the third

one contains 130 gr. of prepared clay-polymer nanocomposite (containing 25% w/w polymer) and 1070 gr. of sand (sieved through <2 mm mesh) and named as S-3. This sample was also mechanically mixed with a mixer at 100 rpm for 5 minutes.

The relative amounts (and also ratios) of sand, clay and nanocomposite in the samples were taken similar to a commercial product containing nanocomposites named as Trisoplast®. Trisoplast® is a mixture of sand, bentonite and polymer. 130 kg of bentonite and 2.6 kg of polymer are mixed with 1000 kg. of sand and 1132.6 kg. of Trisoplast® is produced (Trisoplast, 2007). As a result of this, about 1 kg. (1070 gr.) of sand was mixed with 130 gr of B-1 in the second sample (S-2); and 130 gr. of produced nanocomposite in the third sample (S-3) to produce 1200 gr. (about 1133 gr.) of the commercial sample. The samples were prepared in METU, Geological Engineering Department, Engineering Geology Laboratory.

The permeability tests were done in Hacettepe University, International Research and Application Center for Karst Water Resources, Applied Hydrogeology Laboratory, Ankara.

Test method for the samples S2 (Sand+Bentonite) and S3 is falling head USGS- Johnson type permeameter. Because the sample S1 contains only sand a constant head USGS- Johnson type permeameter method was used for this sample. All the samples were tested according to ASTM- D5084-90 “Test Standard for the Measurement of Hydraulic Conductivity of Saturated Porous Materials Using a Flexible Wall Permeameter”.

Figure 18 describes the generalized flow chart of this study. First, three samples were chosen as previously defined under “Materials” subtitle. Their physicochemical characteristics were defined with swelling capacity, methylene blue adsorption tests and XRD measurements. From these bentonite samples, organoclays named as OB1, OB2 and OB3 were produced. Later, these samples were determined to have quite similar characteristics and OB1 was selected for the preparation of nanocomposite. Single sample was used for both no district variations between the starting B-1, B-2, B-3 samples was seen and for time-saving

purpose. Clay-polymer nanocomposite was produced from OB1. This was mixed with sand to measure permeability.

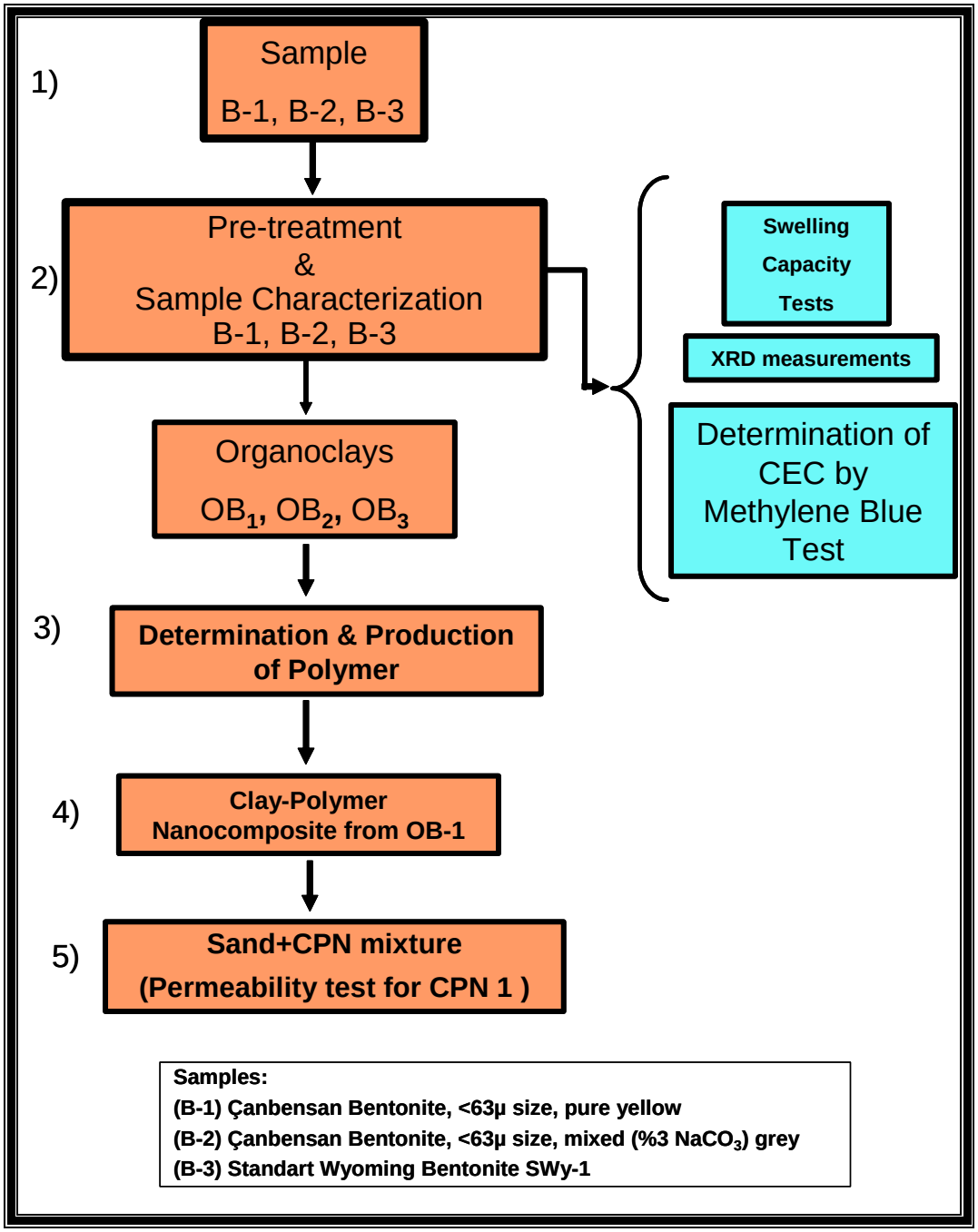

Figure 18. Generalized flow chart of the study

CHAPTER 3

RESULTS AND DISCUSSION

3.1. Results

3.1.1. Swelling Capacity Test

Table 4 and Figure 19 represents the swelling capacity test values of the samples named as B1, B2 and B3. The tests were performed three times to achieve reliability. In Table 3 the swelling capacity values of the sample B-1 are 16 ml. for first experiment, 18 (ml/100 ml). for the second, and finally 16 ml. for the third experiment. For B-2, the swelling capacity values are 20, 19 and 18 ml. for Test 1, Test 2 and Test 3, and the swelling capacity values for B-3 are 30, 30 and 28 (ml/100 ml). for Test 1, Test 2 and Test 3.

Table 4. Measured swelling capacity values for the samples (ml/100 ml).

Sample	Test-1	Test-2	Test-3	Average
B-1	16	18	16	16.67
B-2	20	19	18	19.00
B-3	30	30	28	29.33

The average values of swelling capacity tests for the samples are 16.67, 19.00 and 29.33 (ml/100ml) for B-1, B-2 and B-3 respectively. Figure 17 is a graphical representation of the swelling capacity test results of the samples B-1, B-2

and B-3. It can be seen from the graph that B-3 has the highest swelling capacity value, and B-1 has the lowest swelling capacity.

These values indicate that swelling clay minerals are present in these samples. The reason why B-2 has a higher swelling capacity value than B-1 is that B-2 was activated with soda ash (Na_2CO_3) and the clay minerals in the sample B-2 adsorbs water more than B-1. Higher quantities in B-1 and B-2 resulted in a decrease in the swelling capacity values of the samples compared to B-3. The swelling behaviour of the samples was observed by naked eye after one day. The volume of samples were doubled after 24 hours.

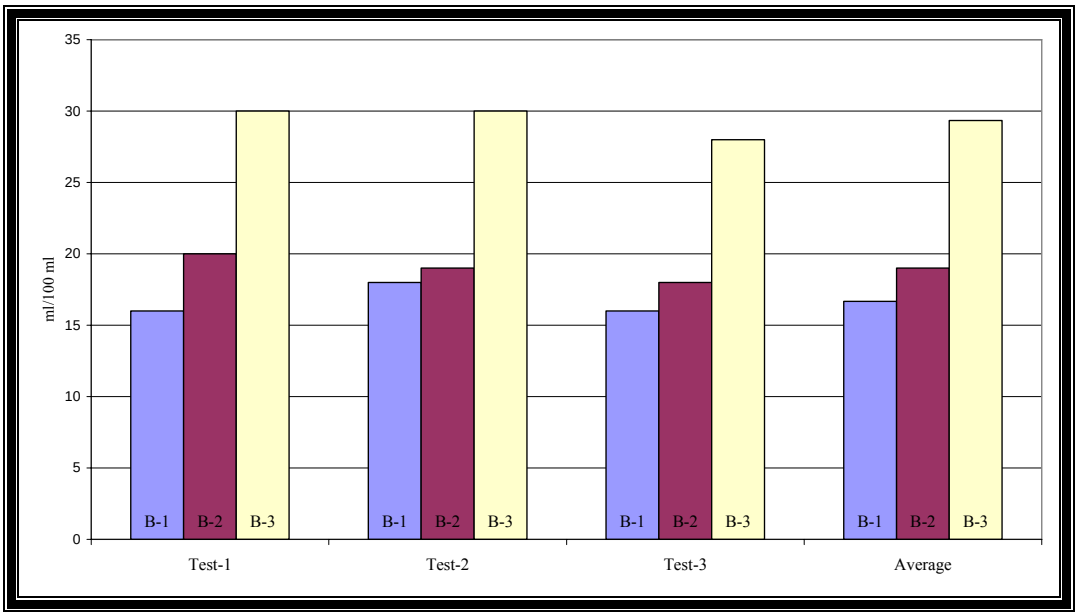

Figure 19. Comparison of swelling capacity values of the samples.

3.1.2 Methylene Blue Adsorption Test

Table 5 represents the MBA (methylene blue adsorption) and CEC (cation exchange capacity) values calculated from the MBA values of the three samples (B1, B2, B3). These tests were also performed three times to achieve reliability. In Test 1, 30 gr of clay sample was used and in Test 2 and Test 3, 7.5 gr of clay sample was used in order to prevent waste of time.

The methylene blue adsorbtion (MBA) values of the sample B-1 are 780 ml for 30 gr of clay sample and 200 and 195 ml for 7.5 gr of clay sample. For B-2, the values are 1100 ml for 30 gr of clay sample, 195 and 160 ml for 7.5 gr of clay sample. Finally, for B-3, 1000 ml for 30 gr of clay sample, 230 and 220 ml for 7.5 gr of clay sample.

Table 5. Determined CEC values of the samples.

Sample	MBA Value (ml)			CEC Value (meq/100 gr)			Average CEC
	Test 1	Test 2	Test 3	Test 1	Test 2	Test 3	
B-1	780	200	195	59.3	60.8	59.2	59.77
B-2	1100	195	160	83.6	59.3	48.7	63.87
B-3	1000	230	220	75.9	69.7	66.7	70.77

The results indicate that B-3 has the highest CEC among three (70.77 meq/100gr). Then B2 has the second highest CEC value (63.87 meq/100gr) and finally B1 has the lowest value (59.77 meq/100 gr). The CEC value of Swy-1 (B-3) is 76.4 meq/100 g as given in literature (Van Olphen, 1979). So, it can be seen that the Methylene Blue test used in this study is a reliable method depending on the CEC values of the samples. These CEC values show that montmorillonite is present in all of the samples. Montmorillonite present in all these samples has the highest CEC value among clay minerals (Grim, 1968).

The reason why these results were achieved is because of the sample B3 is the standard SWy-1 Wyoming bentonite with highest concentration of (> 95%) montmorillonite (Van Olphen, 1979). B2 sample was enriched with soda (thus Na^+ cation) and it was activated resulting in a higher CEC than B1 (unmodified yellow bentonite). Moreover, some impurities such as quartz, feldspar and calcite are present in samples B1 and B2. This situation may have been resulted from a decrease in CEC of the samples compared to B3 (Standard Wyoming bentonite).

This test was performed to learn the CEC of the samples and to determine the amount of HDTMA-Br salt which had to be added to the unmodified bentonites for the organoclay production.

3.1.3. X-Ray Diffraction Analyses of Bentonites

The X-ray diffraction results of the selected samples (Appendix F) show that they contain mostly montmorillonite at with d(001) reflection 14.01 Ångstrom Ca-Montmorillonite peak in B1, at 12.54 Ångstrom Na-montmorillonite peak in B2 and 12.23 Ångstrom peak Na-montmorillonite in B3. Also some organophillic clays exhibit 23.98 Ångstrom peak due to the natural organic content of clay mineral (B-3 AD). Some organic cations originated from those organic components may have substituted cations such as Ca and Na present in the interlayer spaces of montmorillonites. (Oral communication with Prof. Dr. Yűksel Sarıkaya).

The XRD results of air dried (AD), ethylene glycolated (EG), heated to 300 C˚ (300) and 550 C˚ (550) of B-1 B-2 and B-3 show that these samples mainly contain Ca-, Na-montmorillonite and little amounts of natural organophillic montmorillonites, plagioclase, quartz and 1:1 illite/smectite mixed layer formation. When the samples adsorb etyhlene glycol their interlayer space increases and their mineralogy is preserved upon heating of 300 and 550 C˚ (see Appendix F).

3.1.4. X-Ray Diffraction Analyses of Organoclays

The samples produced from B1, B2 and B3 were named as OB1, OB2 and OB3 (Organobentonite). The X-ray diffraction patterns (Appendix G) show that organoclay structure is formed and the peaks appear at 43.21 and 21.63 Ångstrom in B-1, 40.12 and 19.88 Ångstrom in B-2 and finally 42.84 and 19.97 Ångstrom in B-3. These results show that two distinct layered organoclay structure is formed. Pinnavaia et al. (1999) proposed a model for these situations and stated that the

surfactant can be interpositioned in different ways between the two layers of clay mineral (Figure 4). This may be the reason of the formation of two distinct peaks and their reflectance to the XRD patterns. This is undoubtful that all the clay minerals in the sample became organophilic. The peaks of pure montmorillonite were disappeared and shifted towards leftside indicating a swelling behaviour as it can be seen in the XRD patterns. In addition to this, when they adsorb ethylene glycol solution they swell less than pure montmorillonites present in B1, B2, and B3 samples and their structure did not change upon heating 300 and 550 C°.

The results in XRD diffractograms show that all the clay minerals substituted their inorganic cations with the organic cation $HDTMA^+$. The aim of organoclay production is to trigger the mechanism of exfoliation and enhance the exfoliation of clay platelets into polymer matrix.

3.1.5. X-Ray Diffraction Analyses of Nanocomposites

The X-ray diffractograms of prepared clay-polymer nanocomposites (CPN) show that (Appendix F) the clay platelets were intercalated and "partly" exfoliated. The polymers entered into the interlayer galleries of organoclays and filled those pore spaces as discussed in the previous sections (Figure 5). The polymers broke the hexadecyltrimethylammonium ($HDTMA^+$) chains and caused the clay minerals disperse into the polymer and little amount of clay platelets were exfoliated into the matrix. The peaks at 43.21 and 21.63 Ångstrom disappeared and the intensity of the peaks were decreased as the polymer content of nanocomposite increased. It can be seen from the X-Ray diffractograms that the intensity values decreased and some peaks are disappeared at some polymer ratios as the polymer content increased. For example, the 37.40 Ångstrom peak in CPN 30 (30% polymer+ 70% clay) was disappeared in CPN 40. Moreover, the peak at 18.70 Ångstrom in CPN 40 was disappeared in CPN 50.

Depending on these results, it can be estimated that one or both of the peaks disappears depending on a specific ratio of clay and polymer. That means that the

behaviour of exfoliation and intercalation mechanism changes as the polymer content changes.

The clay-polymer nanocomposite containing 25% w/w was chosen considering the prices of acrylamide monomer (57.5 TL/kg) and bentonite. The lower the amount of monomer used, the more economical the nanocomposite is. In addition to this, achievement of intercalation and exfoliation was considered in the selection of tested nanocomposite.

3.1.6. Permeability Test Results

Table 6 represents the hydraulic conductivity test results of the samples S1, S2 and S3. The hydraulic conductivity values of the samples are $9.7*10^{-5}$ m/s for S1 (sand), $1.26*10^{-8}$ m/s for S2 (sand+bentonite) and $6.4*10^{-9}$ m/s for S3 (sand+nanocomposite).

Table 6. Hydraulic conductivity test results for the samples.

Lab. No.	Sample	Hydraulic Conductivity (m/s)
HC-07-112	S1	9,70E-05
HC-07-113	S2	1,26E-08
HC-07-114	S3	6,4E-09

S1: 1200 gr. Sand

S2: 1070 gr sand+130 gr B1

S3: 1070 gr sand + 130 gr CPN 25%

Depending on these results, bentonite addition into sand decreases the hydraulic conductivity of selected material and nanocomposite addition decreases the hydraulic conductivity of selected material more than bentonite addition.

The comparison of Hydraulic Conductivities of samples were done by dividing the Hydraulic Conductivities of S1 to S2, of S1 to S3, and finally S2 to S3. The hydraulic conductivity value for S2 is 7698.4 times smaller than S1 (Figure 20). This indicates that the hydraulic conductivity of sample drastically decreases with the addition of (approximately 10%) bentonite.

The hydraulic conductivity value for S3 is 15156.2 times smaller than S1 while it is 1.968 times smaller than S2. This is the reason for the intercalation of clay samples with organic cations and filling of polymer chains into the interlayer galleries of organoclays resulting in a decreased permeability and little amount of exfoliation of clay platelets into polymer matrix.

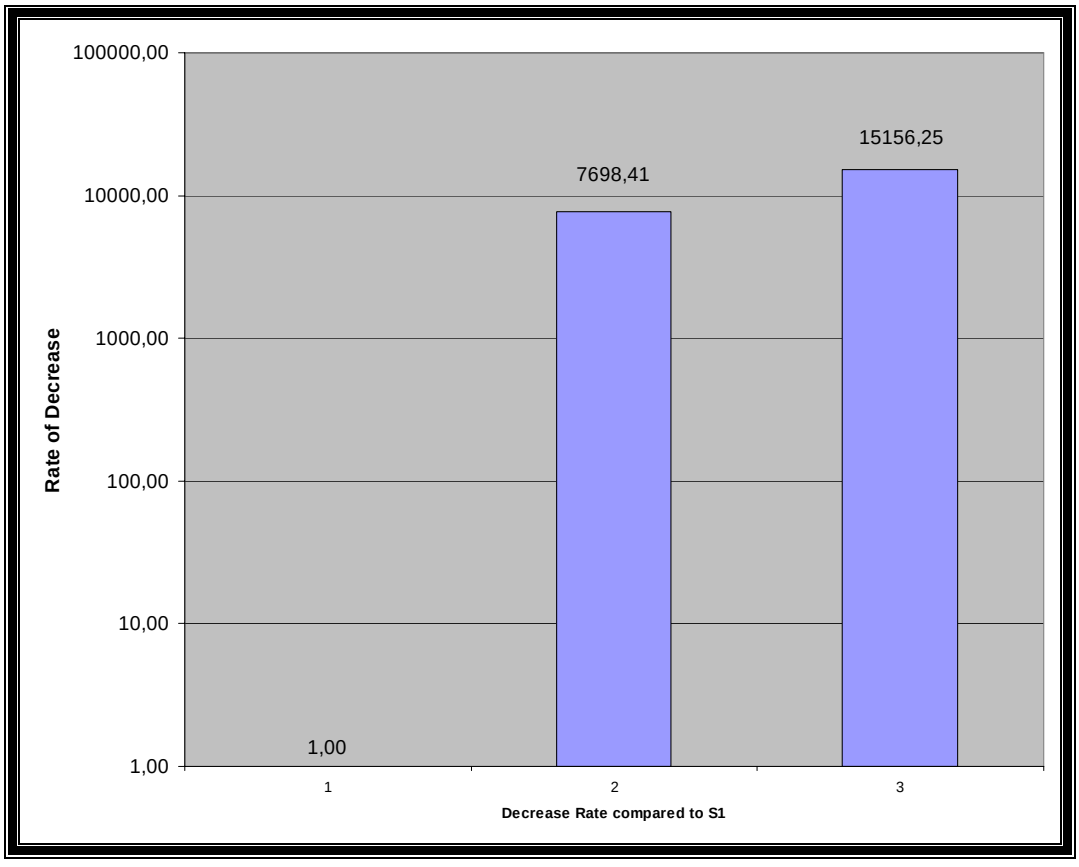

Figure 20. Comparison of the hydraulic conductivity of the samples.

3.2. Discussion

Nanoscience and nanotechnology are rapidly growing fields and the need for nanomaterials and nanocomposites as new products is strongly increasing nowadays. To compensate for this increase, new products are being invented from new research methods by improving some desired mechanical and thermal properties. Therefore, the thing that was desired to emphasize in this study is the importance, the preparation and the application of clay-polymer nanocomposite products namely based on their improved hydraulic conductivities.

For this purpose, bentonite samples containing mostly montmorillonite mineral, that is frequently used in this field to produce nanocomposites, were used because of their crystal structure and their high affinity to react with some chemicals due to their high cation exchange capacity. Three samples were chosen named as B-1, B-2 and B-3. B-1 and B-2 were the bentonite samples obtained from the ÇANBENSAN Trade & Indusrty Co. Çankırı/Turkey. B-3 was the Standard bentonite (SWy-1) obtained from the Clay Mineral Society, USA. The physicochemical properties such as the cation exchange capacity, the swelling capacity were determined to characterize the samples and some XRD measurement were done to establish the crystal structure of minerals that the samples contain.

Their cations that are present in their interlayer spaces were substituted by an organic cation called hexadecyltrimethylammonium ($HDTMA^+$) which is a quaternary ammonium and organoclays were produced from the clay minerals belonging to unmodified bentonite samples. After that, because all the samples B-1, B-2 and B-3 have no district differences, the organoclay samples of B-1 (OB-1) were chosen for the further stages of analysing.

In order to achieve the penetration of polymer chains into the interlayer gallery spaces of organoclays, a neutral monomer called acrylamide (and polymer) was chosen. The monomers were polymerized by in-situ polymerization by free radical reaction (Appendix D). The clay-polymer ratio in the produced clay-polymer nanocomposite were selected as 25% w/w (25% polymer and 75% clay).

In the literature the situation is vice versa. The clay content doesn't exceed 10% (Xiong et.al., 2007, Sarathi et al., 2007, Ahn et al., 2006)

The clay-polymer ratio in the produced clay polymer nanocomposite were selected as 25% w/w considering some economical reasons about both clay and the monomer costs. A detailed feasibility study should be done depending on the latest prices of these materials. Little amount of the clay minerals were exfoliated into the polymer matrix and major part of the clay minerals remained intercalated with polymers within their interlayer gallery spaces. This situation was proven by the XRD analyses of clay-polymer nanocomposite obtained during this study. The produced clay-polymer nanocomposites from sample OB1 were mixed with chosen sand, and then the permeability of the samples were measured. There were three samples containing sand, sand with unmodified bentonite, and finally sand with produced nanocomposite. It was observed that the permeability of the samples decreased with the addition of the clay-polymer nanocomposite down to $6.4*10^{-9}$ m/s which is 1.968 times less than sand+bentonite (S2) mixture.

There are several reasons for the decrease of permeability of samples. First one is the exfoliation of clay platelets into the polymer matrix. This phenomena may have resulted to a distribution of clay platelets randomly into the polymer matrices creating a tortourous path for the water molecules penetrating into them (Yano et al., 1993). Secondly, the intercalated clay platelets contaning highly hydrophilic polyacrylamide chains and these polymers might adsorb the water resulting in a difficult penetration. In this study, the mechanism causing a decrease of permeability of the samples was not determined.

The decrease of hydraulic conductivity of a the final clay-polymer nanocomposite obtained in this study has some advantages if the product is used in landfill sites. One of the major advantages of use is the gain of landfill volume. Because the density of polymer is less than the density of bentonite, the volume of material containing nanocomposite will be less than the material containing bentonite used as landfill liner resulting in a gain of landfill volume. Secondly, the decrease of permeability retards leakage of wastewaters and prevents the

contamination of groundwater. Thirdly, the produced nanocomposite has a plastic behaviour. This is very advantageous for landfill sites having differential settlement movements. Formation of cracks due to the movement of underlying substrate are prevented because of the increased plasticity of liner. Finally, the slope stability is increased and designing steeper slopes without additional reinforcement in landfill sites can be possible by using these materials. Moreover, intercalated organoclays can be used to eliminate the organic content of water penetrating into them. Organophilic smectites prepared by the cation exchange of the interlayer cations with cationic surfactants (mainly long chain alkylammonium cations) swell in organic solvents (Dekany et al., 1986 a,b, 1989) and they can adsorb organic molecules in the interlayer space by hydrophobic interactions.

CHAPTER 4

CONCLUSION

Organophilic clays from $HDTMA^+$ organic cation and composites of polyacrylamide (PAM) with nanodimensional montmorillonite (MMT) were prepared via in situ intercalative polymerization. The following conclusions were made:

- All the samples (B1, B2 and B3) are bentonites and contain mainly montmorillonite and few illite/smectite mixed layer as clay minerals. B1 is an unmodified yellow bentonite and B2 is a grey bentonite modified from B1, by the addition of Na_2CO_3 (Soda Ash). B3 is a standard Wyoming (SWy-1) white bentonite.
- The swelling capacity values of samples have an increasing order of B1, B2 and B3 and the values were foud to be 16.67, 19.00 and 29.33 ml.
- The cation exchange capacity values of samples have an increasing order of B1, B2 and B3 and the values were taken as 60, 65 and 70 meq/100 gr respectively.
- The amount of HDTMA-Br salt were determined from the CEC of samples and organoclays were produced successfully from those clay minerals in bentonite samples (OB-1, OB-2 and OB-3). The XRD characteristics of all the organoclays, on the other hand, were quite similar to each other, so that they exhibited 39 and 19 Å peaks. So OB1 was chosen for the further stages of study.
- The presence of (39 Å and 19 Å) double peaks must be originated from the different orientations of $HDTMA^+$ cations in the interlayer spaces of organoclays.

- Clay-polymer nanocomposite (CPN) production is achieved by in situ intercalative polymerization successfully with intercalation and partly exfoliation of clay minerals. Various clay/polymer ratios were tested in order to achieve the best dispersion of clay platelets within the polymer. Based on XRD analysis of the clay/polymer nanocomposites produced, 25% w/w clay/polymer mixture (25% clay+ 75% polymer) was selected for further studies.
- The samples of sand (S1) with sand+bentonite (S2) and sand+nanocomposite (S3) mixtures were prepared and their permeability values were determined. The values were $9.7*10^{-5}$ m/s for S1 (sand), $1.26*10^{-8}$ m/s for S2 (sand+bentonite) and $6.4*10^{-9}$ m/s for S3 (sand+nanocomposite). As a result, clay-polymer nanocomposite obtained in this study, drastically reduced the conductivity of test water in the mixture.
- The results showed that the permeability of sample decreased resulting in a retardation of water penetration throughout the sample. So, the product has a high potential of use as a retardant for waste water infiltration in landfill sites.

Following recommendations were done for further studies;

1) Several permeability tests can be done with samples containing different amounts of polymer such as 30% and 40% and 50% w/w polymer content to investigate the effect of polymer content on the permeability of sample.

2) During this study, the permeability tests were done with distilled water and if the product will be used in landfills, there will be no distilled water around these sites. So, the samples can be tested with leachate waters having different pH values. In addition, testing water with concentrations of various organic/inorganic solvents may be recommended.

3) The used sand material contain different mineral phases. The effect of mineral compositions on the permeability of sample can be investigated such as by using sand containing only quartz.

4) Finally, the geohydrological properties such as bulk density and specific retention (S_r) of sand is also important and should be investigated to determine the effect of porosity and clogging on the permeability of sand+CPN samples.

REFERENCES

Ada M., 2007, Performance Assessment of Compacted Bentonite/Sand Mixtures Utilized as Isolation Material in Underground Waste Disposal Repositories, Msc Thesis, METU, 110 pp.

Ahn, Young-Cheol, Paul D.R., 2006, Rubber toughening of nylon 6 nanocomposites., Polymer 47, 2830–2838

Alexandre Benjamin, Marais Stéphane , Langevin Dominique, Médéric Pascal, Aubry Thierry , 2006, Nanocomposite-based polyamide 12/montmorillonite: relationships between structures and transport properties, Desalination 199, 164–166

Bailey S. W., Alietti A., Brindley G. W., Formosa M. L. L., Jasmund K., Konta J., Mackenzie R. C., Nagasawa K., Rausell-Colom R. A., and Zvyagin B. B., 1980, Summary of recommendations of AIPEA nomenclature committee, Clays and Clay Minerals; v. 28; no. 1; p. 73-78

Barbosa Renata, Edcleide M. Araújo, Tomas Jeferson A. Melo, Edson N. Ito, 2007, Comparison of flammability behavior of polyethylene/Brazilian clay nanocomposites and polyethylene/flame retardants. Materials Letters 61, 2575–2578

Bergaya F., Lagaly G., 2001, Surface Modification of Clay Minerals, Applied Clay Science, 19, 1-3.

Bergaya, F. and Lagaly, G. 1999, Surface modifications of clay minerals, Applied Clay Science ,19, 1-3.

Bertini Fabio, Canetti Maurizio, Audisio Guido, Costa Giovanna, Falqui Luciano, 2006, Characterization and thermal degradation of polypropylene-mont-morillonite nanocomposites, Polymer Degradation and Stability 91, 600-605

Bhiwankar, N. and Weiss, R. A., 2006, Melt intercalation/ exfoliation of polystyrene-sodium-montmorillonite nanocomposites using sulfonated polystyrene ionomer compatibilities, Polymer, 47, 6684-6691.

Bowman R.S., Sullivan E.J., Li Z., 2000, Uptake of Cations, Anions, and Nonpolar Organic Molecules by Surfactant Modified Clinoptilolite-rich Tuff, Natural Zeolite for Third Millenium, 287-297

Brindley, G. W. and Pedro, G., 1972, Report of the AIPEA Nomenclature committee: AIPEA Newsletter No. 7, 8-13

Calcagno C.I.W., Mariani C.M., Teixeira S.R., Mauler R.S., 2007, The effect of organic modifier of the clay on morphology and crystallization properties of PET nanocomposites, Polymer 48, 966-974

Causin Valerio, Marega Carla, Marigo Antonio, Ferrara Giuseppe, Gulnaz Idiyatullina, Fabiana Fantinel., 2006, Morphology, structure and properties of a poly(1-butene)/montmorillonite nanocomposite., Polymer 47, 4773–4780

Cho Hyun-Hee, Taeyoon Lee, Sun-Jin Hwang, Jae-Woo Park, 2005, Iron and organo-bentonite for the reduction and sorption of trichloroethylene. Chemosphere 58 103–108.

Çokça, E., 1986, An Investigation on the Consolidation Behaviour of Clays, Msc Thesis, METU, 102 pp.

Davis, John C., 1965. Bentonite deposits of the Clay Spur District, Crook and Weston Counties, Wyoming, Preliminary Report No:4, Geological Survey of Wyoming.

Dekany, I., Szanto, F., Nagy, L.G., 1986b. Sorption and immersional wetting on clay-minerals having modified surface: Part 2. Interlamellar sorption and wetting on organic montmorillonites. J. Colloid Interface Sci. 109, 376–384.

Dekany, I., Szanto, F., Weiss, A., Lagaly, G., 1986a. Interactions of hydrophobic layer silicates with alcohol-benzene mixtures: Part 2. Structure and composition of the adsorption layer. Ber. Bunsen-Ges.-Phys. Chem. Chem. Phys. 90, 427–431.

Delozier D.M., Orwoll R.A., Cahoon C.F., Johnston N.J., Smith Jr J.G., Cornell J.W., Preparation and characterization of polyimide/organoclay nanocomposites. Polymer 43, 813-822

Foley, N. K., 1999, Environmental characteristics of clays and clay mineral deposits: USGS Information Handout

Giannelis, E.P., 1996. Polymer layered silicate nanocomposites. Adv. Mater. 8, 29–35.

Grim, R.E., 1953, Clay Mineralogy, Mc Graw-Hill Company, Inc., New York, 384 pp.

Grim, R.E., 1968 Clay Mineralogy. McGraw-Hill, New York, 596 pp.

Guggenheim S., Martin R.T., 1995, Definition Reprot of Clay and Clay Mineral: Joint the AIPEA and CMS Nomenclature Commitees, Clay Minerals 30, 257-259

Ha S.R., Ryu S.H., Park S.J., Rhee K.Y., 2007, Effect of clay surface modification and concentration on the tensile performance of clay/epoxy nanocomposites, Materials Science and Engineering A 448, 264–268

Inam D., 2006, Organoclay Preparation for Anionic Contaminant Removal from Water., Msc Thesis, METU, 99 pp.

Inam D., Gokturk E.H., Turkmenoglu A.G., 2006, Application of organoclays for the removal of anionic contaminants, Fourth Mediterranian Clay Meeting, Abstracts, 5-10 September 2006, METU, Ankara, p.64.

Inyang H.I., Bae S., 2005, Polyacrylamide sorption opportunity on interlayer and external pore surfaces of contaminant barrier clays, Chemosphere 58, 19-31.

Jiang Tao, Wang Yu-hua, Yeh Jen-taot, Fan Zhi-qiang, 2005, Study on solvent permeation resistance properties of nylon6/clay nanocomposite, European Polymer Journal 41, 459–466

Jo Choonghee, Hani E. Naguib, 2007, Constitutive modeling of HDPE polymer/clay nanocomposite foams. Polymer 48 3349-3360

Katti Kalpana S., Debashis Sikdar, Dinesh R. Katti, Pijush Ghosh, Devendra Verma,. 2006, Molecular interactions in intercalated organically modified clay and clay–polycaprolactam nanocomposites: Experiments and modeling., Polymer 47, 403–414

Kim Byung Kyu, Jang Won Seo, Han Mo Jeong, 2003, Morphology and properties of waterborne polyurethane/clay nanocomposites, European Polymer Journal 39, 85–91

Kim Jang-Kyo, Hu, C., Ricky S.C. Woo and Sham, M., 2005, Moisture barrier characteristics of organoclay-epoxy nanocomposites. Composites Science and technology, Volume 65, Issue 5, Pages 805-813.

Knetchtel, Maxwell M. and Sam H. Patterson, 1962. Bentonite Deposits of the Northern Black Hill District, Wyoming, Montana and South Dakota, Bulletin 1082-M, U.S. Geological Survey.

Koçyiğit A., Türkmenoğlu A., Beyhan A., Kaymakçı N., Akyol E., 1995. Post-Collisional Tectonics of Eskişehir-Ankara-Çankırı Segment of İzmir-Ankara-Erzincan Suture Zone (IAESZ): Ankara Orogenic Phase, TAPG Bulletin, v.6-1, 69-86

Lagaly, G., 1986. Interaction of alkylamines with different types of layered compounds. Solid State Ionics 22, 43–51.

Lai, M-C., Chang, K-C., Yeh, J-M., Liou, S-J., Hsieh, M-F., Chang, H-S., Advanced Environmentally Friendly Anticorrosive Materials Prepared From Water-Based Polyacrylate/Na+-MMT Clay Nanocomposite Latexes, European Polymer Journal (2007), doi: 10.1016/j.eurpolymj.2007.05.008

Le Baron, P.C., Wang, Z. and Pinnavaia, T.J., 1999, polymer layered silicate nanocomposites: an overview, Applied Clay Science, 15, 1-2, 11-29.

Li Z., Zou Y., 1999, A Comparison of Chromate Analysis by AA, UV-VIS Spectrometric, and HPLC Methods, Advances in Environmental Research. 125-131

Liu, P., 2007, Polymer modified clay minerals: A review, Applied Clay Science,doi:10. 1016/j.clay. 20078. 01.004.

Luduena Leandro N., Vera A. Alvarez, Analia Vazquez, 2007, Processing and microstructure of PCL/clay nanocomposites, Materials Science and Engineering A 460–461, 121–129

Mandalia T. and Bergaya F., 2006, Organoclay-mineral melted polyolefin nanocomposites. Effect of surfactant/CEC ratio, Journal of Physics and Chemistry of solids, 67, 836-845.

Mark, J.E., 1996. Ceramic-reinforced polymers and polymer-modified ceramics. Polym. Eng. Sci. 36, 2905–2920.

Masami Okamoto, Polymer/Layered Silicate Nanocomposites, Rapra Technology Limited, United Kingdom, 2003

Matyjaszewski K., Davis T.P., 2002, Handbook of Radical Polymerization, p.118, 131, 162, John Wiley and Sons, Inc. Pub., Germany.

Michael Alexandre, Philippe Dubois, 2000, Polymer-layered silicate nanocomposites: preparation, properties and uses of a new class of materials, Materials Science and Engineering, 28, 1-63,

Nanocompositech, http://www.nanocompositech.com/glossary-nanocomposite-nanotechnology.htm, (last retrieved on 15.09.2007)

Novak, B.M., 1993. Hybrid nanocomposites materials between inorganic glasses and organic polymers. Adv. Mater. 5, 422–433.

Ogasawara Toshio, Yuichi Ishida, Takashi Ishikawa, Takahira Aoki, Toshiyuki Ogura., , 2006. Helium gas permeability of montmorillonite/epoxy nanocomposites, Composites: Part A 37, 2236–2240

Okada A., Usuki, A., 1995. The chemistry of polymer–clay hybrids. Mater. Sci. Eng. C 3, 109.

Osterwald, Frank W., Doris B. Osterwald, Joseph S. Long, Jr., and William H. Wilson, 1966, Mineral Resources of Wyoming, Bulletin No.50, Geological Survey of Wyoming (Revised by William H. Wilson).

Önal M. and Çelik, M., 2006, polymethacrylamide/Na-montmorillonite nanocomposites synthesized by free-radical polymerization, Materials Letters, 60, 48-52.

Paul D.R., Zeng Q.H., Yu A.B., Lu G.Q., 2005, The interlayer swelling and molecular packing in organoclays., Journal of Colloid and Interface Science 292, 462–468

Peneva Y., Tashev E., Minkova L., 2006, Flammability, microhardness and transparency of nanocomposites based on functionalized polyethylenes, European Polymer Journal 42, 2228–2235

Peprnicek T., Duchet J., Kovarova L., Malac J., Gerard J.F., Simonik J., 2006, Poly(vinyl chloride)/clay nanocomposites: X-ray diffraction, thermal and rheological behaviour., Polymer Degradation and Stability 91, 1855-1860

Picard E., Vermogen A., Gerard J.-F., Espuche E., 2007, Barrier properties of nylon 6-montmorillonite nanocomposite membranes prepared by melt blending: Influence of the clay content and dispersion state Consequences on modelling. Journal of Membrane Science 292, 133–144.

Powell Clois E., Beall Gary W., 2006, Physical properties of polymer/clay nanocomposites, Current Opinion in Solid State and Materials Science 10, 73–80

Ray, S.S. and Okamoto, M., 2003 Polymer/layeredsilicate nanocomposites: a review from preparation to processing, Progress in Polymer Science, 28, 1539-1641.

Rehab Ahmed, Salahuddin Nehal, 2005, Nanocomposite materials based on polyurethane intercalated into montmorillonite clay, Materials Science and Engineering A 399, 368–376

Santiago Francisca, Mucientes Antonio E., Osorio Monica, Rivera Carlos, 2007, Preparation of composites and nanocomposites based on bentonite and poly(sodium acrylate). Effect of amount of bentonite on the swelling behaviour, Macromolecular Nanotechnology – Review, European Polymer Journal 43, 1–9

Sarathi R., Sahu R.K., Rajeshkumar P., 2007, Understanding the thermal, mechanical and electrical properties of epoxy nanocomposites, Materials Science and Engineering A 445–446, 567–578

Schmidt H., 1985. New type of non-crystalline solids between inorganic and organic materials. J. Non-Cryst. Solids 73, 681–691.

Slaughter M. and J.W. Earley, 1965. Mineralogical and Geological Significance of the Mowry Bentonites, Wyoming, Special Paper 83, Geological Survey of America

Sugama Toshifumi, 2006, Polyphenylenesulfied/montomorillonite clay nanocomposite coatings: Their efficacy in protecting steel against corrosion, Materials Letters 60, 2700–2706

Sun Q.,F. Schork, J. and Deng, Y., 2006, Water based polymer/clay nanocomposite suspension for improving water and moisture barrier in coating, Composites science and technology, doi:10.1016/j.compositech.2006.10.022.

Taşkın A., 2007, Synthesis of Poly(Methyl Metacrylic Acid) Salt in Aqueous Medium With Potassium Peroxidisulfate By Free Radical Reaction. 17 pages.

Trisoplast, http://www.trisoplast.nl/index1.php?t=3., (last retrieved on 15.09.2007)

Türkmenoğlu A.G., Koçyiğit A., and Özalp T., 1994, Anadolu`daki bazı űst Tersiyer havzalarının evrimi ve ekonomik potansiyeli için tip alan çalışması: Gűneybatı Çankırı Havzası, TUBITAK Project ID: YBAG-0058, 317 pages.

Türkmenoğlu A.G., Koçyiğit A., and Özalp T., 1995, Kalecik-Hasayaz Havzasındaki Tersiyer göl sedimanlarının jeolojisi ve kil mineralojisi, VII. National Clay Symposium. 55-63.

Van Olphen, H. and Fripiat, J.J., 1979, Data Handbook for Clay Minerals and Other Non-metallic Minerals. Pergamon Press, Oxford, England, 346 pp.

Wang Guo-An, Cheng-Chien Wang, The disorderly exfoliated LDHS/PMMA nanocomposite synthesized by in situ bulk polymerization, Polymer, 46, 5065- 5074, 2005

Wang Xiaoying, Yumin Du, Jiwen Luo, Baofeng Lin, John F. Kennedy, 2007, Chitosan/organic rectorite nanocomposite films: Structure, characteristic and drug delivery behaviour. Carbohydrate Polymers 69, 41–49.

Xiong, J., Zheng, Z., Jiang, H., Ye, S. and Wang, X., 2007. Reinforcement of polyurethane composites with an organically modified montmorillonite. Composites Part A: Applied Science and Manufacturing, Volume 38, Issue 1, Pages 132-137.

Xu Yijin Brittain William J., Richard A. Vaia, Price Gary., 2006, Improving the physical properties of PEA/PMMA blends by the uniform dispersion of clay platelets., Polymer 47, 4564–4570

Xu, S. Sheng, G., Boyd, S.A., 1997. Use of organoclays in pollution abatement. Advances in Agronomy 59, 25–62.

Yano, K. Usuki, A., Okada, A., Kurauchi, T., Kamigaito, O., 1993. Synthesis a properties of polyimide–clay hybrid. J. Polym. Sci., Part A: Polym. Chem. 31, 2493–2498.

Yeh Jui-Ming, Tai-Hung Kuo, Hou-Ju Huang, Kung-Chin Chang, Mei-Ying Chang, Jen-Chang Yang, 2007, Preparation and characterization of poly(o-methoxyaniline)/Na+–MMT clay nanocomposite via emulsion polymerization: Electrochemical studies of corrosion protection. European Polymer Journal 43, 1624–1634.

Zeng Q.H., Yu, A.B., Lu, G.Q., and Paul D.R., 2005, Clay based plymer nanocomposites: research and commercial development, Journal of Nanoscienceand Nanotechnology , 5, 1574-1592.

Zheng Qiang, Bo Xu, Yihu Song, Yonggang Shangguan, 2006, Calculating barrier properties of polymer/clay nanocomposites: Effects of clay layers., Polymer 47, 2904–2910

APPENDIX A

METHODOLOGY FOR METHYLENE BLUE ADSORPTION TEST

During analysis, the spot method is used to determine MBA (Methylene Blue Adsorption) and CEC of an unknown sample. The spot method is a simplified titration technique. A certain amount of methylene blue solution added in definite volumes to a suspension of fine grained soil or ground rock particles. The total amount of methylene blue solution adsorbed is used for the calculation of methylene blue and CEC of the soil or rock. The method is very simple, convenient and quick (Çokça, 1991).

The methylene blue hydrochloride ($Ci_6H_{18}N_3SCl$) consists of a base in combination with an acid. The methylene blue molecule contains a negatively charged chloride (Cl^-) ion in a large positively charged ion. The methylene blue replaces natural cations of clay irreversably (Eqn 3).

$$Ca-Na\ CLAY + MB\ Hydrochloride \rightarrow MB\ CLAY + Ca-Na\ Chloride \quad \text{....(Eqn. 3)}$$

The replacement of natural cations by methylene blue

When a methylene blue solution is added to a clay water mixture, the positive methylene blue ion drives away the positive ions at the external surface of the clay. The process continues until all the positive ions have been expelled. Upto that point, all the cations attach to the clay mineral surface. Then, the methylene blue ions replace the positive ions present in the interlayer.

From then on, the remaining methylene blue ions stay in solution. The maximum adsorption indicates the CEC.

Apparatus and Procedure

Various standart equipments and reagents are used during the methylene blue test (Table A1).

Table A1. The apparatus for methylene blue test

A 100 ml burette
Whatman No.40 filter paper with 12,5 cm diameter
Glass stirring rod
Magnetic stirrer
500 ml glass container
Medical quality methylene blue
Distilled water
Over dried clay sample (sieved through no.170 sieve)

Preparation of Solutions

A. Methylene Blue Solution

10 g methylene blue with known normality is placed in a glass container. Then, 1 l of distilled water is added and mixed for 45 minutes with a magnetic stirrer. The normality of methylene blue dye can be calculated by a definite formula (Eqn. 4).

$$NMB = \left(weight\ of\ MB\ in\ gram\right)/320 * \left[(100 - \mathrm{X})/100\right] \quad \text{.....(Eqn. 4)}$$

The normality of methylene blue dye (X: the moisture content of methylene blue dye)

B. Soil Solution

7,5 g (alternatively 30 g) of soil sample sieved through no.170 sieve is placed in a glass container and 50 ml (alternatively 200 ml) distilled water is added and then mixed by using magnetic stirrer at a speed of about 700 rpm. The methylene blue solution already prepared is put into a burette and 5 ml of this solution is added to soil solution which is continuosly being stirred. In order to perform titration, successive volumes of methylene blue are added to soil solution. After each addition, the mixed solution is agitated for 1 minute and drop of dispersion is removed with a glass rod. This is dabbed carefully on a sheet of fitler paper. Initially a circle of dust is formed which is colored dark blue and has a distinct edge, and is surrounded by a ring of clear water. When the edge of the dust circle appears fuzzy and/or is surrounded by a narrow light blue halo, another spot test is done after 1 minute. If the halo disappears, more methylene blue is added. If there is still a halo, the test is repeated four more times at 1 minute intervals. If the light halo still exists at the 5th spot (Figure A1, A2, A3), this indicates the end point and the total volume of methylene blue dye added is recorded (Çokça 1991).

The methylene blue adsorption value (MBA) is normally expressed in grams. Methylene blue adsorbed by 100 g of sample material is mostly given as g/100 g.

$$MBA = V_{cc} / f$$

The Methylene Blue Adsorption (MBA) Value. V_{cc} : volume of the methylene blue solution injected to the soil solution (ml), f: dry weight of the sample used (g)

Since the normality of the methylene blue solution is known (0,0228), the net CEC may be calculated from the following formula.

$$CEC = (100/f)*V_{cc}*Normality$$

Calculation of cation exchange capacity (CEC)

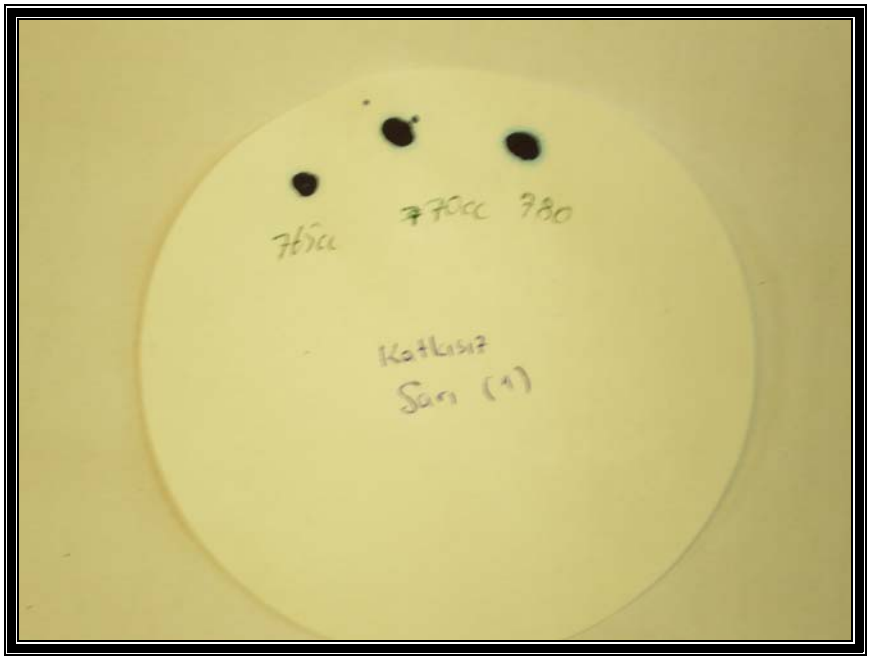

Figure A1. MBA value of the sample B-1.

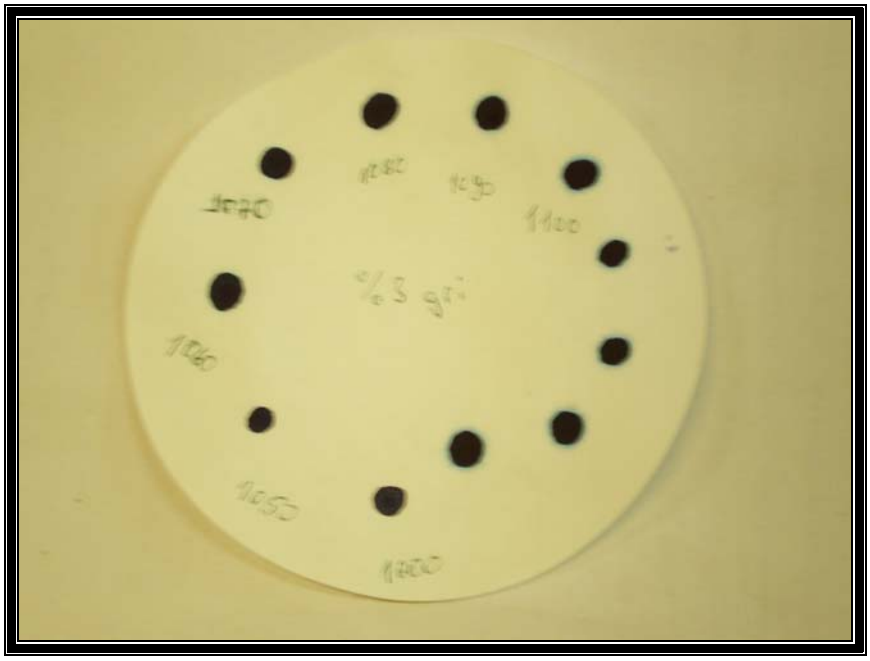

Figure A2. MBA value of the sample B-2.

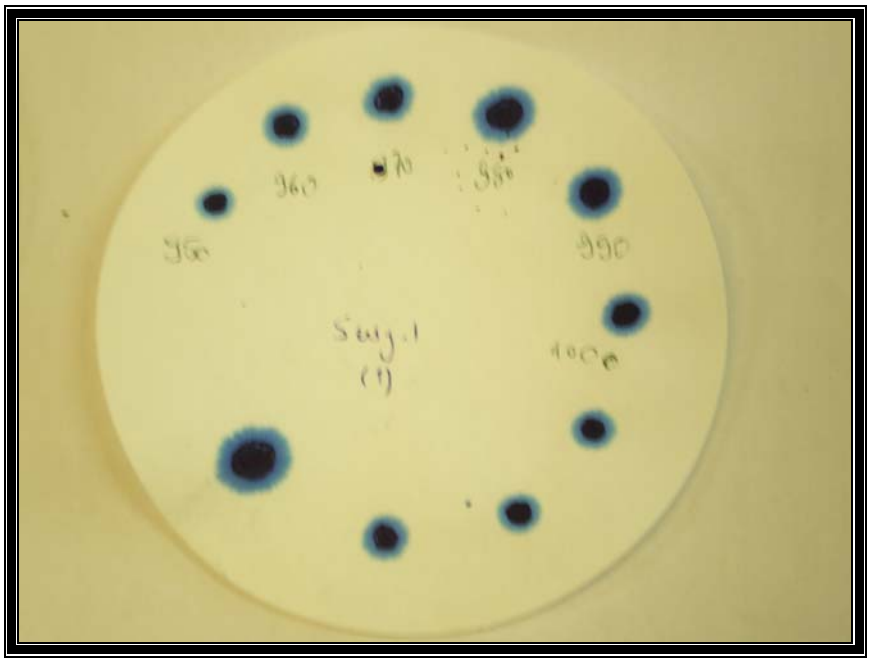

Figure A3. MBA value of the sample B-3.

APPENDIX B

METHODOLOGY FOR SWELLING CAPACITY

Apparatus and Procedure

The apparatus for the test is given in Table B1.

Table B1. Apparatus for swelling capacity test

1.	Graduated cylinder (Figure B1)
2.	High precision (0.01 g) digital balance
3.	Distilled water

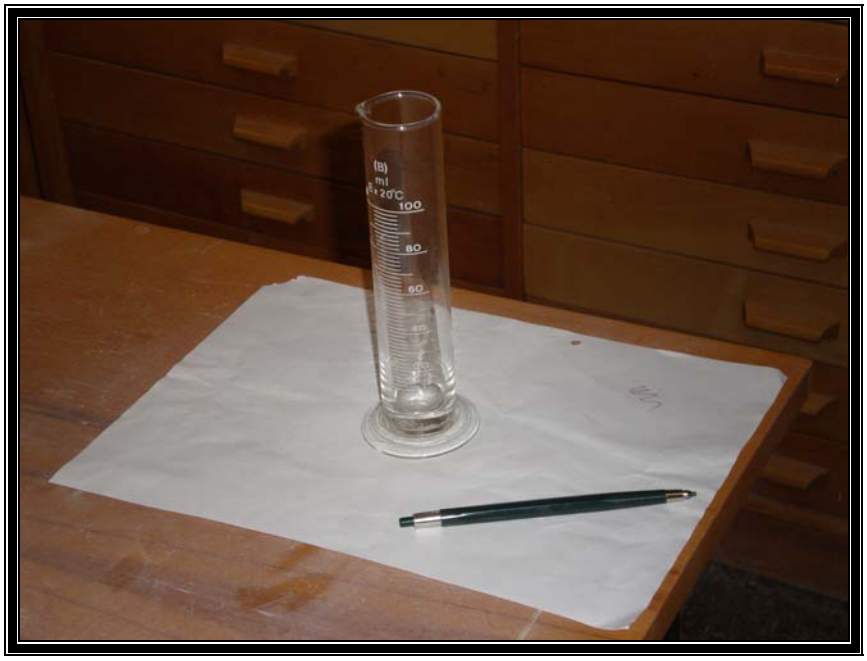

Figure B1. Apparatus for determination of swelling capacity

2 g. of sample is weighed using high precision digital balance. 100 ml distilled water is put into graduated cylinder. Weighed sample is added into distilled water gradually with spatula. After 24 hours, the swelling capacity is read in units of ml/100 ml.

APPENDIX C

METHODOLOGY FOR THE PREPARATION OF ORGANOCLAY

Apparatus and Procedure

The apparatus is given in Table C1.

Table C1. Apparatus for organoclay preparation

A 20 ml burette
A glass rod
Magnetic stirrer
Distilled water
500 ml glass container
A thermometer
HDTMA-Br Salt Alrich™
Laboratory Shaker

The sample is dried in an oven at 50 °C for 2 days to remove the moisture and put into a dessicator a half day for rest. 15 ml distilled water is put into the a glass container. A little amount of HDTMA-Br salt is weighed corresponding to twice of cation exchange capacity of clay sample which was determined with The Methylene Blue Test.

The weighed HDTMA-Br salt is put into distilled water and stirred for 15 minutes in a magnetic stirrer. Then, the solution is heated up to 27-28 °C and the

solution becomes transparent gradually indicating that the salt is solved in the water and $HDTMA^+$ and Br^- ions are formed in the solution The solution`s temperature must be kept below 30 $^\circ$C. If the solution exceeds that temperature, the salt present in the solution becomes recrystallized when the solution`s temperature decreases to room temperature (24-25 $^\circ$C). So with the help of a thermometer the solution temperature must be controlled simultaneously while the solution is being stirred.

2 g. of clay sample, weighed previously with a high precision digital balance, is put into a centrifuge tube and the prepared solution is poured into this tube. The tube`s cap is enclosed and the tube is hand-shaken for 1 minute. Then the sample is placed onto a laboratory shaker and laterally shaken for 24 hours at room temperature.

After 24 hours, the sample is centrifuged for 15 minutes at 3000 rpm. Then, the solution in the tube is removed and some distilled water is added into the tube to wash the sample and again the solution is centrifuged for 15 minutes at 3000 rpm. This process is repeated for three times. The logic for doing this process is wash the sample and remove the excess of $HDTMA^+$ cation.

The clay sample is put into a container with a glass rod and the sample is dried at 80 $^\circ$C until all the sample becomes dried. Finally, the sample is grinded and sieved through No. 170 mesh.

APPENDIX D

METHODOLOGY FOR THE PREPARATION OF NANOCOMPOSITE

Apparatus and Procedure

The apparatus is given in Table D1. The previously prepared organoclay sample is put into a beaker and 100 ml distilled water is added and stirred for 1 minute. A desired amount of (depending on the percentage of clay-polymer) acrylamide monomer is added and solved in 50 ml distilled water. The two solutions are poured into a 500 ml glass container and mixed with each other for 30 minutes at 60 $^{\circ}$C.

Table D1. Apparatus for nanocomposite preparation

Mechanical mixer
Distilled water
500 ml beaker
A thermometer
Acrylamide Merck™ monomer
$FeCl_3$ stock solution (5 M)
Potassium persulfate ($K_2S_2O_8$)

After 30 minutes, 0.300 gr of potassium persulfate is solved in 5 ml distilled water. 3-4 ml $FeCl_3$ stock solution and potassium persulfate solution are put into two small containers. Then, potassium persulfate solution and 3-4 ml $FeCl_3$ stock solution is poured into the organoclay-monomer solution simultaneously. Then this mixture is mixed about 1 hour at 60 $^{\circ}$C and after 1 hour (Figure D1), the mixture is

put into the oven for drying. Finally, after the drying process, the sample is grinded and sieved through no. 170 mesh.

Figure D1. Apparatus for the preparation of nanocomposite

APPENDIX E

CALCULATION OF THE AMOUNT OF HDTMA-Br SALT FOR THE PRODUCTION OF ORGANOCLAY

For B1 (~60 meq/ 100 gr of clay),

$100\ g \rightarrow 120\ mmol\ HDTMA$

$2\ g \rightarrow X\ mmol$

$X = 2.4\ mmol$

2.4 mmol sample is dissolved in 15 ml distilled water to obtain 0.16 molar HDTMA solution using the equation $M = \frac{n}{V}$.

For 15 ml solution,

using equation $n = \frac{m}{m_W}$

2.4 *x* 10^{3-} *x* 364.46 = 0.88 g of HDTMA-Br salt is dissolved for one tube.

Molecular weight of HDTMA-Br salt (m_W) = 364.46 g/mol

For B2 (~65 meq/ 100 gr of clay),

$100\ g \rightarrow 130\ mmol\ HDTMA$

$2\ g \rightarrow X\ mmol$

$X = 2.6\ mmol$

2.6 mmol sample is dissolved in 15 ml distilled water to obtain 0.173 molar HDTMA solution using the equation $M = \frac{n}{V}$.

For 15 ml solution,

using equation $n = \frac{m}{m_W}$

2.6 *x* 10^{3-} *x* 364.46 = 0.95 g of HDTMA-Br salt is dissolved for one tube.

Molecular weight of HDTMA-Br salt (m_W) = 364.46 g/mol

For B3 (~70 meq/ 100 gr of clay),

$100\ g \rightarrow 140\ mmol\ HDTMA$

$2\ g \rightarrow X\ mmol$

$X = 2.8\ mmol$

2.8 mmol sample is dissolved in 15 ml distilled water to obtain 0.19 molar HDTMA solution using the equation $M = \frac{n}{V}$.

For 15 ml solution,

using equation $n = \frac{m}{m_W}$

2.8 *x* 10^{3-} *x* 364.46 = 1.02 g of HDTMA-Br salt is dissolved for one tube.

Molecular weight of HDTMA-Br salt (m_W) = 364.46 g/mol

APPENDIX F

XRD GRAPHS FOR THE SAMPLES B1, B2 And B3

Figures F-1 to F-15 show the X-ray diffraction patterns of the selected samples B-1, B-2 and B-3. The samples were placed onto glass lamellas and air-dried. Then they were put into a dessicator containing ethylene glycol. The samples were ethylene glycol solvated and kept in the dessicator for a half day at 60 C°. Those samples were named as "EG". Later on, the samples were placed onto glass lamellas and heated up to 300 C° for 1 hr. in an oven and named as "300". Finally, the samples were again placed onto glass lamellas and heated up to 550 C° for 1 hr. and named as "550". Eventually, 5 diffractograms were obtained from each sample named as Random, AD, EG, 300 and 500.

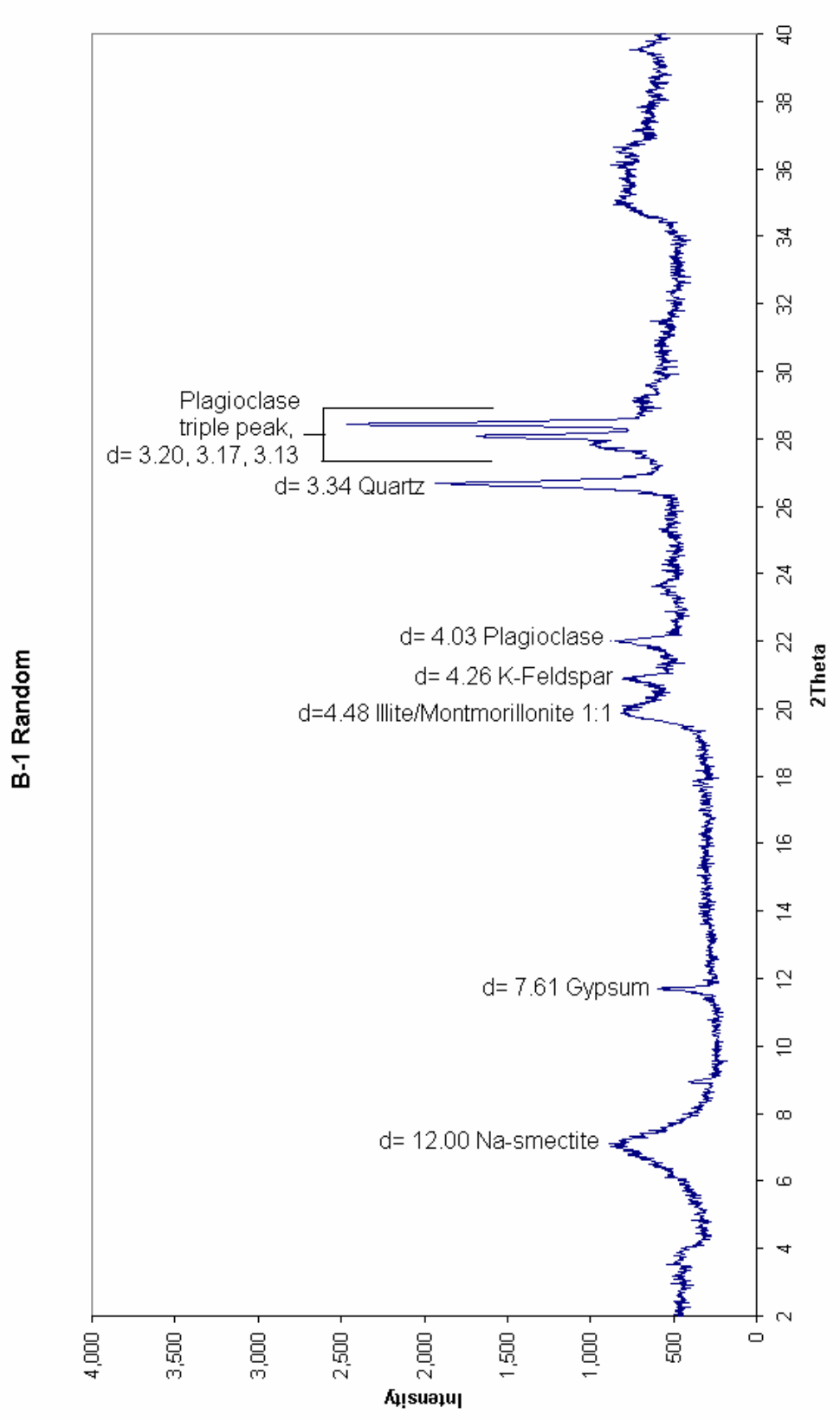

Figure F1. XRD Graph for the Sample B-1 (Random)

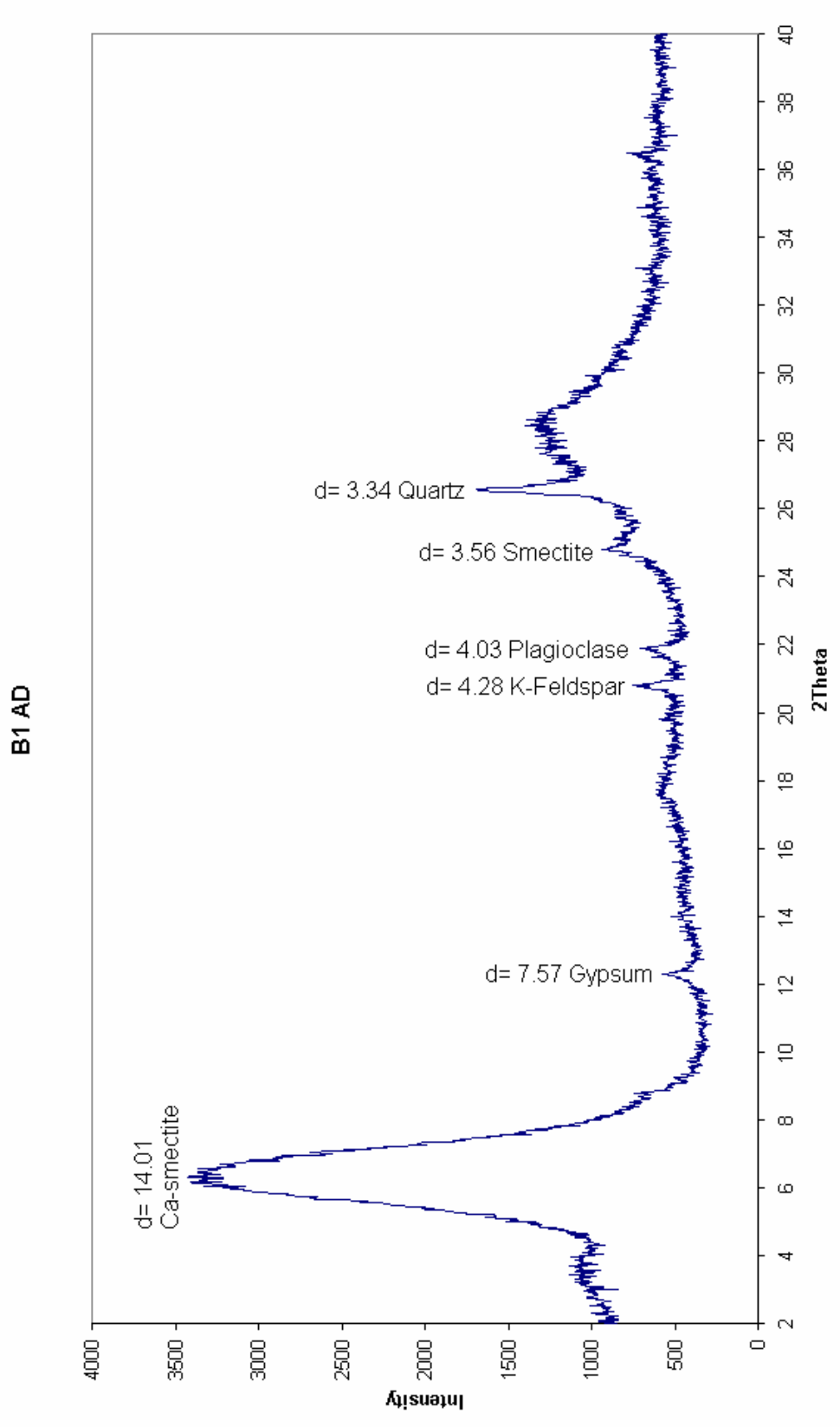

Figure F2. XRD Graph for the Sample B-1 (Air Dried)

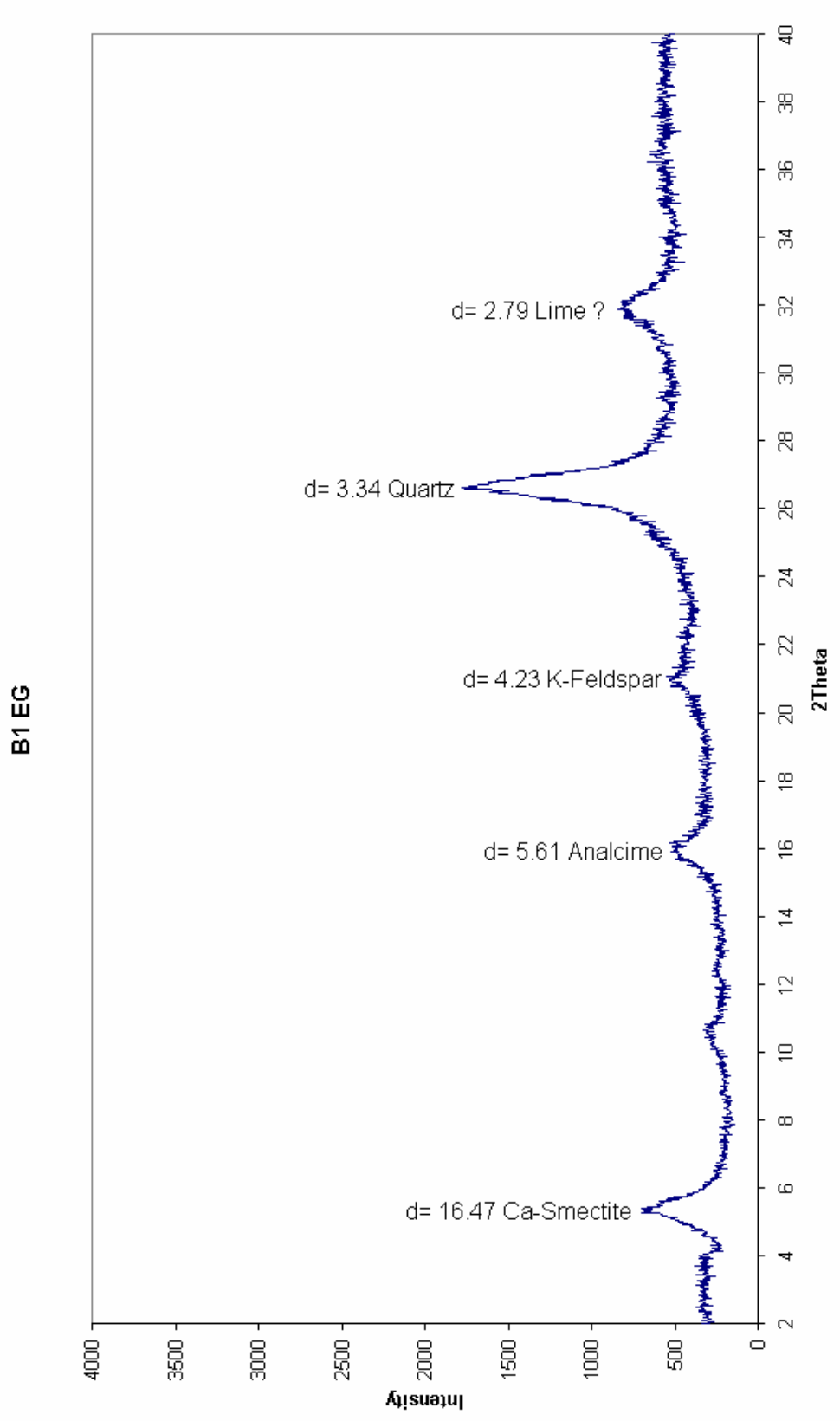

Figure F3. XRD Graph for the Sample B-1 (Ethylene Glycolated)

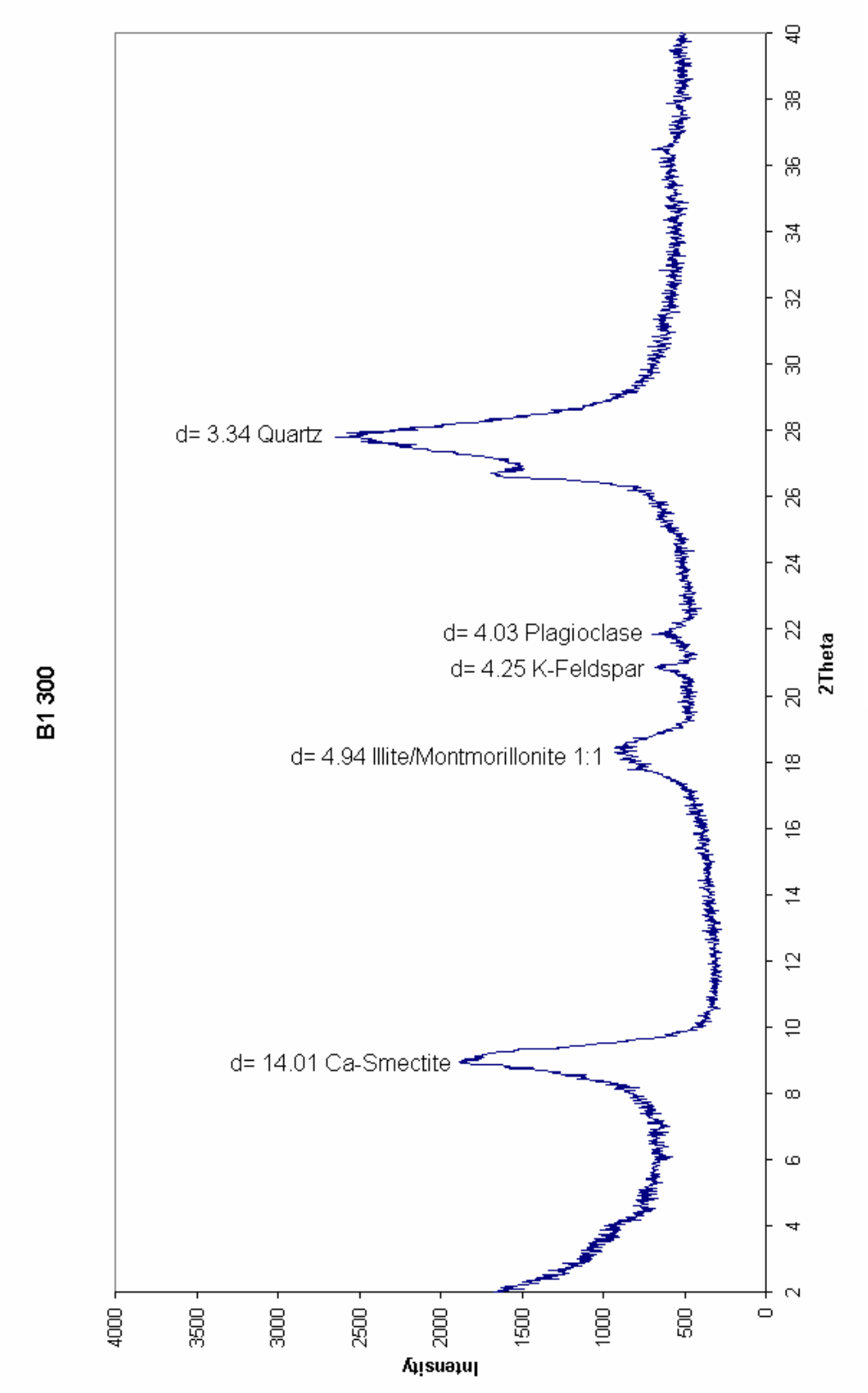

Figure F4. XRD Graph for the Sample B-1 (Heated to 300°C)

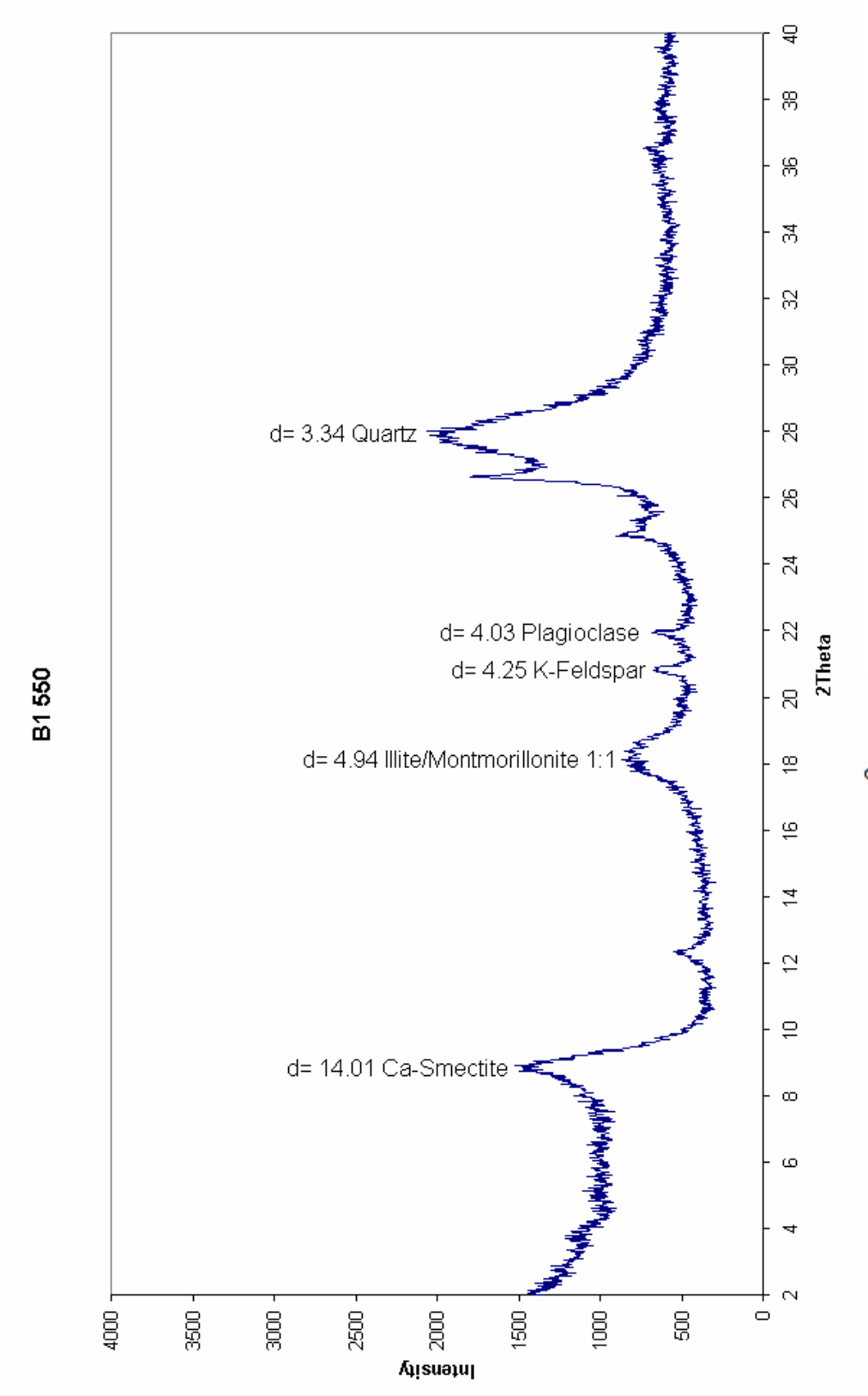

Figure F5. XRD Graph for the Sample B-1 (Heated to 550^{o}C)

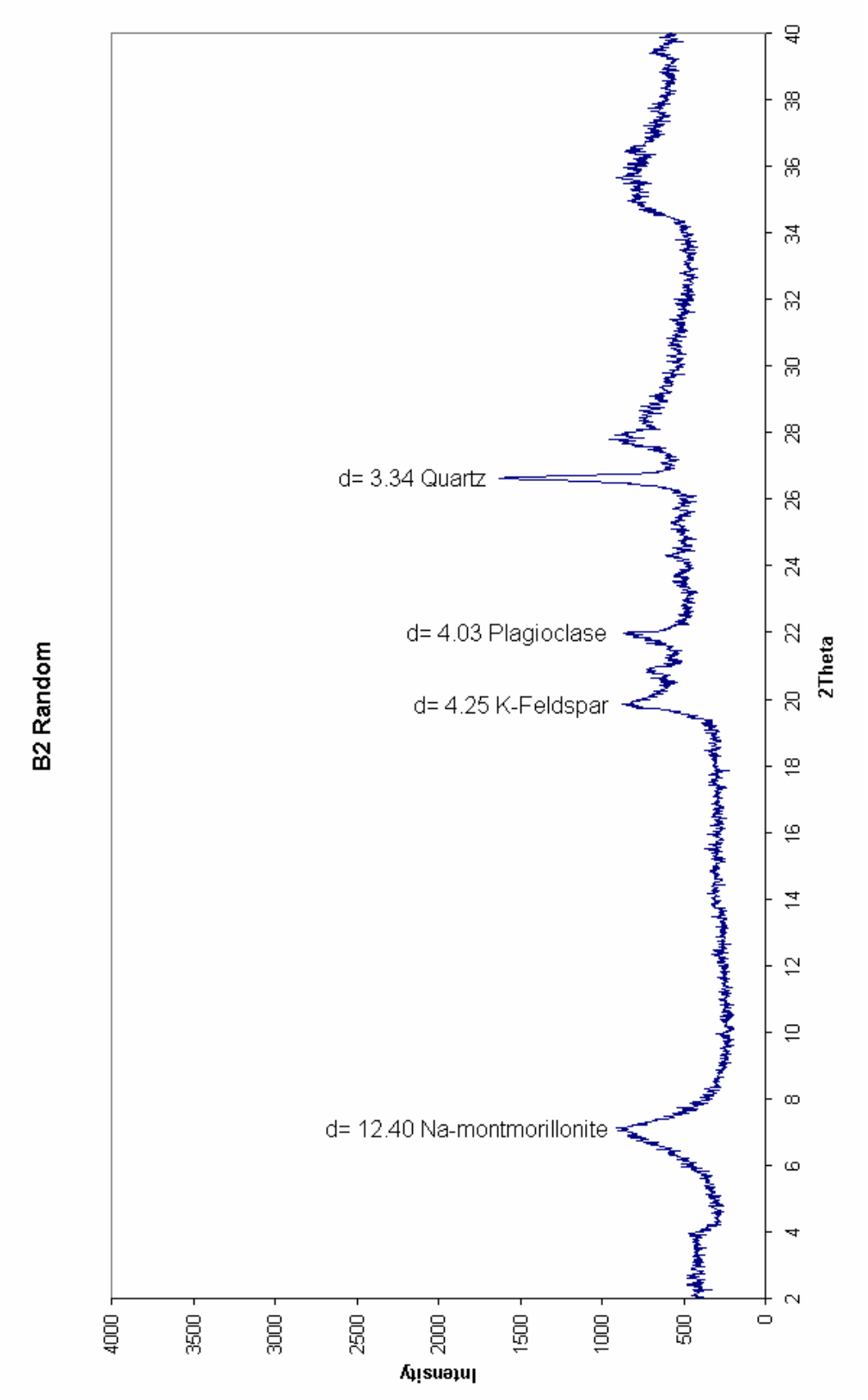

Figure F6. XRD Graph for the Sample B-2 (Random)

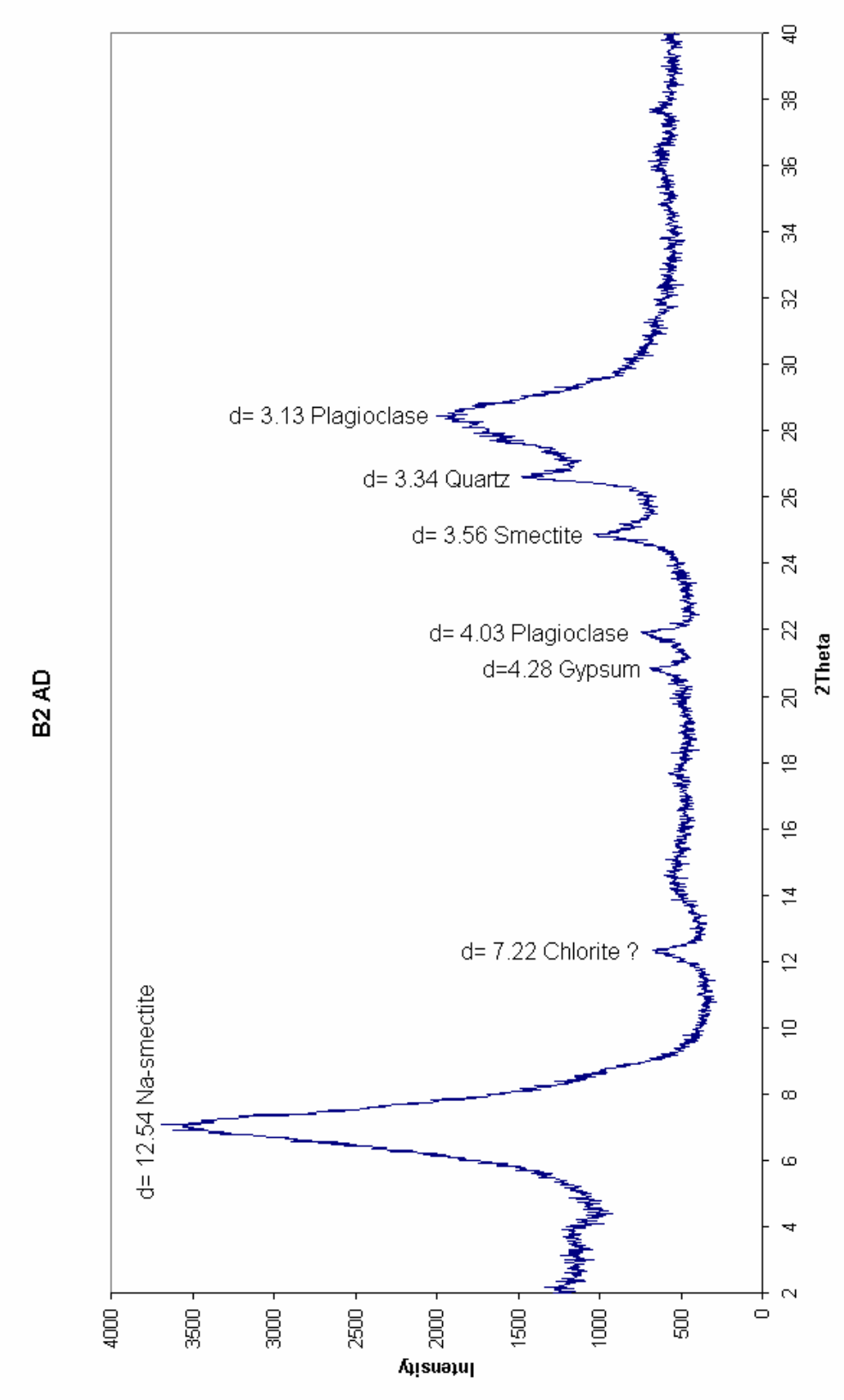

Figure F7. XRD Graph for the Sample B-2 (Air Dried)

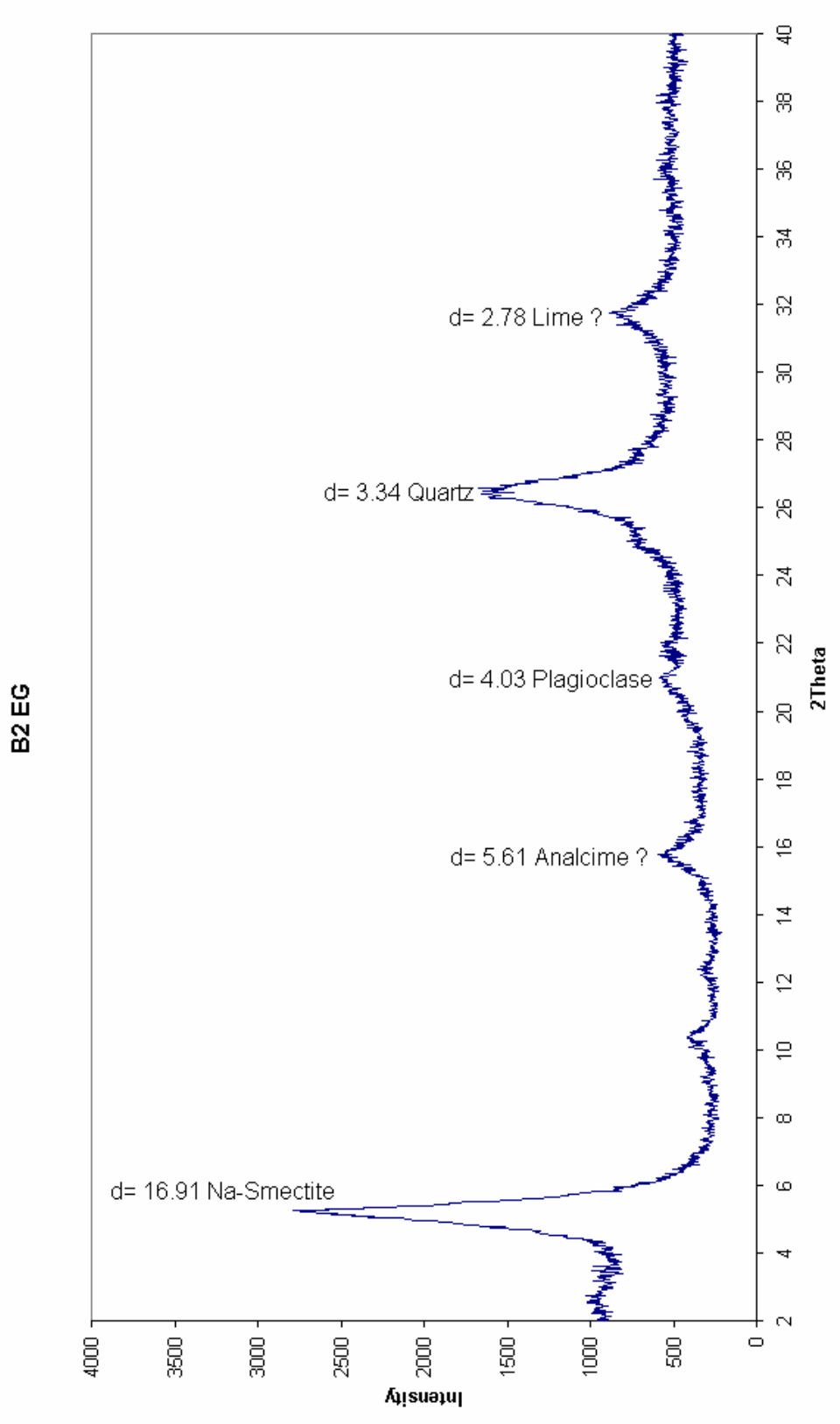

Figure F8. XRD Graph for the Sample B-2 (Ethylene Glycolated)

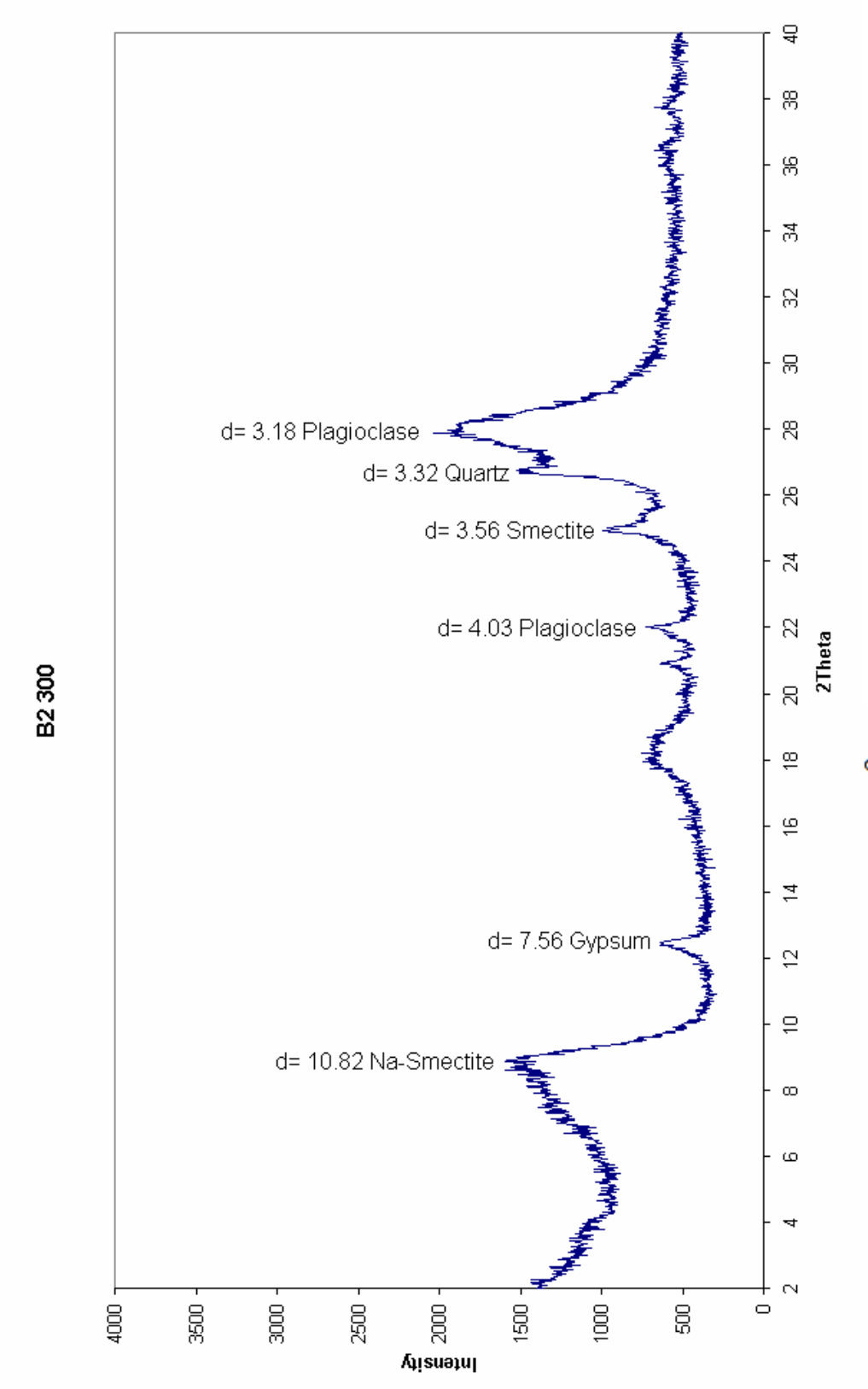

Figure F9. XRD Graph for the Sample B-2 (Heated to 300°C)

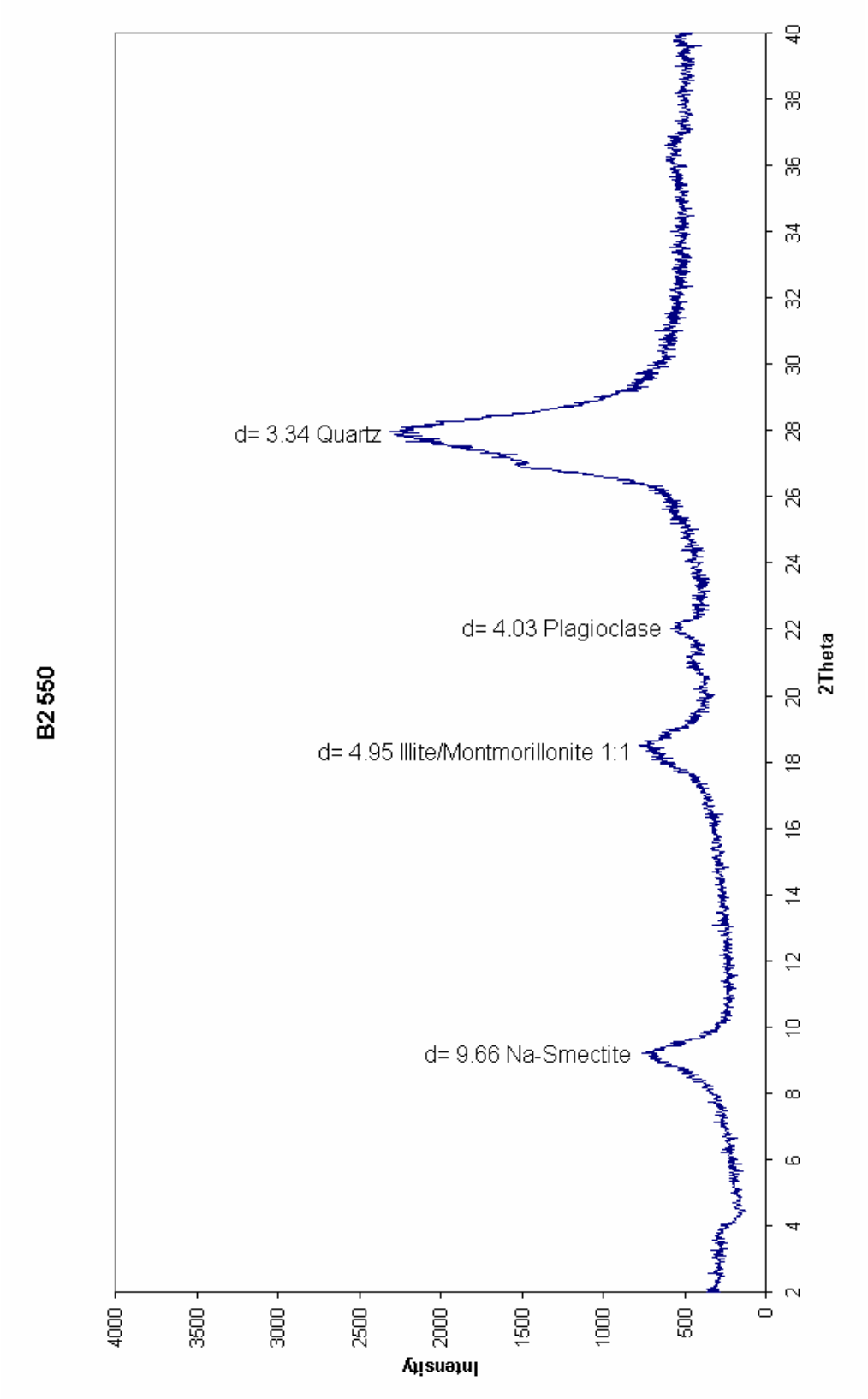

Figure F10. XRD Graph for the Sample B-2 (Heated to 550^{o}C)

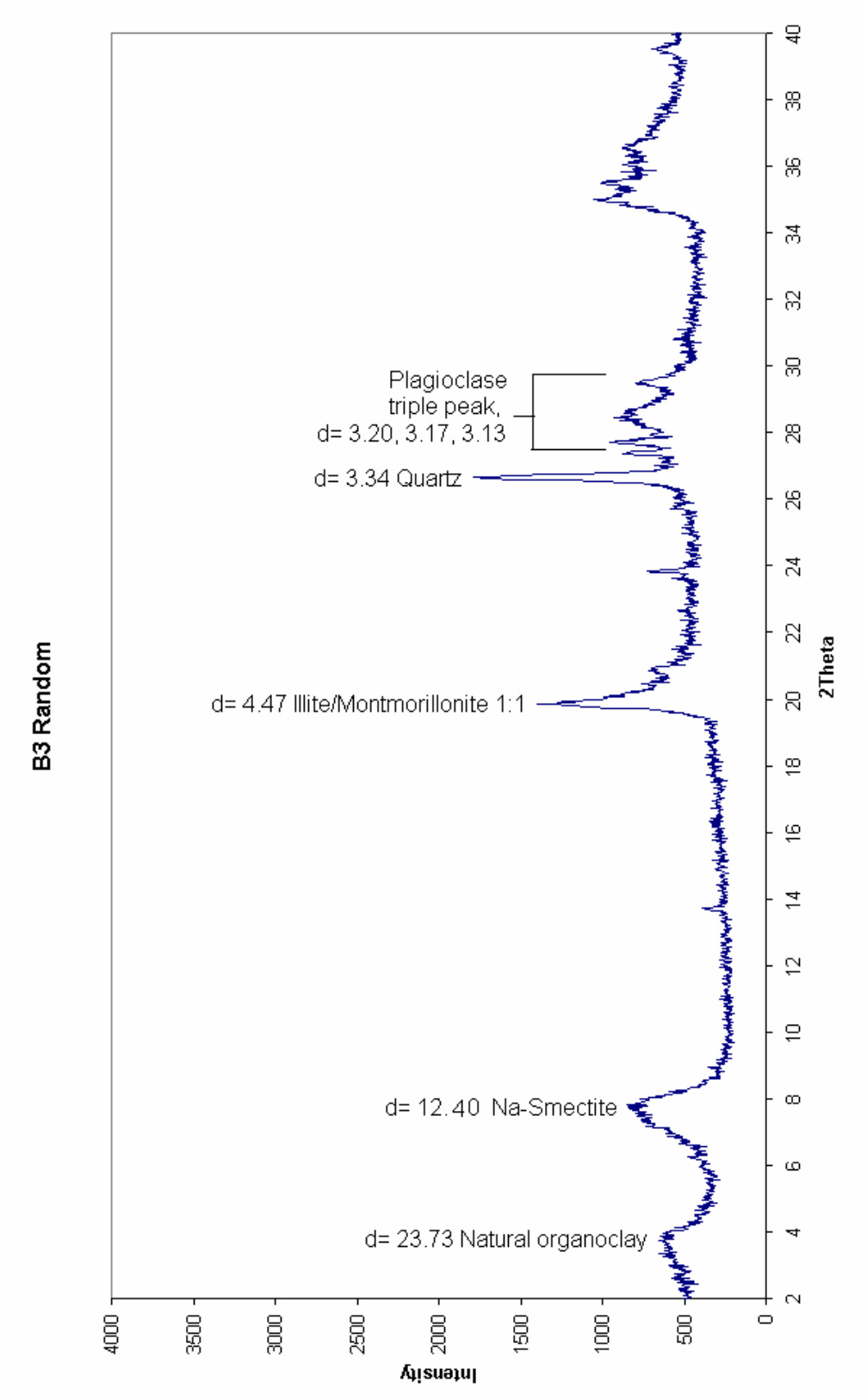

Figure F11. XRD Graph for the Sample B-3 (Random)

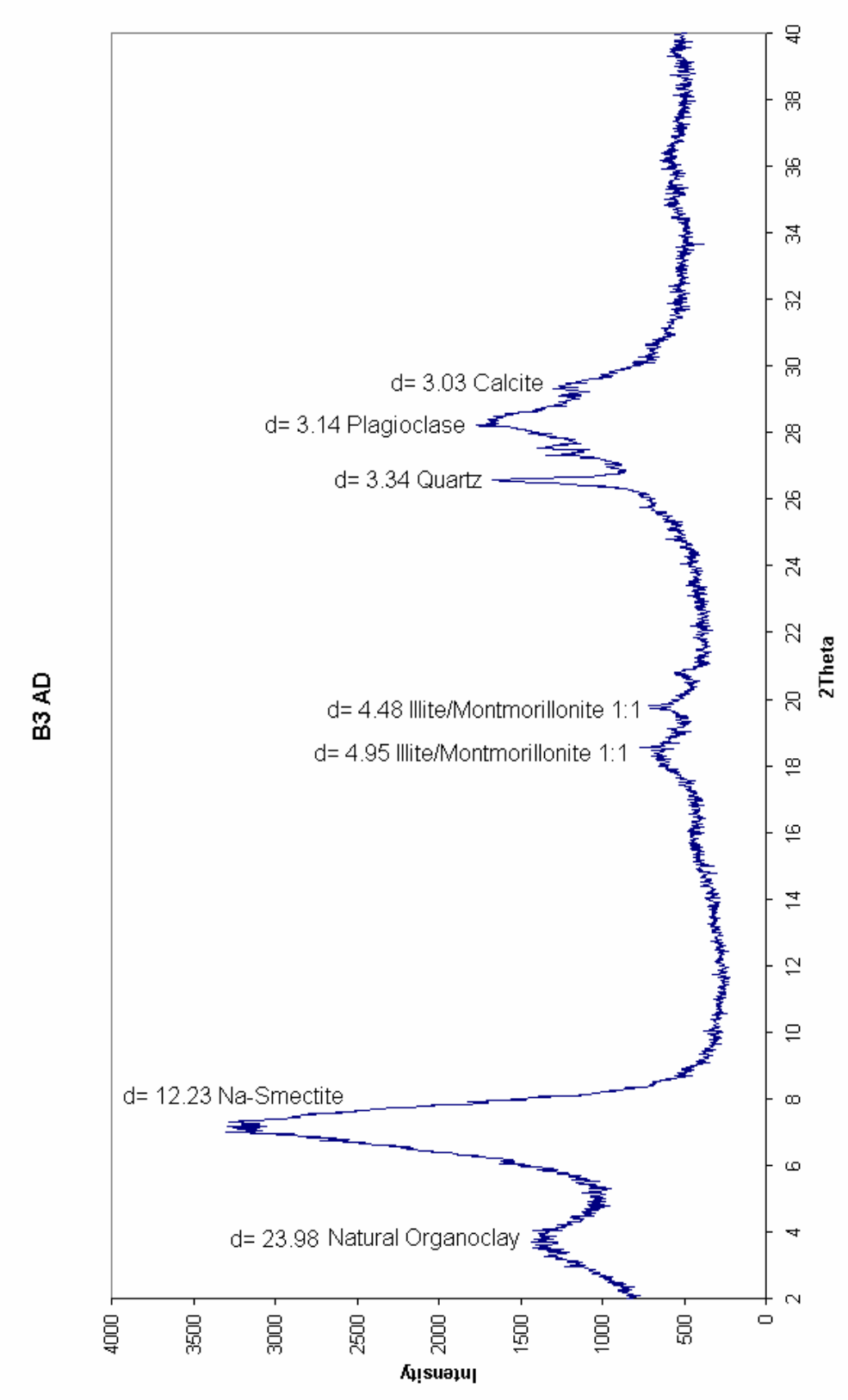

Figure F12. XRD Graph for the Sample B-3 (Air Dried)

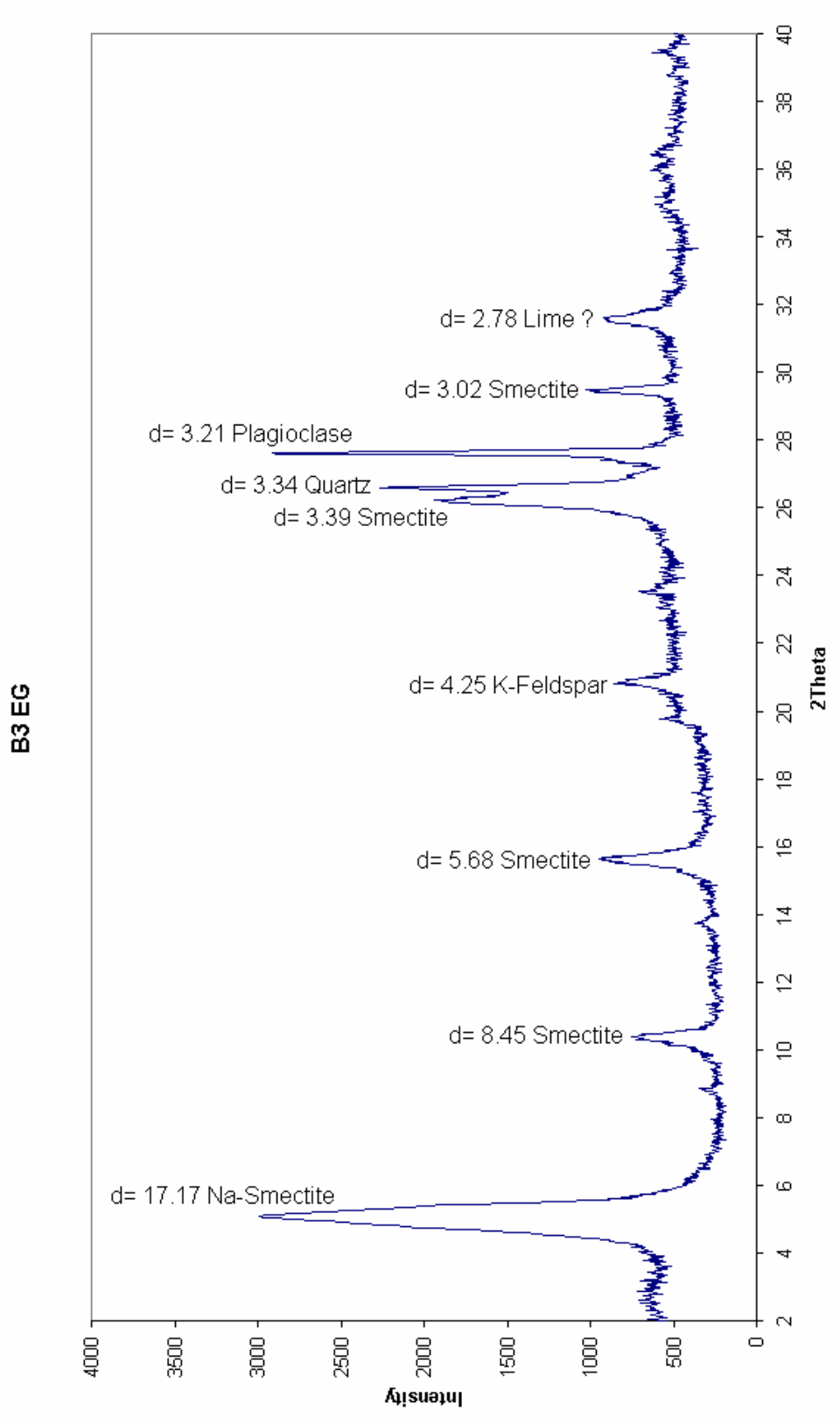

Figure F13. XRD Graph for the Sample B-3 (Ethylene Glycolated)

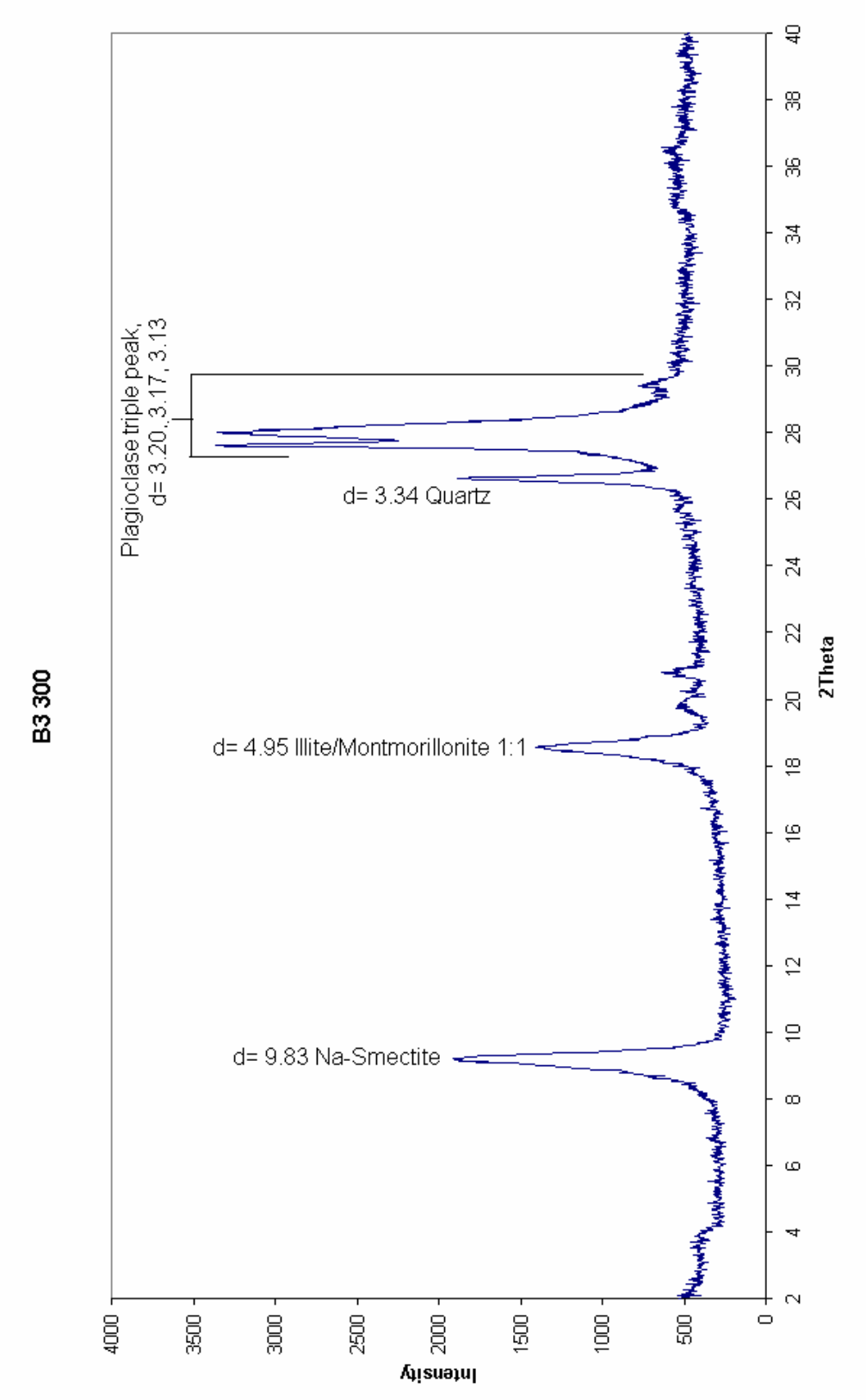

Figure F14. XRD Graph for the Sample B-3 (Heated to 300°C)

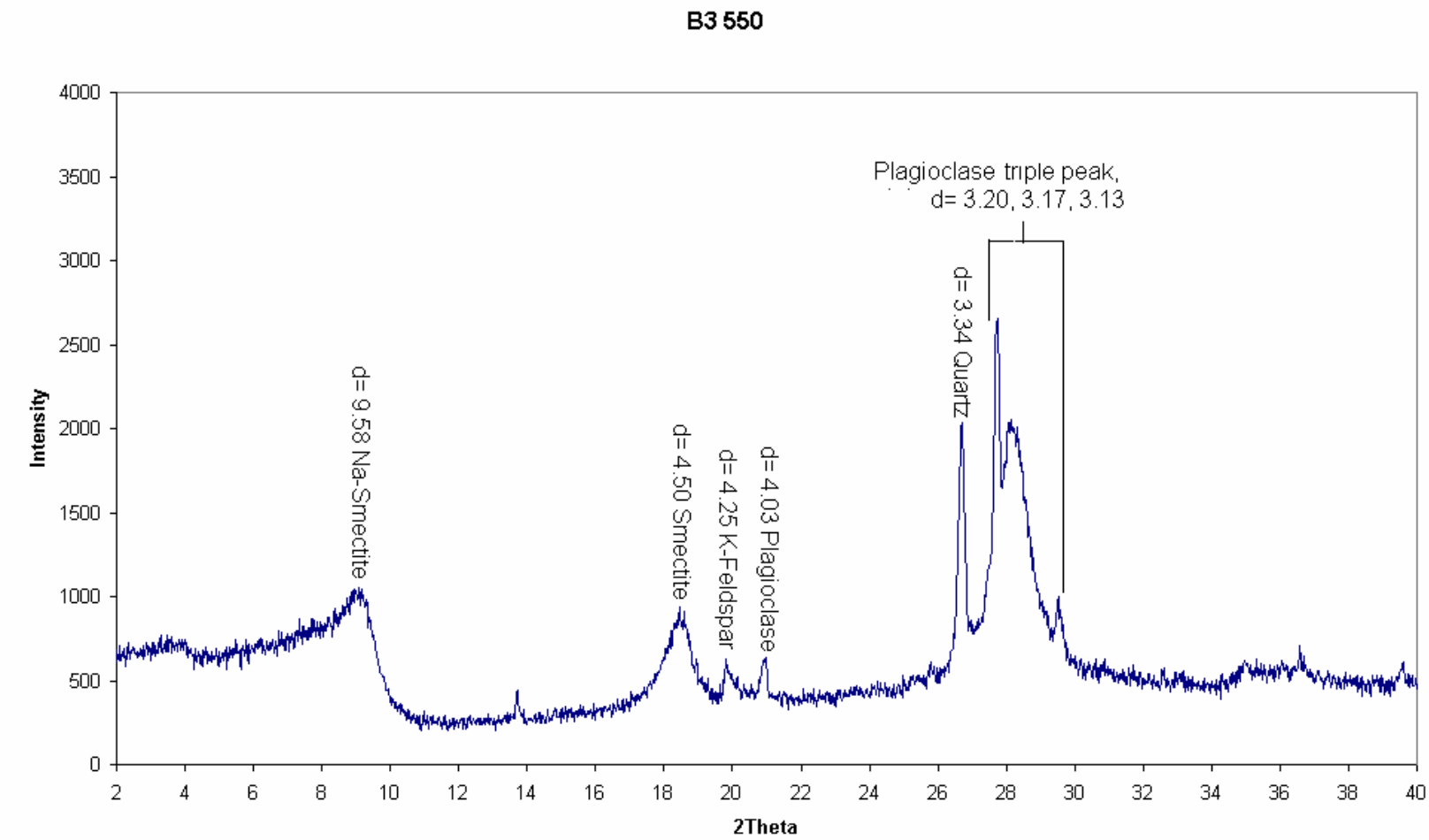

Figure F15. XRD Graph for the Sample B-3 (Heated to 550^{o}C)

APPENDIX G

XRD GRAPHS FOR THE SAMPLES OB1, OB2 AND OB3

Figures G-1 to G-15 show the X-ray diffraction patterns of the selected samples OB-1, OB-2 and OB-3. The samples were placed onto glass lamellas and air-dried. Then they were put into a dessicator containing ethylene glycol. The samples were ethylene glycol solvated and kept in the dessicator for a half day at 60 C°. Those samples were named as "EG". Later on, the samples were placed onto glass lamellas and heated up to 300 C° for 1 hr. in an oven and named as "300". Finally, the samples were again placed onto glass lamellas and heated up to 550 C° for 1 hr. and named as "550". Eventually, 5 diffractograms were obtained from each sample named as Random, AD, EG, 300 and 500.

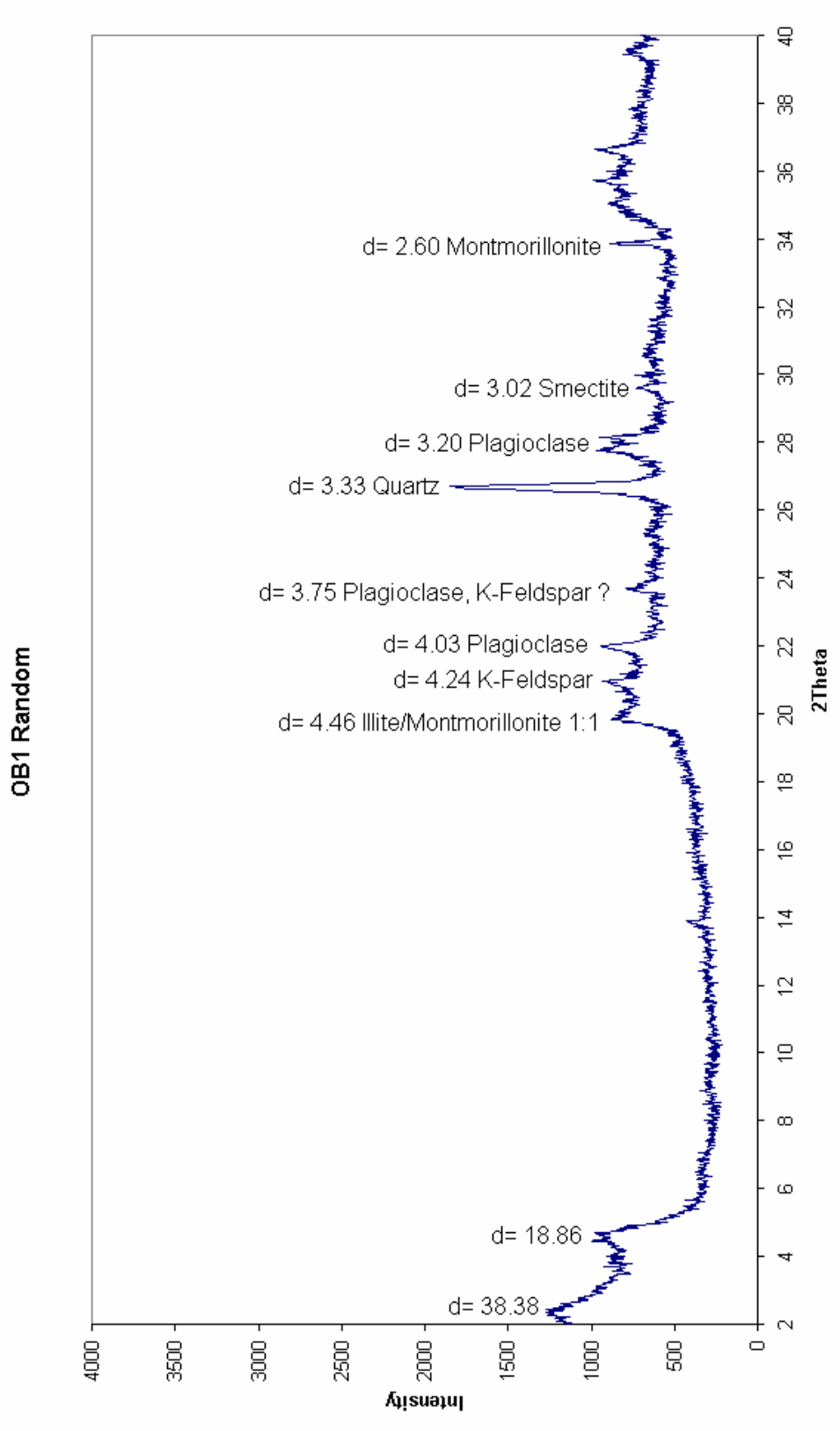

Figure G1. XRD Graph for the Sample OB-1 (Random)

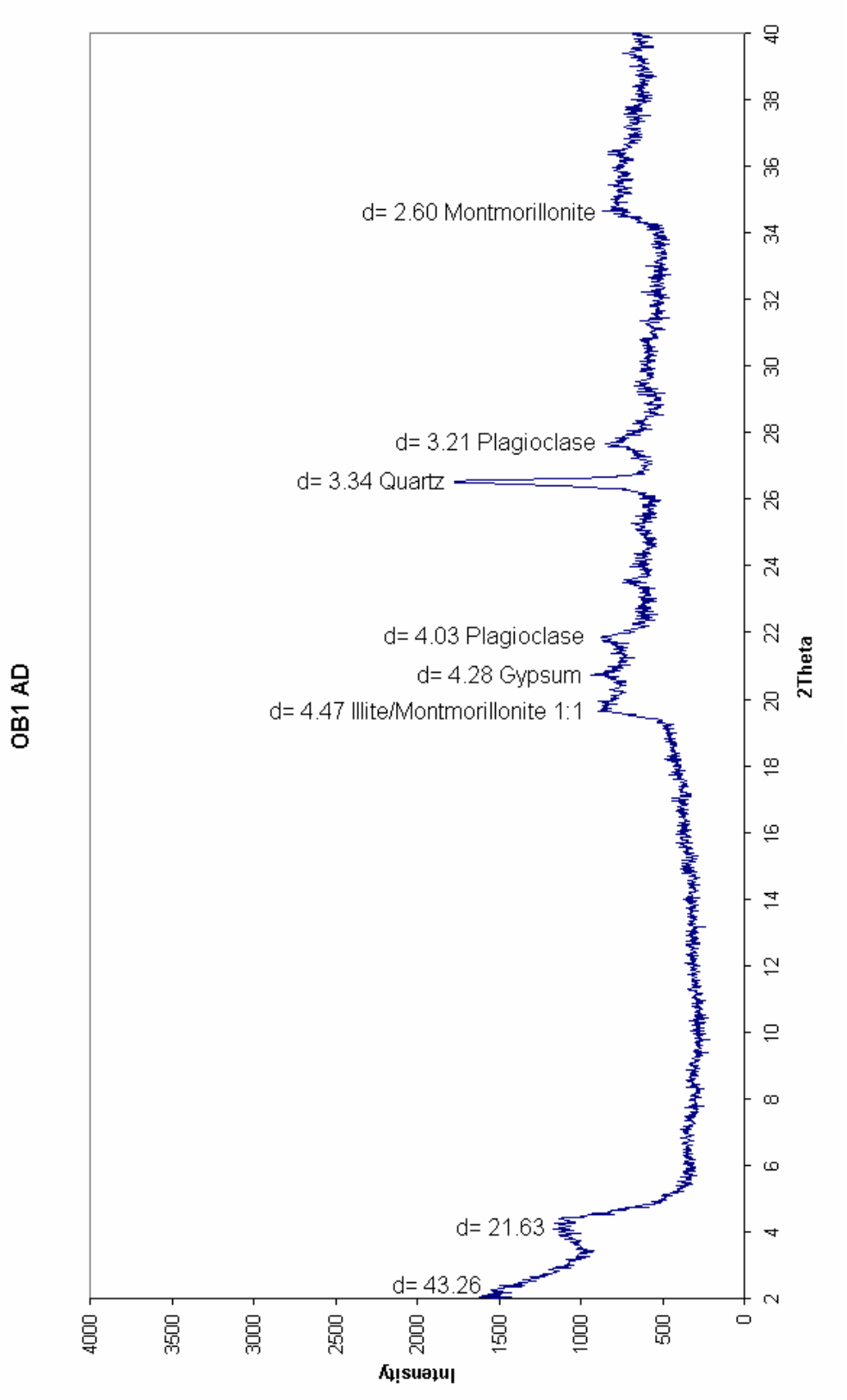

Figure G2. XRD Graph for the Sample OB-1 (Air Dried)

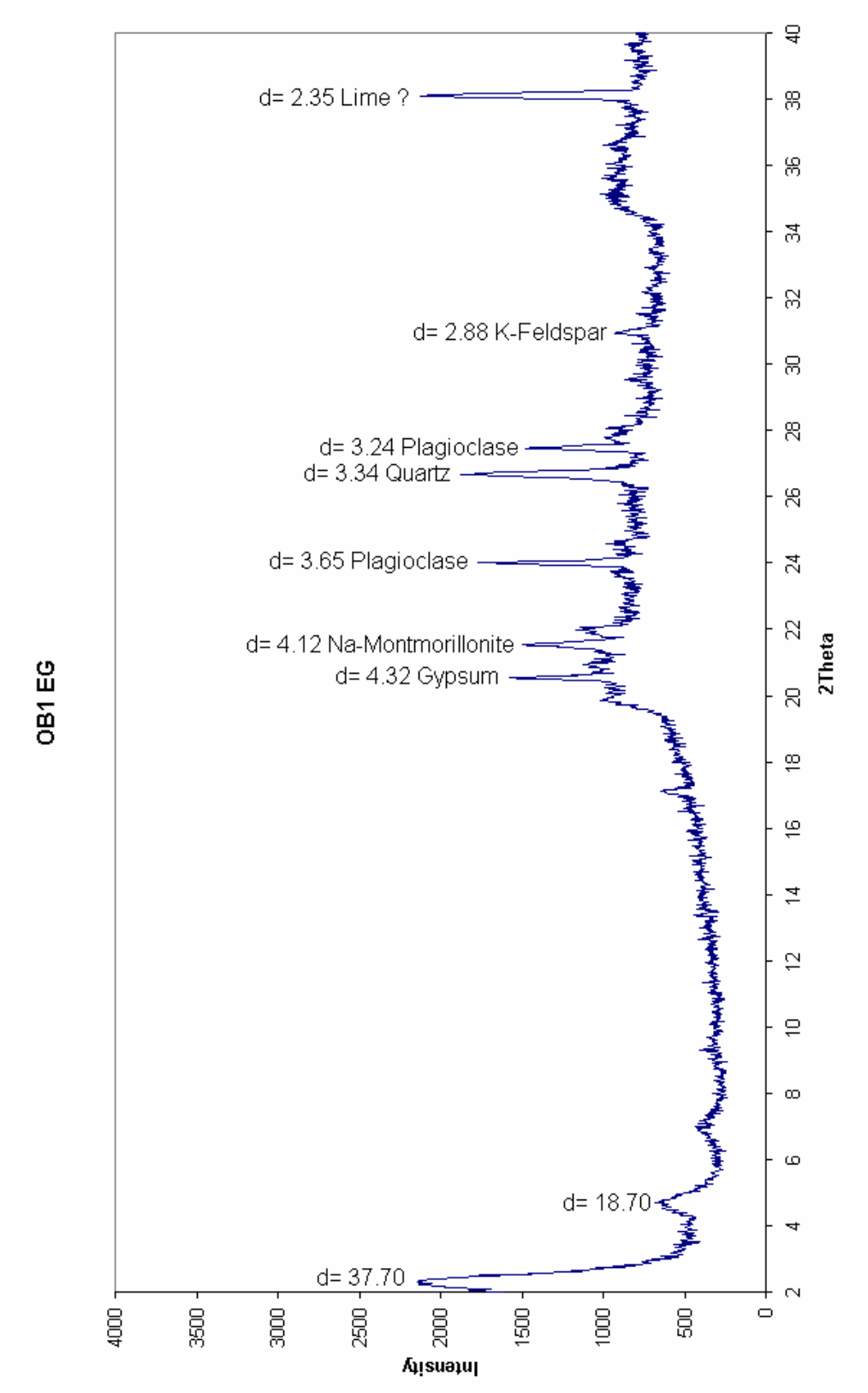

Figure G3. XRD Graph for the Sample OB-1 (Ethylene Glycolated)

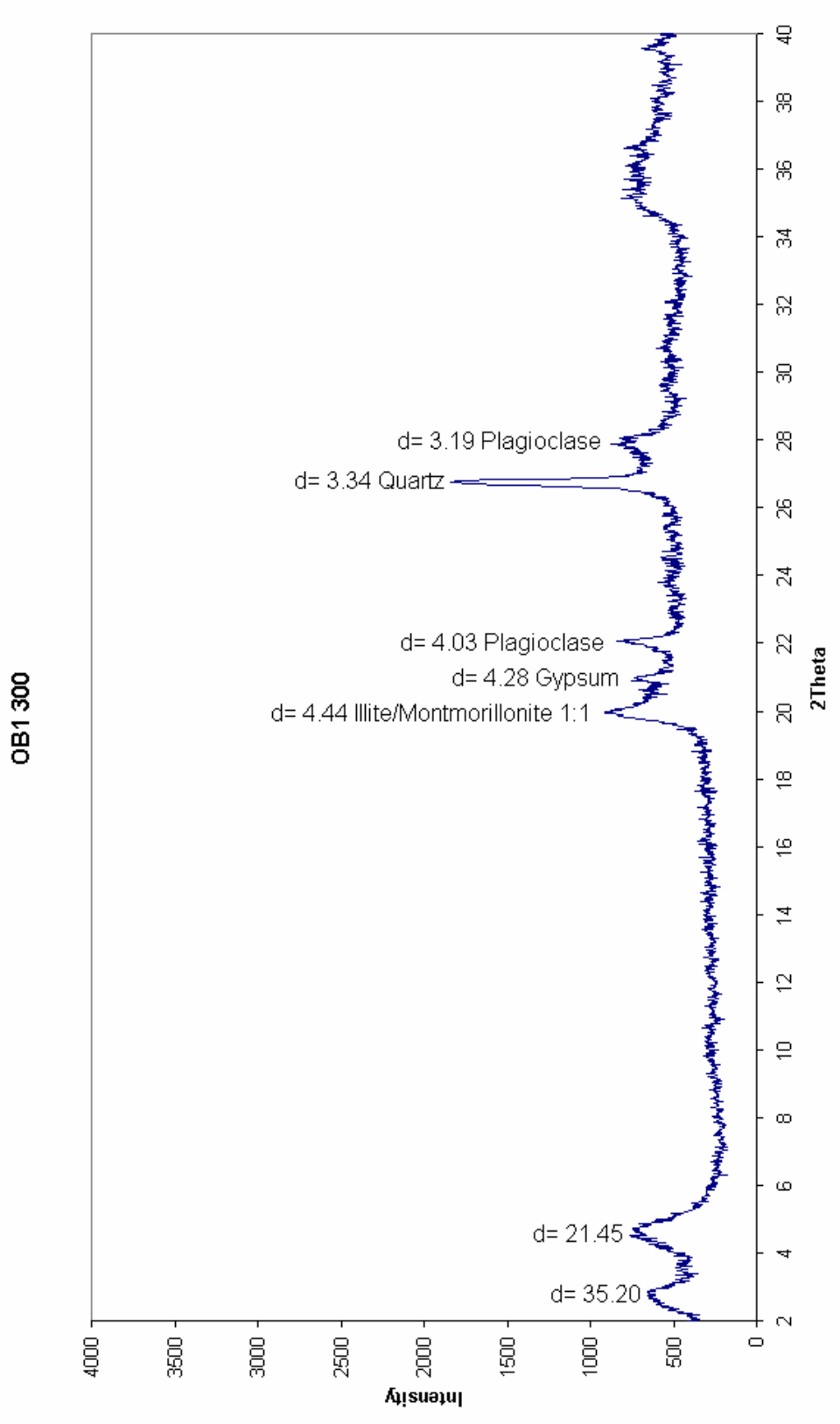

Figure G4. XRD Graph for the Sample OB-1 (Heated to 300°C)

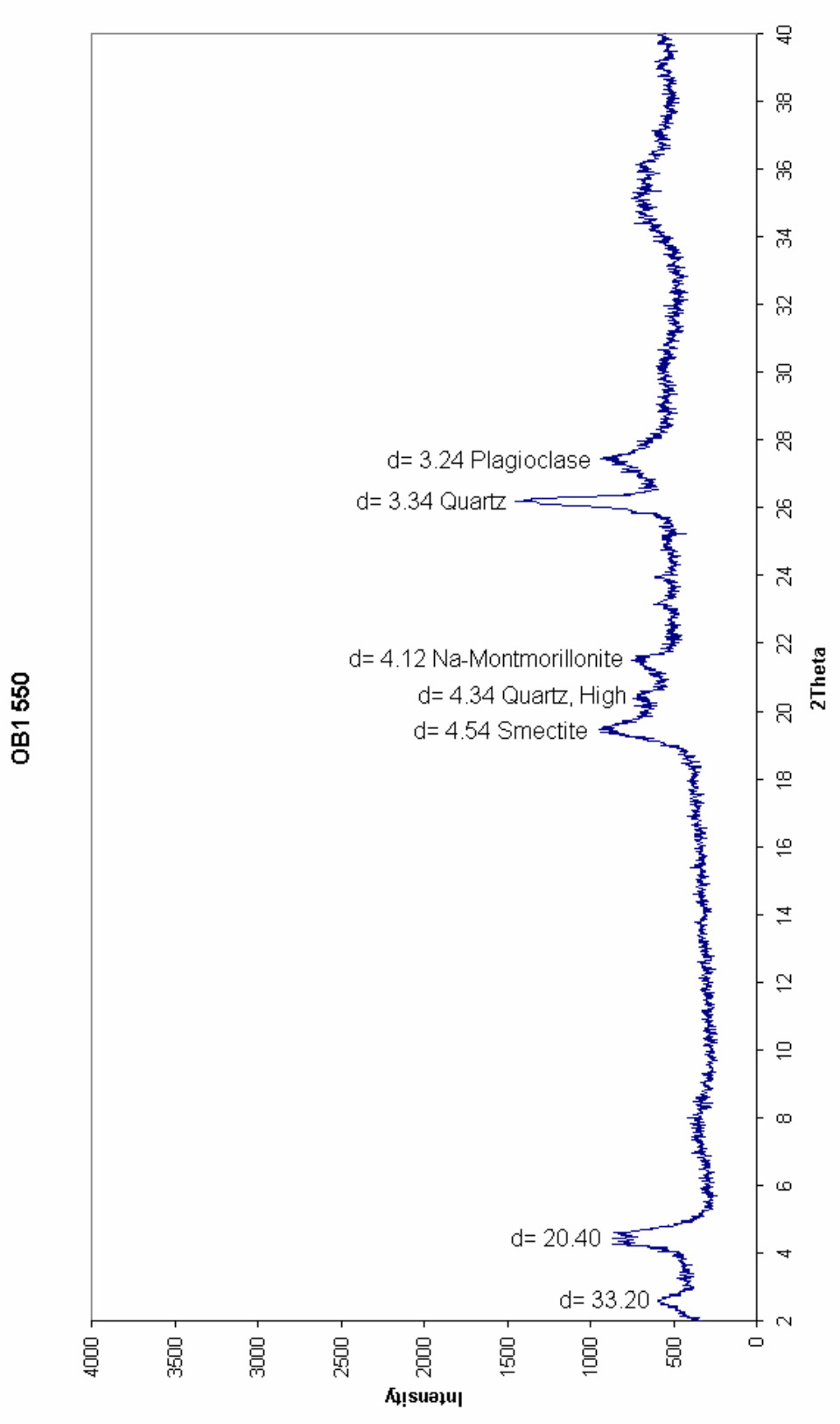

Figure G5. XRD Graph for the Sample OB-1 (Heated to 550^{o}C)

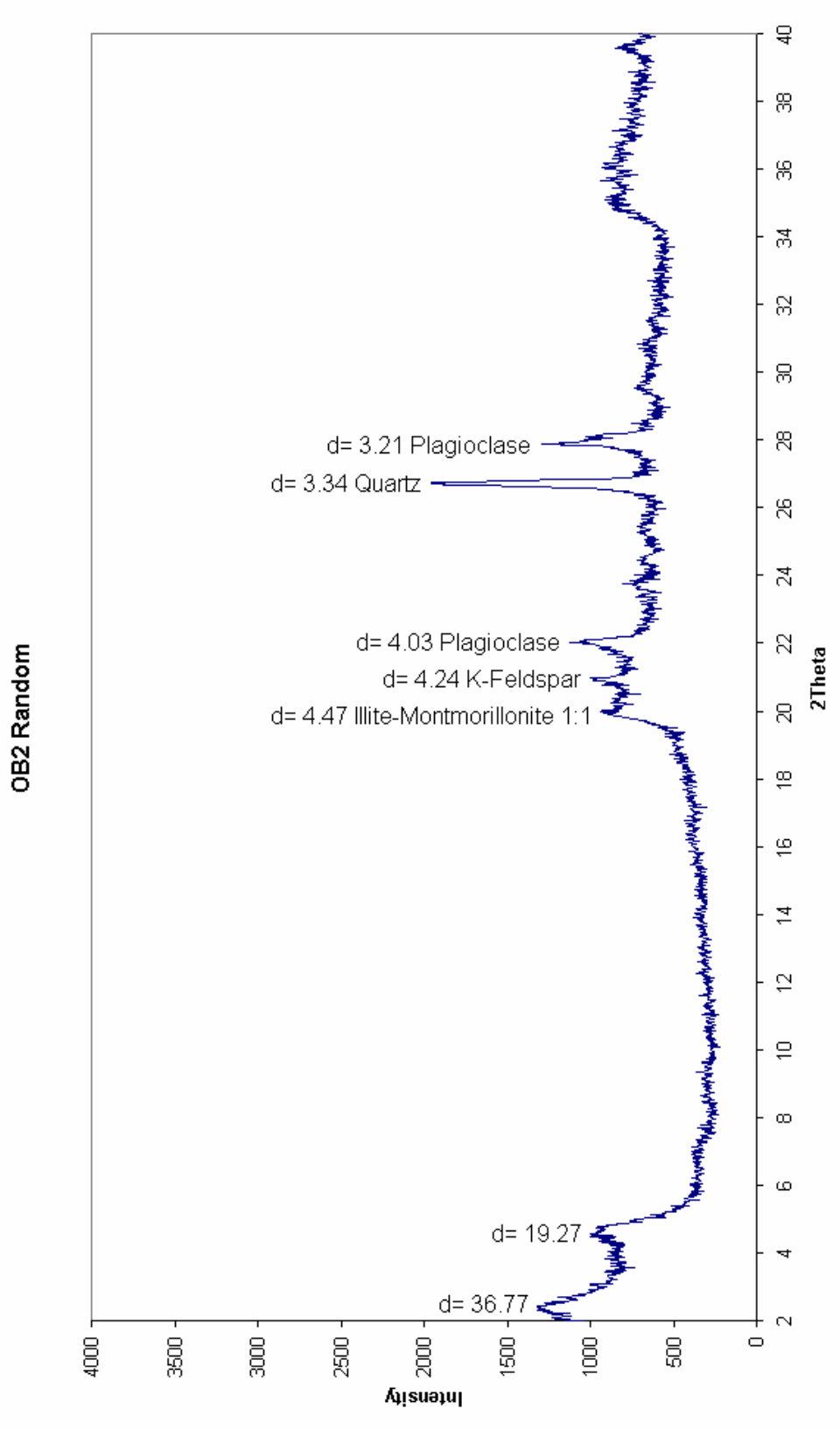

Figure G6. XRD Graph for the Sample OB-2 (Random)

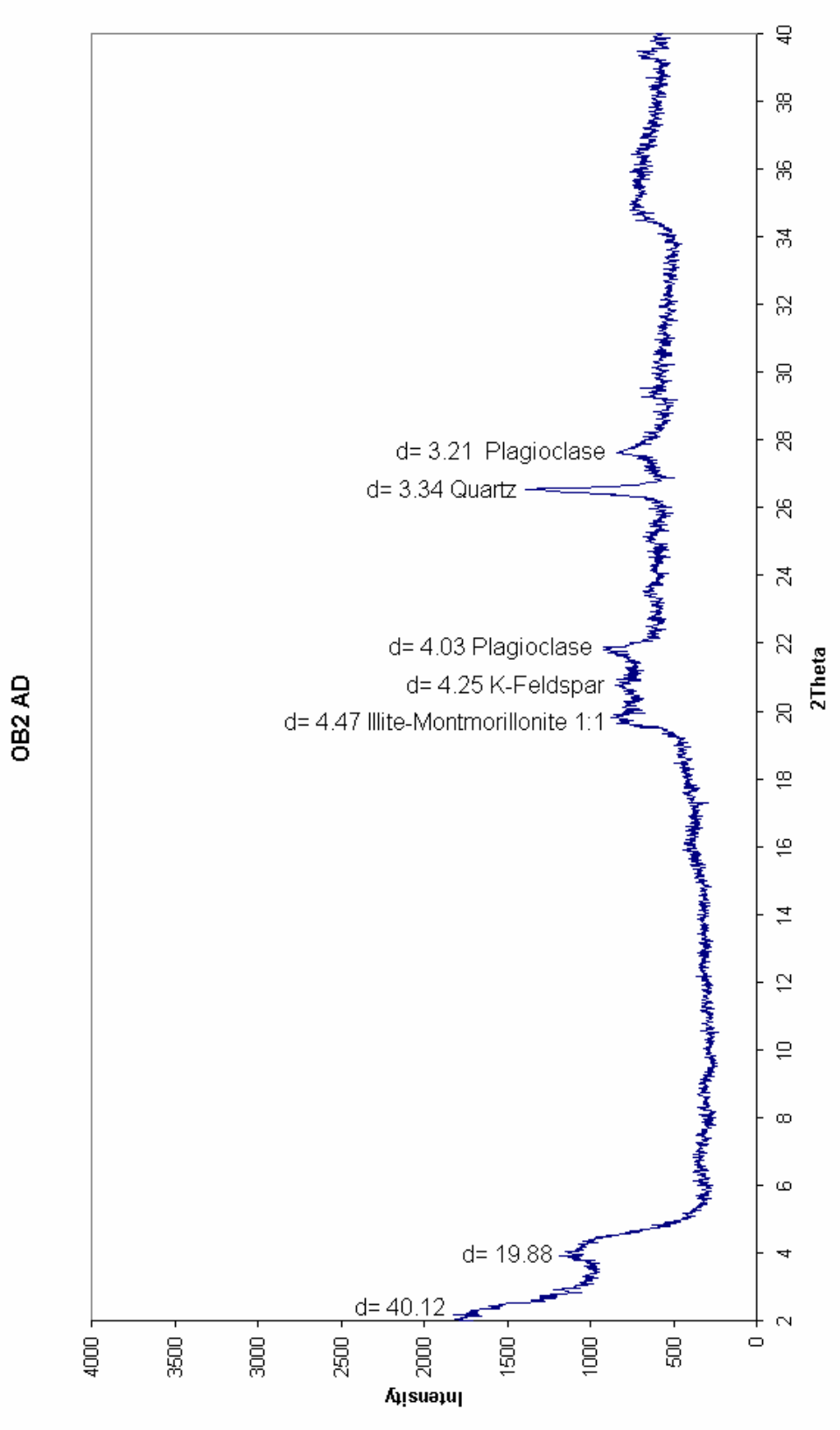

Figure G7. XRD Graph for the Sample OB-2 (Air Dried)

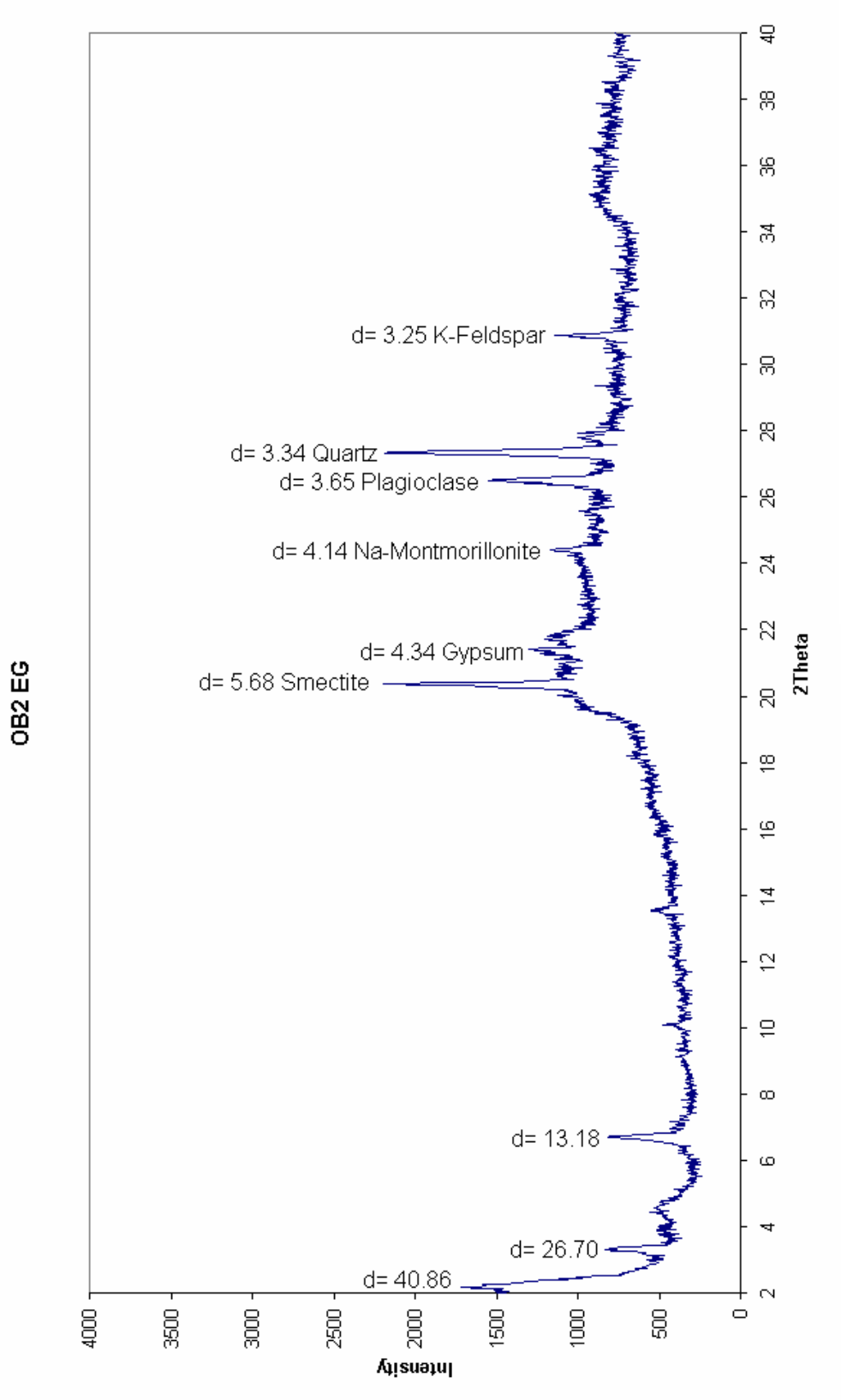

Figure G8. XRD Graph for the Sample OB-2 (Ethylene Glycolated)

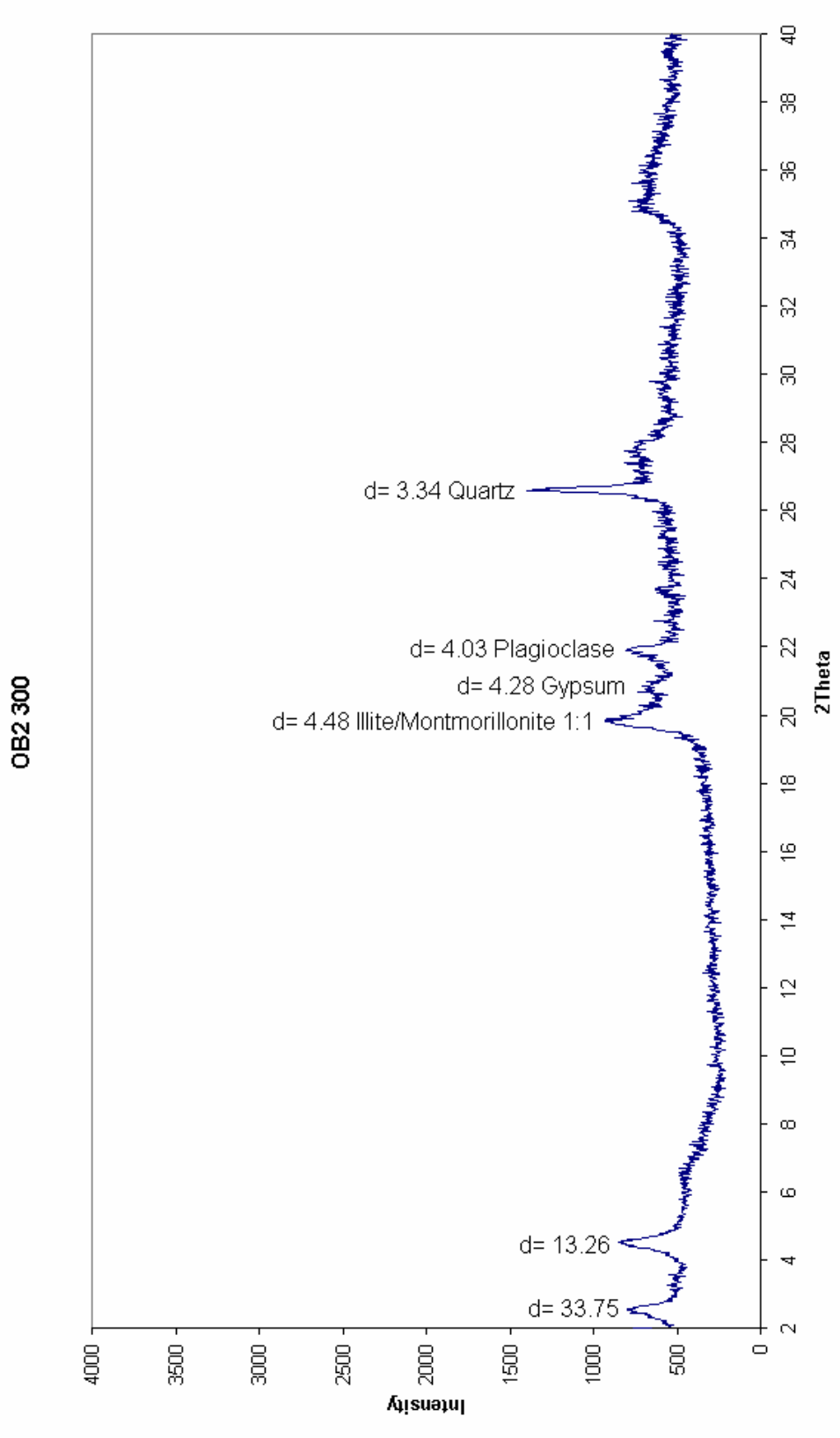

Figure G9. XRD Graph for the Sample OB-2 (300°C)

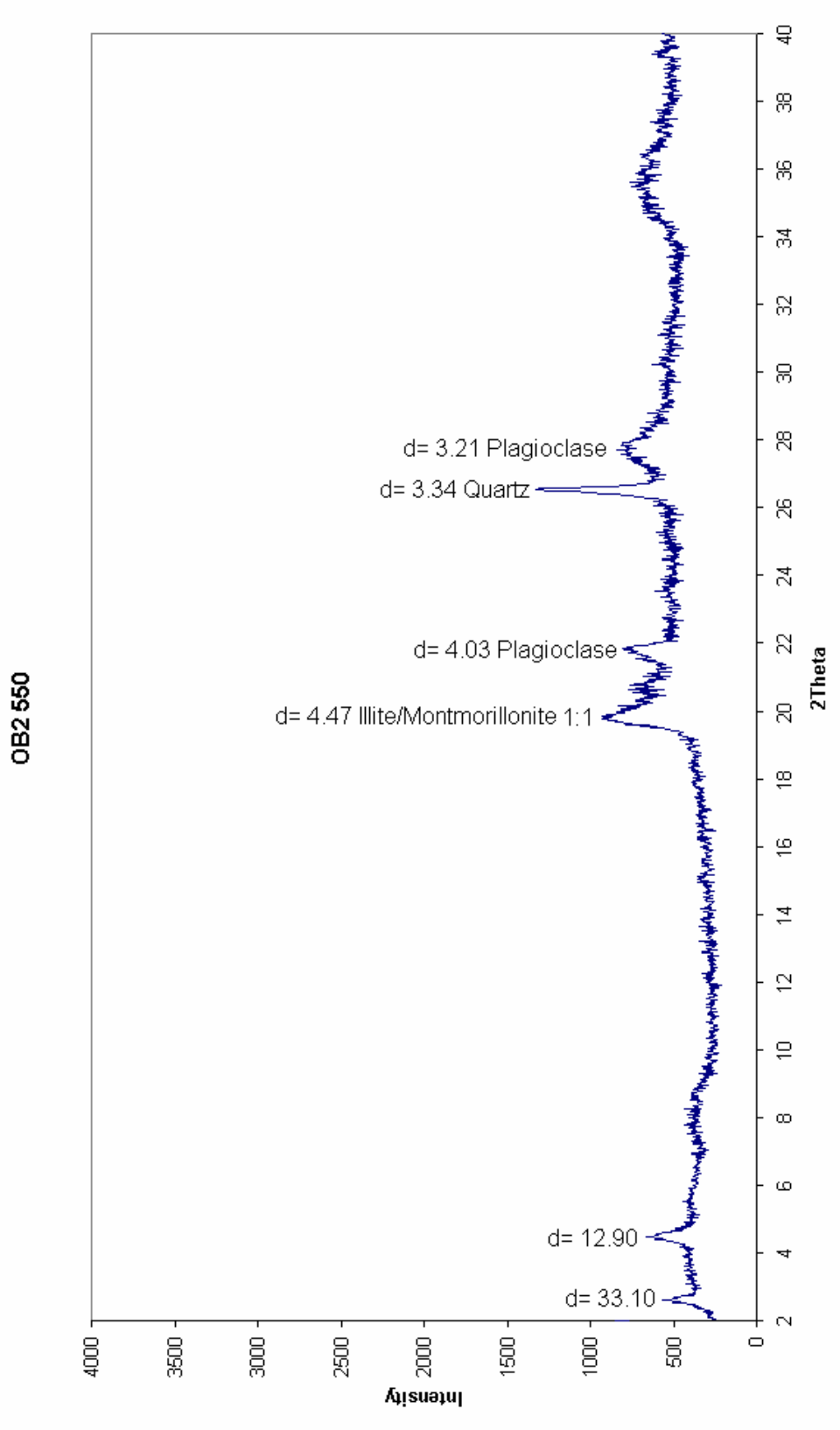

Figure G10. XRD Graph for the Sample OB-2 (Heated to 550°C)

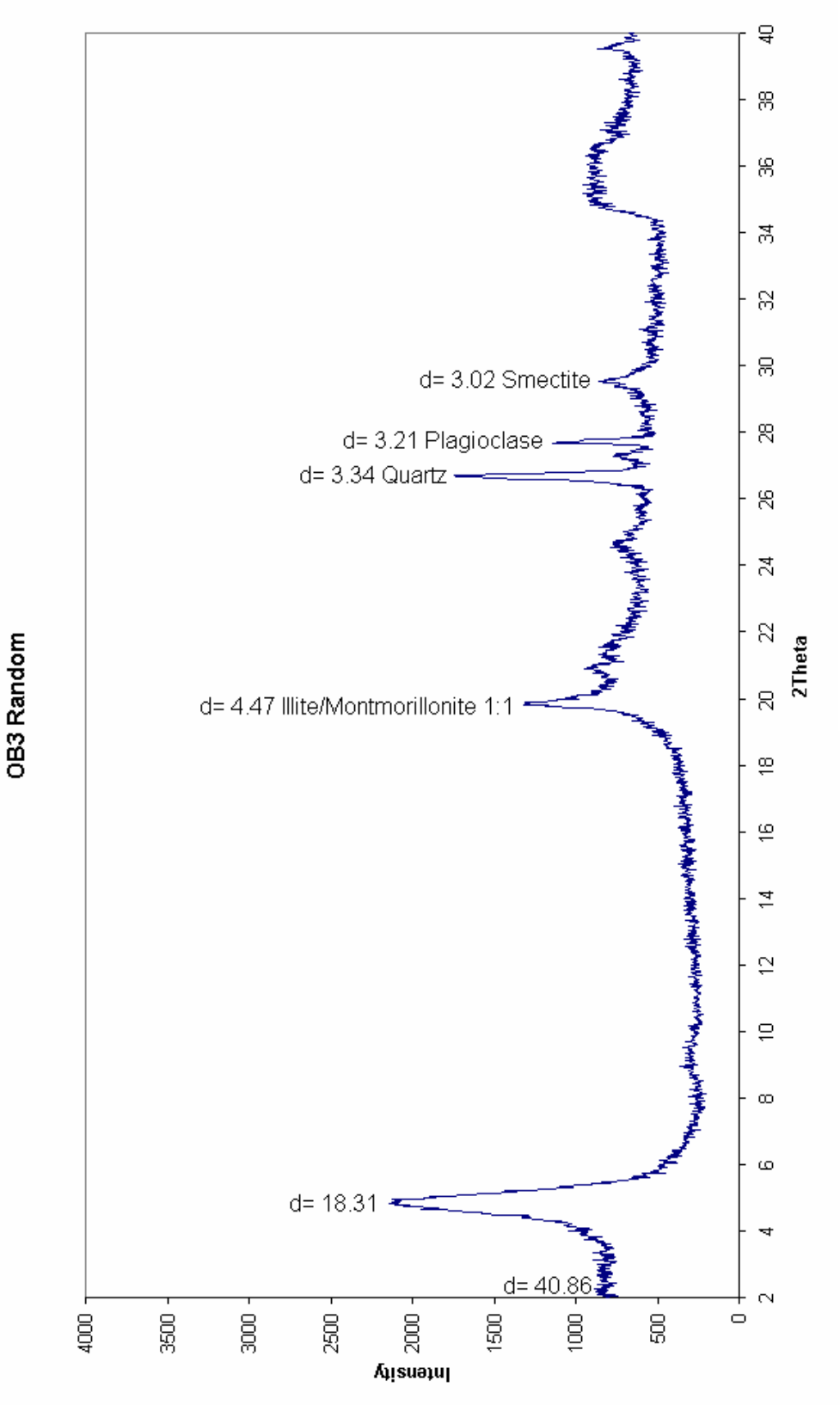

Figure G11. XRD Graph for the Sample OB-3 (Random)

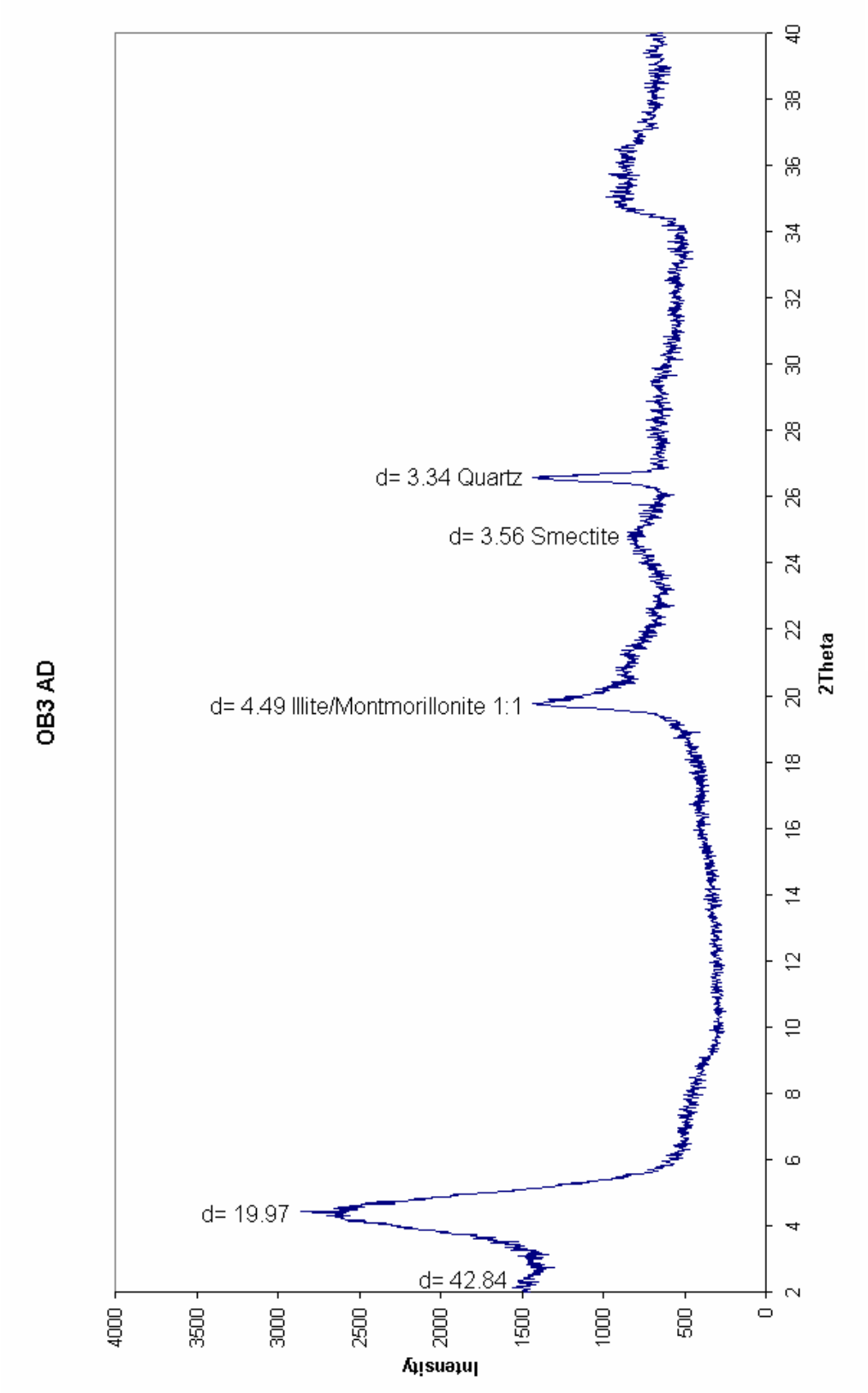

Figure G12. XRD Graph for the Sample OB-3 (Air Dried)

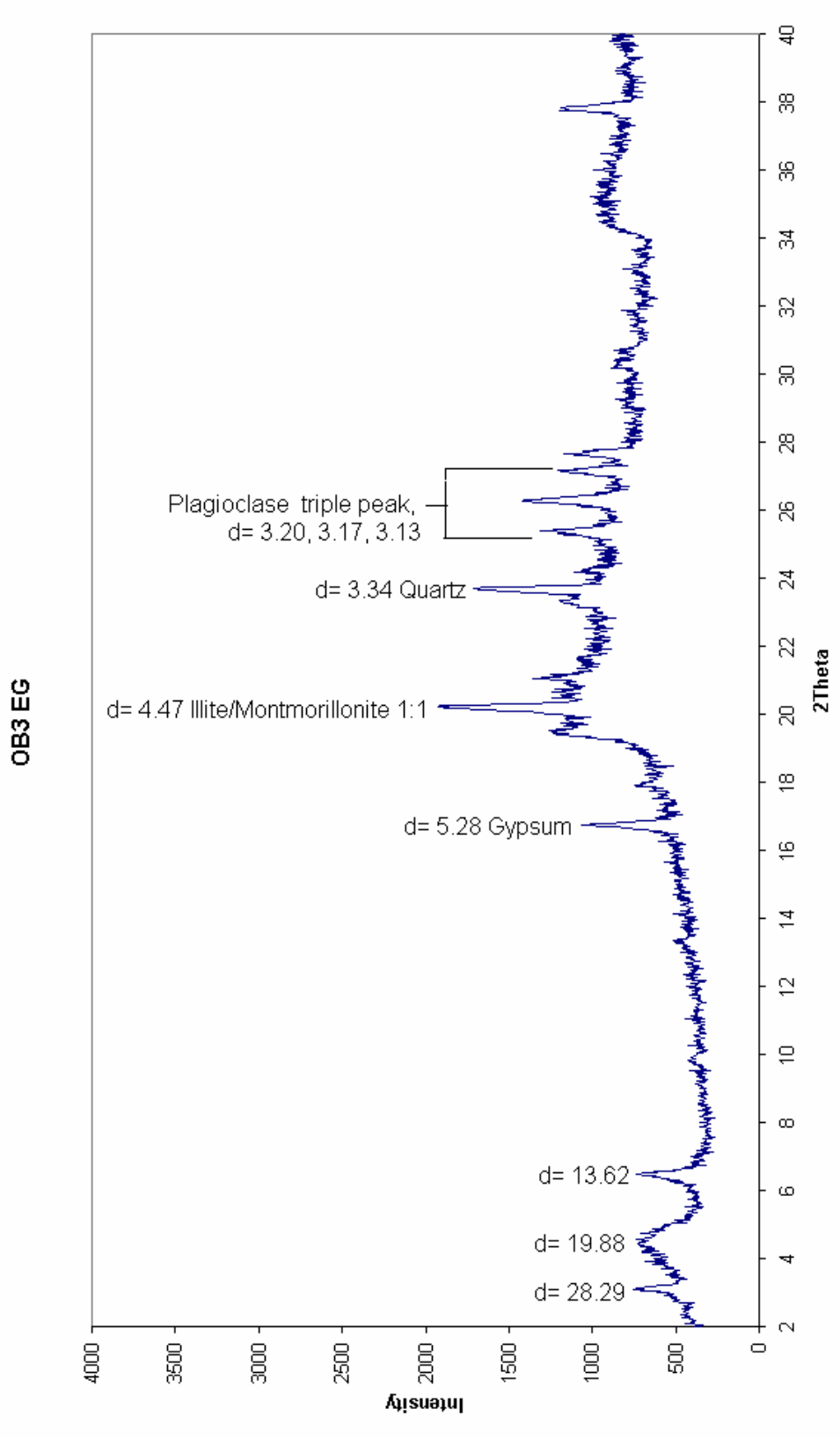

Figure G13. XRD Graph for the Sample OB-3 (Ethylene Glycolated)

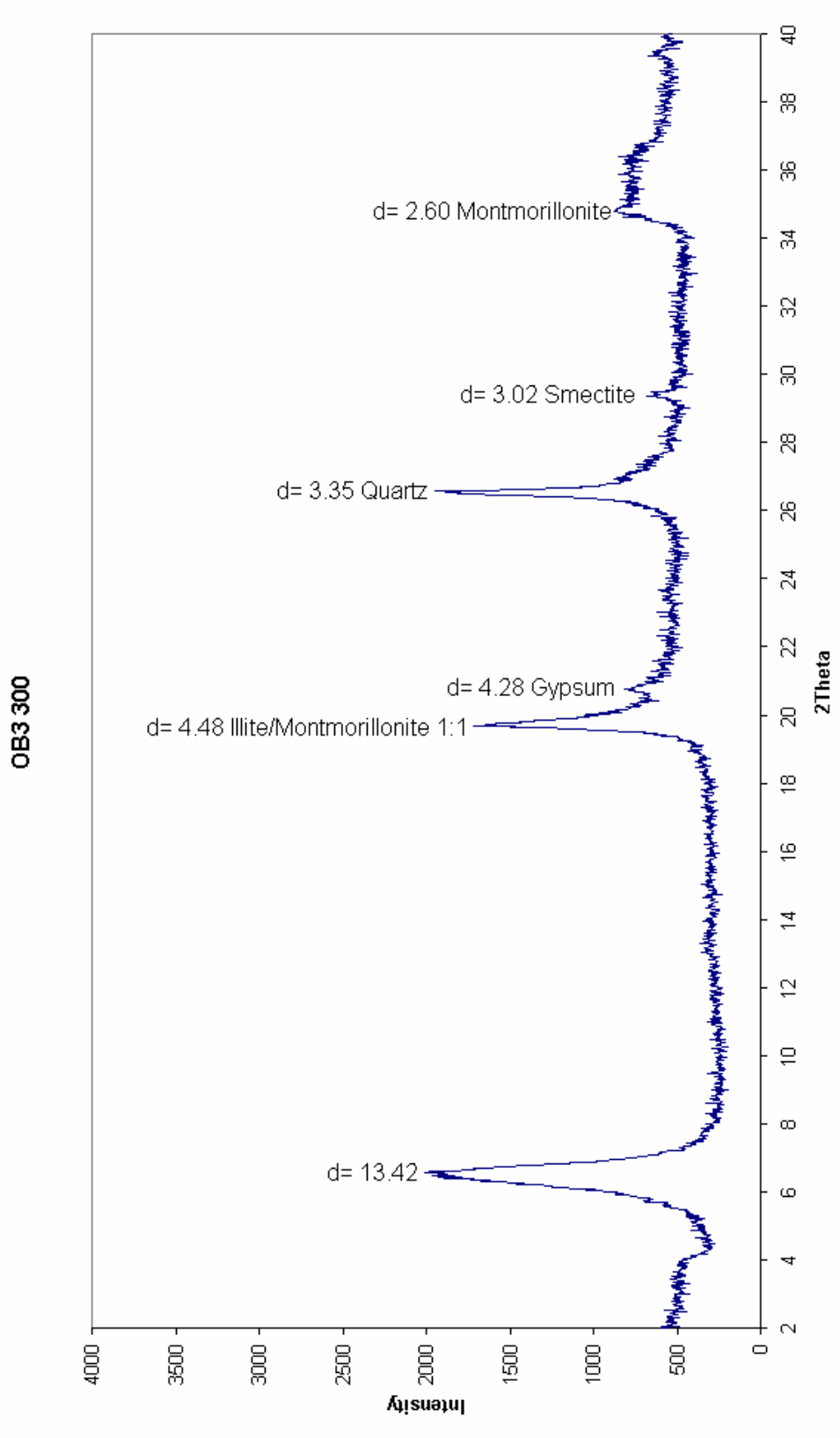

Figure G14. XRD Graph for the Sample OB-3 (Heated to 300^{o}C)

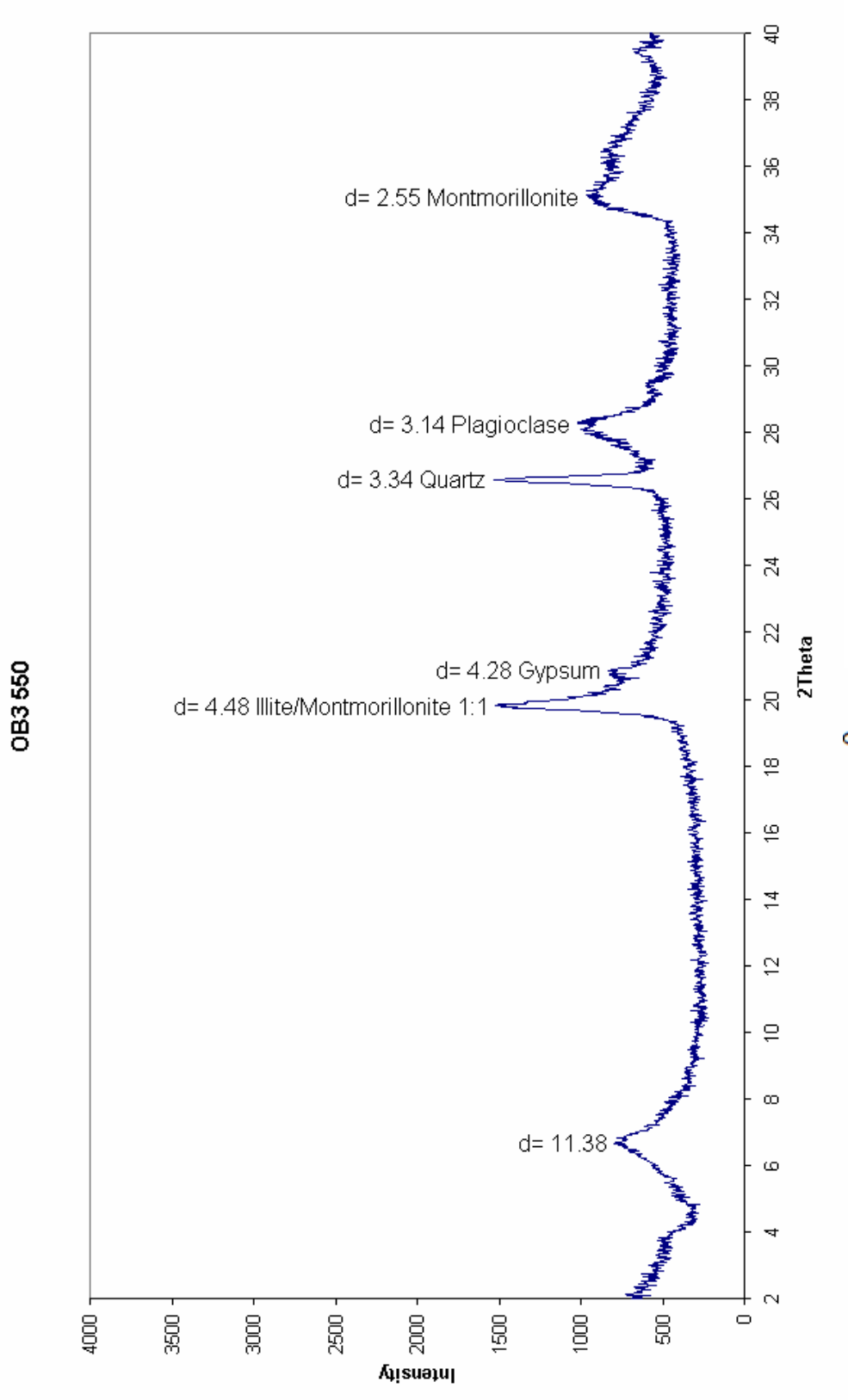

Figure G15. XRD Graph for the Sample OB-3 (Heated to 550^{o}C)

APPENDIX H

XRD GRAPHS FOR CLAY-POLYMER NANOCOMPOSITES WITH VARYING POLYMER CONTENT

Figures H1 to H6 show X-ray diffraction patterns of the samples produced from the sample OB-1. The samples contain 7, 17, 25, 30, 40, 50 % w/w polyacrylamide and named as CPN 7%, CPN 17%, CPN 25%, CPN 30%, CPN 40 % and CPN 50% respectively. The X-ray diffractograms of produced clay-polymer nanocomposites were taken randomly and named as "CPN". For example, a nanocomposite containing 30% w/w polymer content was named as CPN 30.

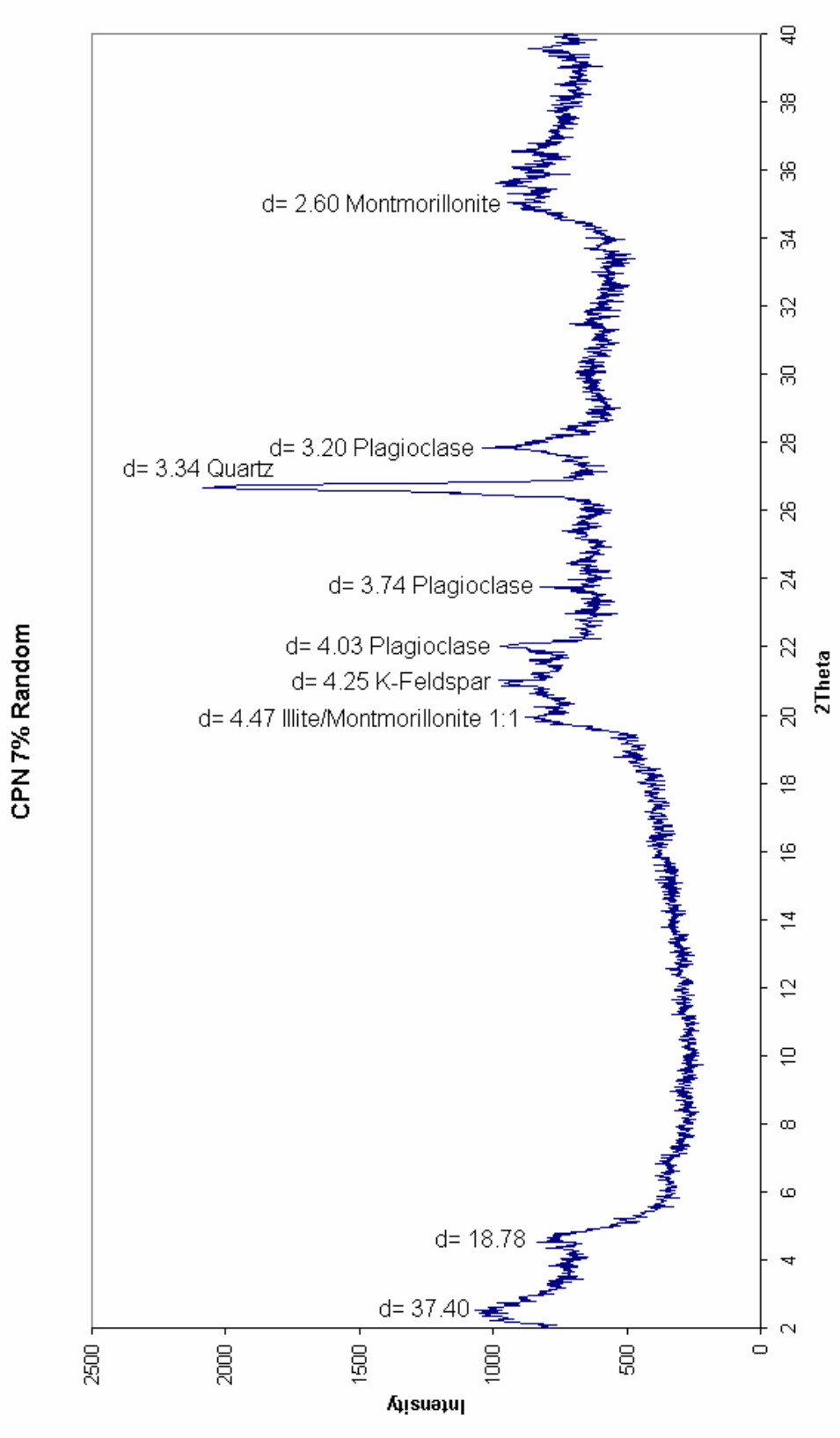

Figure H1. XRD Graph for Clay-Polymer Nanocomposite with 7% Polymer (Random)

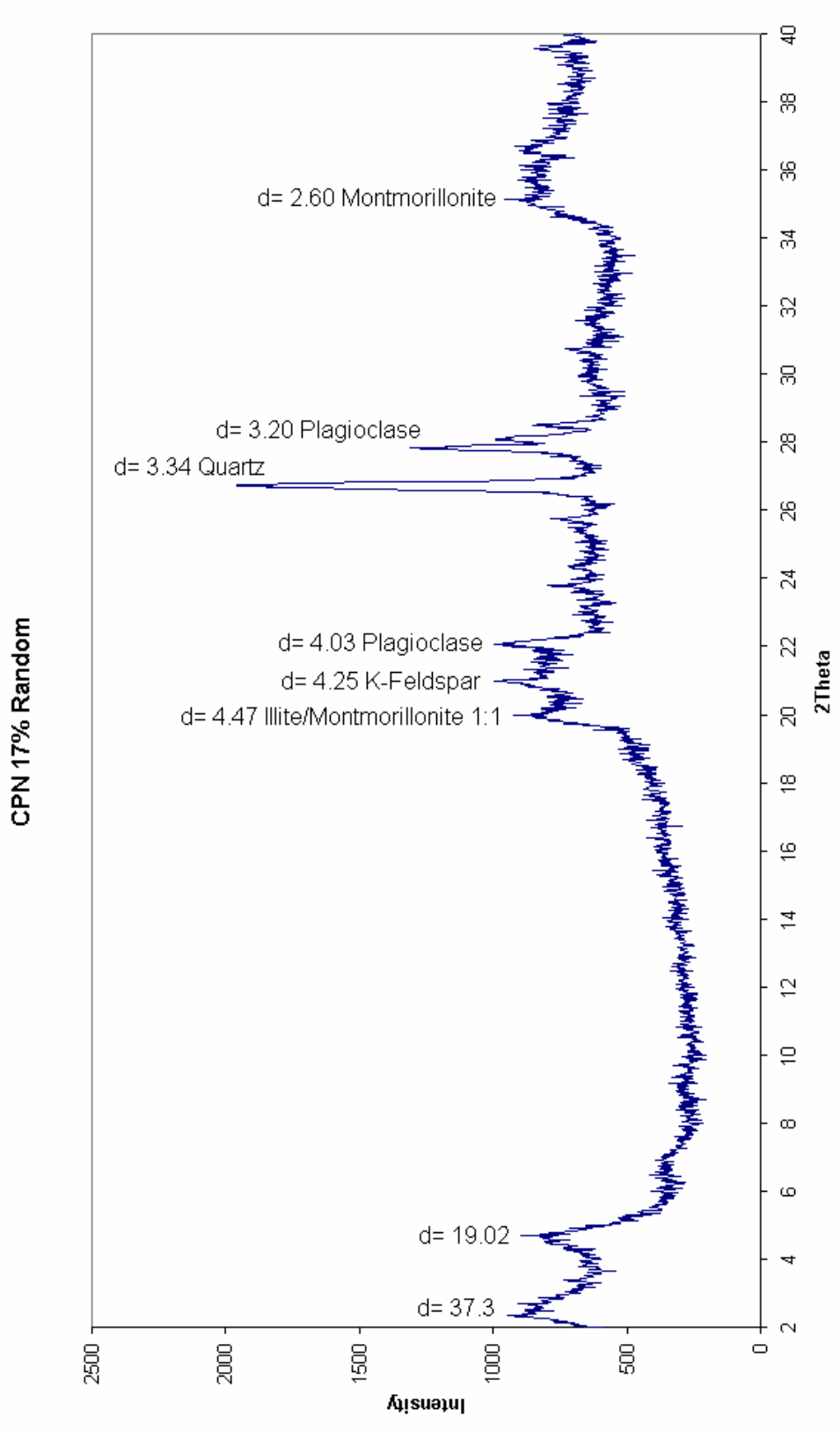

Figure H2. XRD Graph for Clay-Polymer Nanocomposite with 17% Polymer (Random)

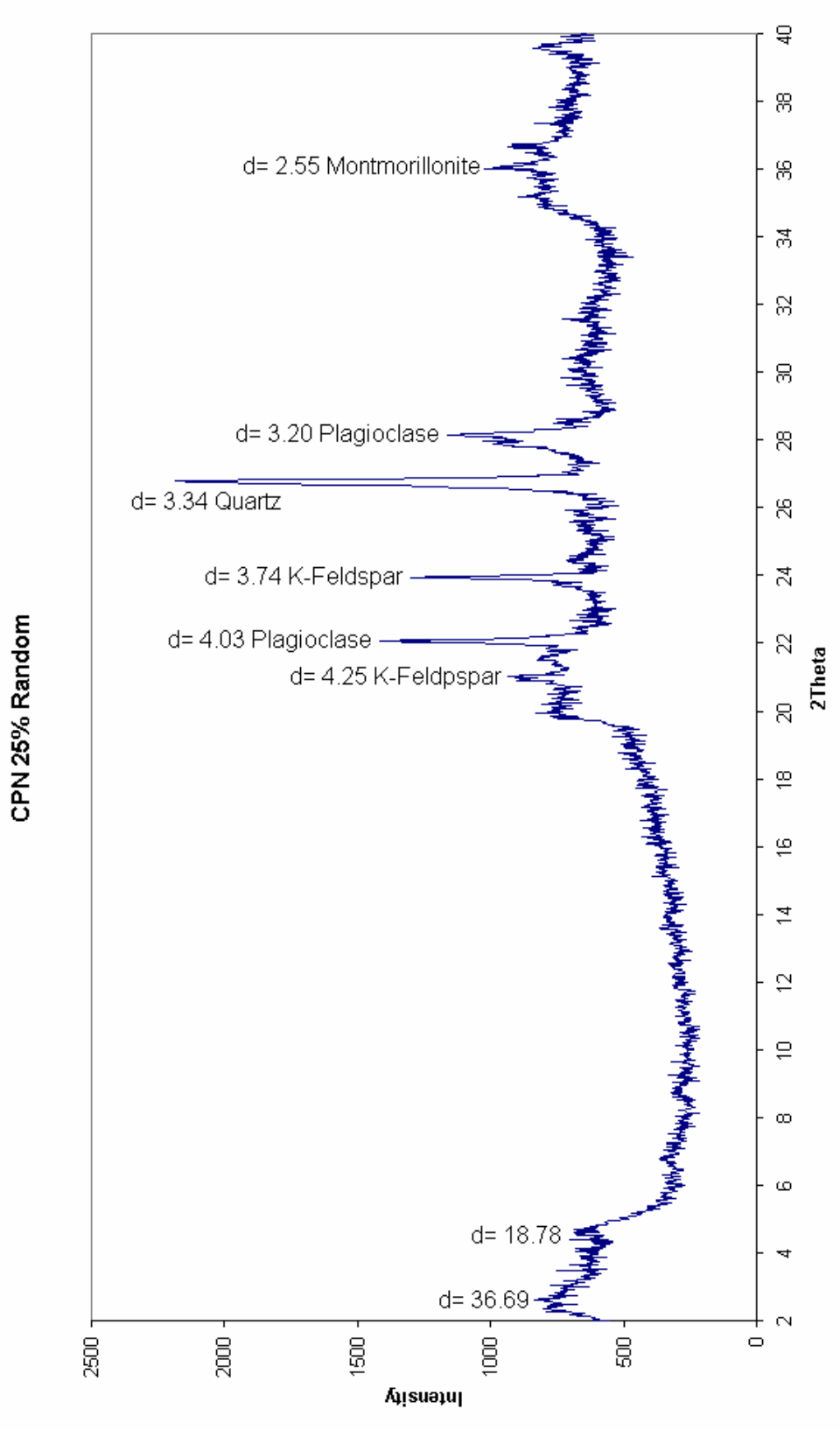

Figure H3. XRD Graph for Clay-Polymer Nanocomposite with 25% Polymer (Random)

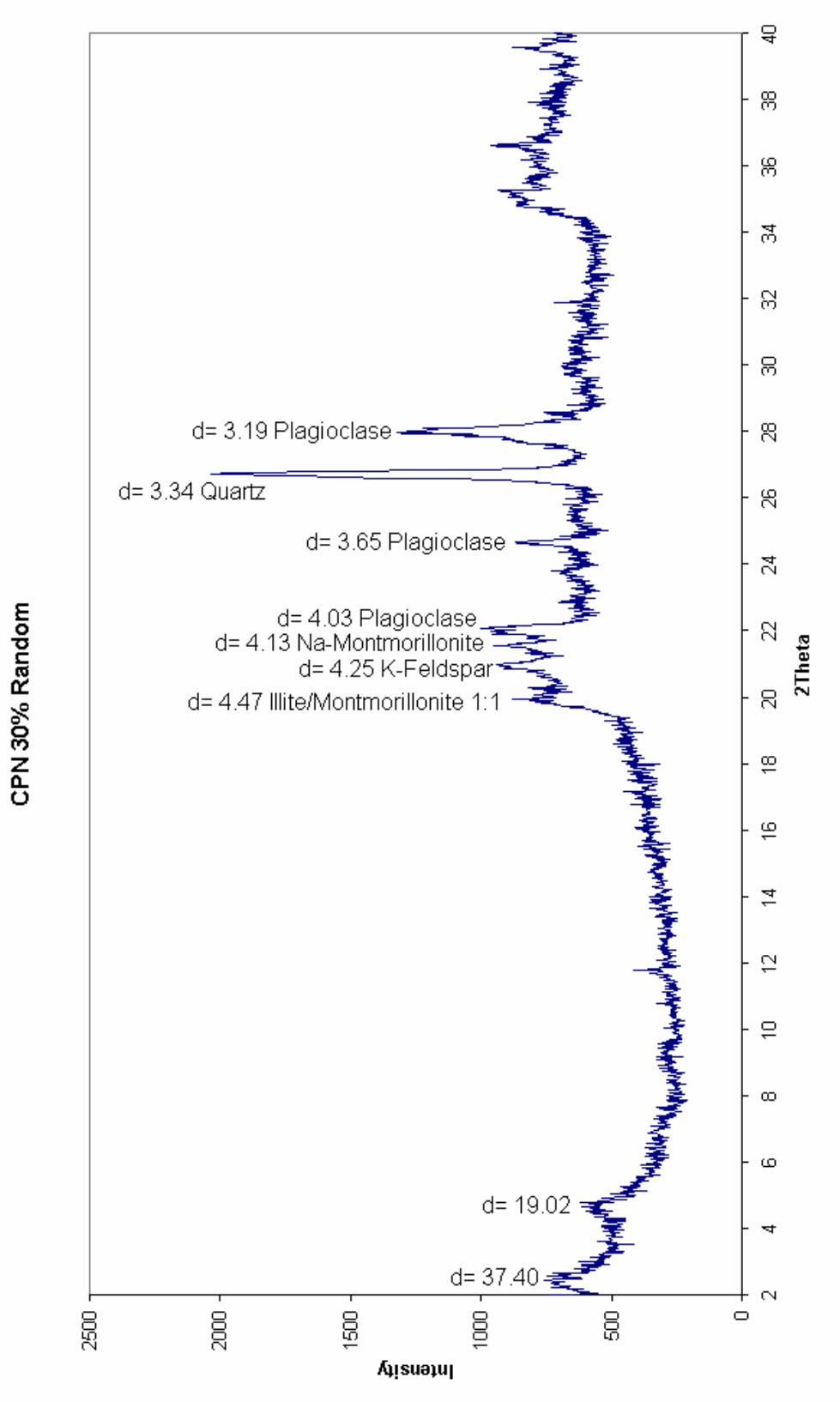

Figure H4. XRD Graph for Clay-Polymer Nanocomposite with 30% Polymer (Random)

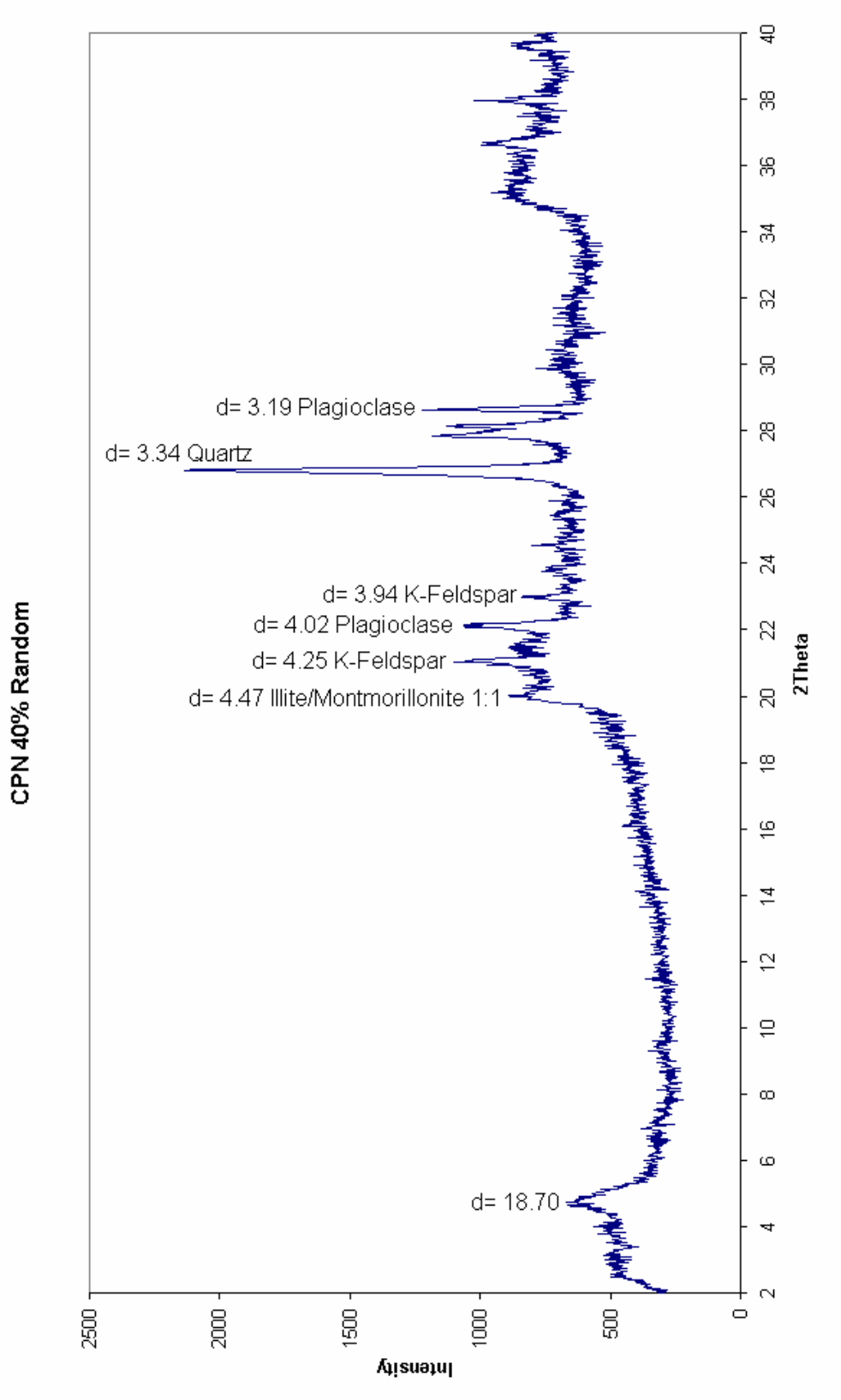

Figure H5. XRD Graph for Clay-Polymer Nanocomposite with 40% Polymer (Random)

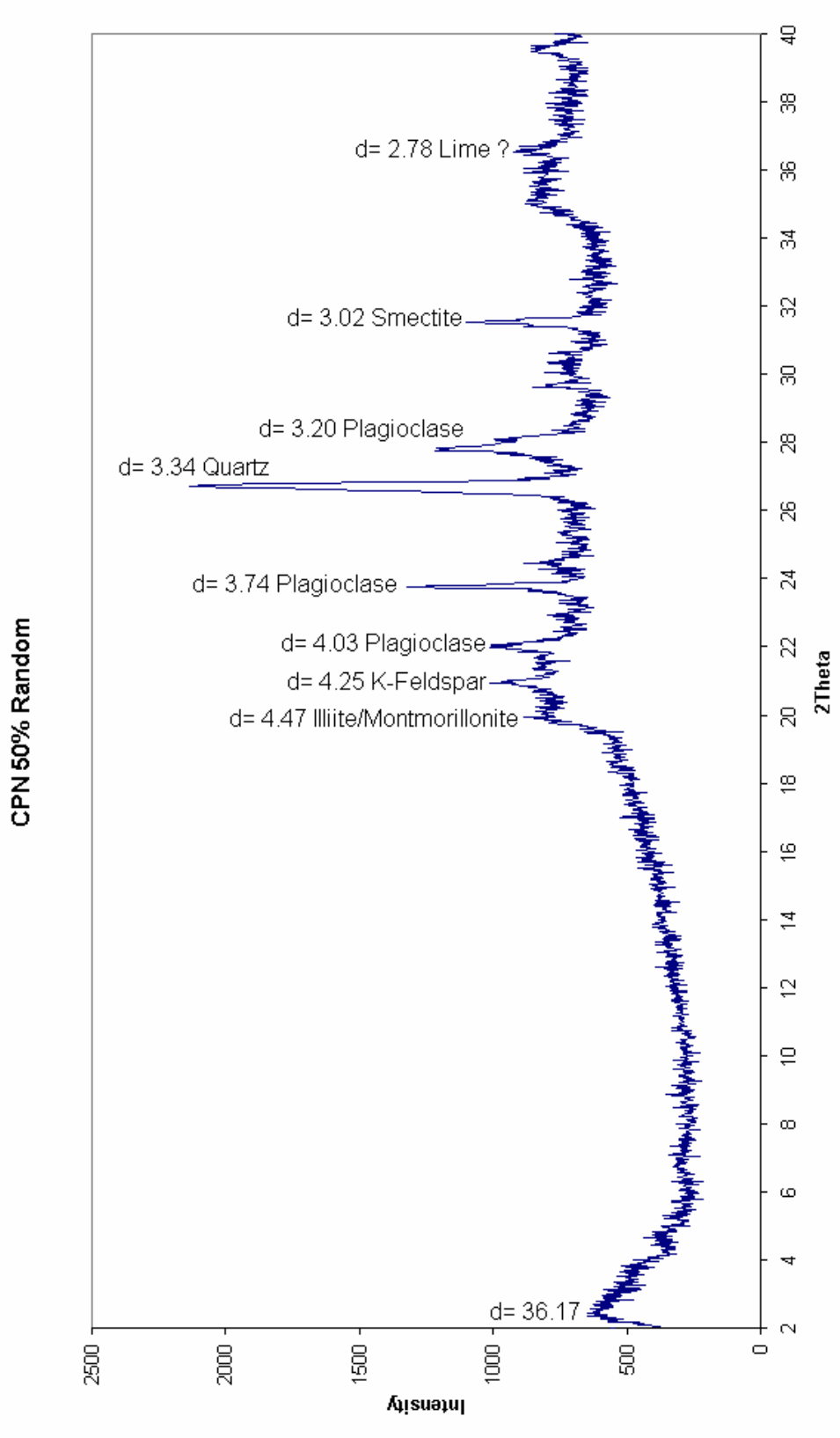

Figure H6. XRD Graph for Clay-Polymer Nanocomposite with 50% Polymer (Random)